IAEA RADIOISOTOPES AND RADIOPHARMACEUTICALS REPORTS No. 2

Cyclotron Based Production of Technetium-99m

IAEA
International Atomic Energy Agency

IAEA RADIOISOTOPES AND RADIOPHARMACEUTICALS SERIES PUBLICATIONS

One of the main objectives of the IAEA Radioisotope Production and Radiation Technology programme is to enhance the expertise and capability of IAEA Member States in deploying emerging radioisotope products and generators for medical and industrial applications in order to meet national needs as well as to assimilate new developments in radiopharmaceuticals for diagnostic and therapeutic applications. This will ensure local availability of these applications within a framework of quality assurance.

Publications in the IAEA Radioisotopes and Radiopharmaceuticals Series provide information in the areas of: reactor and accelerator produced radioisotopes, generators and sealed sources development/production for medical and industrial uses; radiopharmaceutical sciences, including radiochemistry, radiotracer development, production methods and quality assurance/quality control (QA/QC). The publications have a broad readership and are aimed at meeting the needs of scientists, engineers, researchers, teachers and students, laboratory professionals, and instructors. International experts assist the IAEA Secretariat in drafting and reviewing these publications. Some of the publications in this series may also be endorsed or co-sponsored by international organizations and professional societies active in the relevant fields.

There are two categories of publications: the **IAEA Radioisotopes and Radiopharmaceuticals Series** and **IAEA Radioisotopes and Radiopharmaceuticals Reports**.

IAEA RADIOISOTOPES AND RADIOPHARMACEUTICALS SERIES

Publications in this category present guidance information or methodologies and analyses of long term validity, for example protocols, guidelines, codes, standards, quality assurance manuals, best practices and high level technological and educational material.

IAEA RADIOISOTOPES AND RADIOPHARMACEUTICALS REPORTS

In this category, publications complement information published in the IAEA Radioisotopes and Radiopharmaceuticals Series in areas of the: development and production of radioisotopes and generators for medical and industrial applications; and development, production and QA/QC of diagnostic and therapeutic radiopharmaceuticals. These publications include reports on current issues and activities such as technical meetings, the results of IAEA coordinated research projects, interim reports on IAEA projects, and educational material compiled for IAEA training courses dealing with radioisotope and radiopharmaceutical related subjects. In some cases, these reports may provide supporting material relating to publications issued in the IAEA Radioisotopes and Radiopharmaceuticals Series.

All of these publications can be downloaded cost free from the IAEA web site:

http://www.iaea.org/Publications/index.html

Further information is available from:

Marketing and Sales Unit
International Atomic Energy Agency
Vienna International Centre
PO Box 100
1400 Vienna, Austria

Readers are invited to provide feedback to the IAEA on these publications. Information may be provided through the IAEA web site, by mail at the address given above, or by email to:

Official.Mail@iaea.org

CYCLOTRON BASED PRODUCTION OF TECHNETIUM-99m

The following States are Members of the International Atomic Energy Agency:

AFGHANISTAN
ALBANIA
ALGERIA
ANGOLA
ANTIGUA AND BARBUDA
ARGENTINA
ARMENIA
AUSTRALIA
AUSTRIA
AZERBAIJAN
BAHAMAS
BAHRAIN
BANGLADESH
BARBADOS
BELARUS
BELGIUM
BELIZE
BENIN
BOLIVIA, PLURINATIONAL STATE OF
BOSNIA AND HERZEGOVINA
BOTSWANA
BRAZIL
BRUNEI DARUSSALAM
BULGARIA
BURKINA FASO
BURUNDI
CAMBODIA
CAMEROON
CANADA
CENTRAL AFRICAN REPUBLIC
CHAD
CHILE
CHINA
COLOMBIA
CONGO
COSTA RICA
CÔTE D'IVOIRE
CROATIA
CUBA
CYPRUS
CZECH REPUBLIC
DEMOCRATIC REPUBLIC OF THE CONGO
DENMARK
DJIBOUTI
DOMINICA
DOMINICAN REPUBLIC
ECUADOR
EGYPT
EL SALVADOR
ERITREA
ESTONIA
ETHIOPIA
FIJI
FINLAND
FRANCE
GABON
GEORGIA
GERMANY
GHANA
GREECE
GUATEMALA
GUYANA
HAITI
HOLY SEE
HONDURAS
HUNGARY
ICELAND
INDIA
INDONESIA
IRAN, ISLAMIC REPUBLIC OF
IRAQ
IRELAND
ISRAEL
ITALY
JAMAICA
JAPAN
JORDAN
KAZAKHSTAN
KENYA
KOREA, REPUBLIC OF
KUWAIT
KYRGYZSTAN
LAO PEOPLE'S DEMOCRATIC REPUBLIC
LATVIA
LEBANON
LESOTHO
LIBERIA
LIBYA
LIECHTENSTEIN
LITHUANIA
LUXEMBOURG
MADAGASCAR
MALAWI
MALAYSIA
MALI
MALTA
MARSHALL ISLANDS
MAURITANIA
MAURITIUS
MEXICO
MONACO
MONGOLIA
MONTENEGRO
MOROCCO
MOZAMBIQUE
MYANMAR
NAMIBIA
NEPAL
NETHERLANDS
NEW ZEALAND
NICARAGUA
NIGER
NIGERIA
NORWAY
OMAN
PAKISTAN
PALAU
PANAMA
PAPUA NEW GUINEA
PARAGUAY
PERU
PHILIPPINES
POLAND
PORTUGAL
QATAR
REPUBLIC OF MOLDOVA
ROMANIA
RUSSIAN FEDERATION
RWANDA
SAN MARINO
SAUDI ARABIA
SENEGAL
SERBIA
SEYCHELLES
SIERRA LEONE
SINGAPORE
SLOVAKIA
SLOVENIA
SOUTH AFRICA
SPAIN
SRI LANKA
SUDAN
SWAZILAND
SWEDEN
SWITZERLAND
SYRIAN ARAB REPUBLIC
TAJIKISTAN
THAILAND
THE FORMER YUGOSLAV REPUBLIC OF MACEDONIA
TOGO
TRINIDAD AND TOBAGO
TUNISIA
TURKEY
TURKMENISTAN
UGANDA
UKRAINE
UNITED ARAB EMIRATES
UNITED KINGDOM OF GREAT BRITAIN AND NORTHERN IRELAND
UNITED REPUBLIC OF TANZANIA
UNITED STATES OF AMERICA
URUGUAY
UZBEKISTAN
VANUATU
VENEZUELA, BOLIVARIAN REPUBLIC OF
VIET NAM
YEMEN
ZAMBIA
ZIMBABWE

The Agency's Statute was approved on 23 October 1956 by the Conference on the Statute of the IAEA held at United Nations Headquarters, New York; it entered into force on 29 July 1957. The Headquarters of the Agency are situated in Vienna. Its principal objective is "to accelerate and enlarge the contribution of atomic energy to peace, health and prosperity throughout the world''.

IAEA RADIOISOTOPES AND RADIOPHARMACEUTICALS REPORTS No. 2

CYCLOTRON BASED PRODUCTION OF TECHNETIUM-99m

INTERNATIONAL ATOMIC ENERGY AGENCY
VIENNA, 2017

COPYRIGHT NOTICE

Marketing and Sales Unit, Publishing Section
International Atomic Energy Agency
Vienna International Centre
PO Box 100
1400 Vienna, Austria
fax: +43 1 2600 29302
tel.: +43 1 2600 22417
email: sales.publications@iaea.org
http://www.iaea.org/books

Printed by the IAEA in Austria
June 2017
STI/PUB/1743

IAEA Library Cataloguing in Publication Data

Names: International Atomic Energy Agency.
Title: Cyclotron based production of technetium-99m / International Atomic Energy Agency.
Description: Vienna : International Atomic Energy Agency, 2017. | Series: IAEA radioisotopes and radiopharmaceuticals reports, ISSN 2413–9556 ; no.2 | Includes bibliographical references.
Identifiers: IAEAL 17-01090 | ISBN 978–92–0–102916–4 (paperback : alk. paper)
Subjects: LCSH: Radiopharmaceuticals. | Cyclotrons. | Technetium — Isotopes. | Nuclear medicine.
Classification: UDC 621.039.574.5 | STI/PUB/1743

FOREWORD

Owing to the widespread availability of technetium-99m (^{99m}Tc) generators supplied from fission production of molybdenum-99 (^{99}Mo), alternative sources of supply, such as the production of technetium radioisotopes directly from conventional medical cyclotrons, has long been neglected. Given the shortage of ^{99}Mo caused by the unexpected prolonged shutdown of the Chalk River (Canada) and Petten (Netherlands) reactors, and the permanent cessation of ^{99}Mo production at Chalk River in 2016, the exploration of alternative methods of producing technetium radioisotopes has attracted significant interest. Such alternative methods would enable the continued use of all existing radiopharmaceuticals designed for ^{99m}Tc in nuclear medicine, for example, as diagnostic imaging agents, if another shortage should arise.

Over the years, IAEA support of research and development and technical cooperation activities has significantly enhanced Member States' capabilities in the field of medical isotope production. To continue with this approach, and as a result of a recently completed coordinated research project (CRP) on Accelerator-based Alternatives to Non-HEU Production of ^{99}Mo/^{99m}Tc, the IAEA decided to issue this publication as guidance on enhancing the utilization of medical cyclotrons for the production of ^{99m}Tc. The CRP was intended to improve production routes and to improve the separation and purification of this radionuclide so as to achieve high specific activity and chemical purity suitable for labelling molecules of medical interest, and to utilize the spare capacity available at medical cyclotron centres.

This IAEA publication is a compilation of inputs from dedicated experts in the field as well as from the results of the above mentioned CRP. Consequently, the first part of this publication contains sections on the production of ^{99m}Tc, techniques for the preparation of targets, the irradiation of targets under high beam currents, target processing, target recovery and so on. The intended audience of this publication includes: scientists interested in translating the theory of accelerator-based ^{99m}Tc production technology into practice; technologists already working with cyclotrons in Member States who wish to enhance the utility of their existing machines; and managers who are in the process of setting up facilities in their State. In addition, students working towards higher level degrees in related fields may also benefit from this publication. The attached CD-ROM contains contributed accounts of the participants' work during the CRP, demonstrating the successful application of the principles described in the main body of the publication.

The IAEA wishes to thank all CRP participants and contributors to this publication for their valuable contributions. The IAEA officers responsible for this publication were M. Haji-Saeid and J. Osso of the Division of Physical and Chemical Sciences.

EDITORIAL NOTE

Guidance provided here, describing good practices, represents expert opinion but does not constitute recommendations made on the basis of a consensus of Member States.

This report does not address questions of responsibility, legal or otherwise, for acts or omissions on the part of any person.

Although great care has been taken to maintain the accuracy of information contained in this publication, neither the IAEA nor its Member States assume any responsibility for consequences which may arise from its use.

The use of particular designations of countries or territories does not imply any judgement by the publisher, the IAEA, as to the legal status of such countries or territories, of their authorities and institutions or of the delimitation of their boundaries.

The mention of names of specific companies or products (whether or not indicated as registered) does not imply any intention to infringe proprietary rights, nor should it be construed as an endorsement or recommendation on the part of the IAEA.

The authors are responsible for having obtained the necessary permission for the IAEA to reproduce, translate or use material from sources already protected by copyrights.

Material prepared by authors who are in contractual relation with governments is copyrighted by the IAEA, as publisher, only to the extent permitted by the appropriate national regulations.

The IAEA has no responsibility for the persistence or accuracy of URLs for external or third party Internet web sites referred to in this book and does not guarantee that any content on such web sites is, or will remain, accurate or appropriate.

The material on the accompanying CD-ROM has been prepared from the original materials as submitted by the authors.

CONTENTS

1. INTRODUCTION

1.1. BACKGROUND

Efforts and studies to investigate alternative production routes of molybdenum-99 (^{99}Mo) and technetium-99m (^{99m}Tc) are ongoing all over the world. The direct production of ^{99m}Tc using accelerators is one of the proposed alternatives that utilizes the ^{100}Mo(p,2n)^{99m}Tc reaction on highly ^{100}Mo-enriched target material [1–5]. A Coordinated Research Project (CRP) on Accelerator-based Alternatives to Non-HEU Production of ^{99}Mo/^{99m}Tc was initiated with the aim of developing an alternative direct method of production of ^{99m}Tc using dedicated high current cyclotrons.

There are several potential methods for the production of ^{99m}Tc from accelerators. These have been explored in a recent publication by the OECD Nuclear Energy Agency in 2010 [6]. An IAEA consultants meeting was held in 2011 to review the current status of research and development of and the perspective for the accelerator based production of ^{99m}Tc. The meeting concluded with the suggestion that the IAEA initiate a CRP on the development of accelerator based alternatives to the ^{99}Mo/^{99m}Tc generator, with an emphasis on several outstanding issues that need further research and development, including:

— The purity of the final ^{99m}Tc product with regard to both the isotopic ratio of the molybdenum starting material and the proton energy.
— Approaches to isolating and purifying the ^{99m}Tc extracted from the target material. A more complete understanding regarding reproducibility, purity and efficiency for these approaches is needed and should use prescribed metrics for direct comparisons.
— The impact of specific activity (^{99m}Tc / all Tc isotopes including ^{99g}Tc) has to be determined in order to define the shelf life of accelerator produced ^{99m}Tc compared with generator produced ^{99m}Tc in the formulation of radiopharmaceutical kits.
— The path to recovery of the enriched ^{100}Mo target material including the tracking of the isotopic composition and chemical and radionuclidic impurities.

It was noted by the expert panel assembled that the proposed CRP on direct production may also be a long term solution and is quite sufficient to manufacture ^{99m}Tc on-site for supplying regional radiopharmacies and may supplement or in some instances even replace ^{99}Mo generators.

In the CRP, the focus was on one of several feasible accelerator based technologies: the direct production of ^{99m}Tc from proton bombardment of enriched molybdenum. Usable quantities of ^{99m}Tc can be produced by the ^{100}Mo(p,2n)^{99m}Tc reaction, which has a peak in the cross-section at 15–16 MeV, well within the reach of many commercial cyclotrons. A higher current cyclotron has been used to produce 350 GBq (>9 Ci) of ^{99m}Tc, which could supply a large metropolitan area (18 MeV protons, 250μA, 6 h irradiation). Higher yields can be reached with higher energy cyclotrons and/or with a more intense beam current (>1.184 TBq (32 Ci) at 24 MeV and 450 μA). However, there are several considerations that may affect the practicality of this production method. The 6 h half-life of ^{99m}Tc is a factor that constrains the time (and therefore the distance) from production to use. The distribution model and the ability to make use of existing distribution networks will influence practicality. A local distribution model would include a small accelerator and lower power target and would produce only enough for the local vicinity, whereas a regional or national distribution model would include a larger accelerator and higher power targets to enable a wider distribution of the ^{99m}Tc. These models have other implications, such as delivery schedules and the influence of irradiation parameters on isotopically enriched molybdenum supply and recovery. Another aspect of practicality is the cost per MBq of accelerator produced ^{99m}Tc when compared with the price of generator produced ^{99m}Tc, assuming the Organisation for Economic Co-operation and Development (OECD) goal of full cost recovery. Although an exact estimate is probably not possible at this time, rough estimates put the cost per MBq at about the same level for both production methods, although this will again depend on the distribution model chosen and whether existing cyclotron facilities can use the time when the cyclotron is not occupied with other radionuclide production for the production of ^{99m}Tc. ^{100}Mo is a naturally occurring isotope of molybdenum and is sold by a commercial isotope suppliers with greater than 99% enrichment.

Both the isotopic composition of the enriched molybdenum starting material and the incident proton energy have an impact on the purity of the final ^{99m}Tc product. The irradiation parameters impacting radiation dose (patient dose and specific activity) include target enrichment, bombarding energy and length of irradiation.

The stability of the isolated ^{99m}Tc pertechnetate solution as a function of time and the stability of the prepared radiopharmaceutical will affect the shelf life of the product and must be assessed.

The impact of specific activity (^{99m}Tc / all Tc isotopes including ^{99g}Tc) has to be determined in order to define the shelf life of the accelerator produced ^{99m}Tc in comparison with generator produced ^{99m}Tc in the formulation of radiopharmaceutical kits.

The path to recovery of the enriched ^{100}Mo target material should be optimized and involves tracking isotopic composition and chemical and radionuclidic impurities in order to determine recycling protocols.

There are several approaches to isolating and purifying the ^{99m}Tc extracted from the target material. A more complete understanding regarding reproducibility, purity and efficiency for these approaches using prescribed metrics for direct interlaboratory comparisons is needed. With these aspects in mind, the CRP goal was to address each component through a variety of approaches, and the findings are reported in this publication.

1.2. OBJECTIVE

This IAEA publication was initiated following a CRP on Accelerator-based Alternatives to Non-HEU production of ^{99}Mo/^{99m}Tc. The CRP had 12 participating institutions worldwide and the aim of enhancing the capability of Member States to directly produce ^{99m}Tc for medical applications in order to meet the demand for diagnostic agents for specific diseases. This publication is intended to provide broad information on improved production routes and improved separation and purification of cyclotron based ^{99m}Tc to achieve the high specific activity and chemical purity needed for labelling molecules of medical interest and to also enable the fruitful use of spare capacity available in medical cyclotron centres. The references cited in this publication may also be useful as sources of further information.

1.3. SCOPE

This publication provides guidelines and methods, using standardized nuclear data, for the development of targets for cyclotron based ^{99m}Tc production capable of producing sufficient quantities of this radionuclide for clinical investigations and on the chemistry for the separation of radionuclides from target materials. In addition, this publication provides information on: the purity of the final ^{99m}Tc product in terms of both the isotopic composition of the enriched molybdenum starting material and the incident proton energy; the irradiation parameters impacting radiation dose including target enrichment, bombarding energy and length of irradiation; approaches to isolating and purifying the ^{99m}Tc extracted from the target material; a more complete understanding of reproducibility, purity and efficiency; the assessment of the stability of the isolated ^{99m}Tc pertechnetate solution as a function of time and the stability of the prepared radiopharmaceutical, which will affect the shelf life of the products; the impact of specific activity (^{99m}Tc / all Tc isotopes including ^{99g}Tc) in order to define the shelf life of the accelerator produced ^{99m}Tc compared with generator produced ^{99m}Tc in the formulation of radiopharmaceutical kits; and finally the optimized path to recovery of the enriched ^{100}Mo target material which is involved in tracking the isotopic composition and chemical/radionuclidic impurities in order to determine recycling protocols.

1.4. STRUCTURE

Section 2 of this publication disucsses nuclear data and facilities, while Section 3 describes target preparation. Section 4 describes target dissolution and separation. Section 5 focuses on quality control and Section 6 on recycling. Preclinical and clinical studies are discussed in Section 7, while good manufacturing processes (GMP) are described in Section 8, and Section 9 forms a conclusion to the publication. The accompanying CD-ROM, which supports the book, contains accounts of the participants' work during the CRP demonstrating the successful

application of the principles described in the main body of the publication; these are the unedited reports of the CRP participants as presented at the final research coordination meeting.

2. NUCLEAR DATA AND FACILITES

The direct production of ^{99m}Tc using accelerators can be considered as an alternative to reactor based ^{99}Mo/^{99m}Tc generator production. Several different approaches are available for the accelerator production of ^{99m}Tc. In principle, using Mo as a target material, 12 reactions are available:

- ^{100}Mo(p,2n)^{99m}Tc
- ^{100}Mo(p,x)^{99}Mo
- ^{100}Mo(d,3n)^{99m}Tc
- ^{100}Mo(d,x)^{99}Mo
- ^{98}Mo(d,n)^{99m}Tc
- ^{98}Mo(d,p)^{99}Mo
- ^{98}Mo(p,γ)^{99m}Tc
- ^{100}Mo(p,2p)^{99}Nb → ^{99}Mo
- ^{97}Mo(d,γ)^{99m}Tc
- ^{100}Mo(γ,n)^{99}Mo
- ^{96}Mo(α,p)^{99m}Tc
- ^{97}Mo(α,2p)^{99}Mo

These production reactions, although viable from the nuclear physics point of view, require different technical and technological developments, and, when using accelerators on a large scale, produce ^{99m}Tc with different specific activities and radionuclidic purities. In this CRP, only the ^{100}Mo(p,2n)^{99m}Tc production route was considered [7, 8]. However, this publication will also discuss other production routes.

The direct accelerator production of ^{99m}Tc is possible on ^{100}Mo-enriched molybdenum targets with yields high enough to provide a suitable amount of activity to cover most local and regional needs. The final quality of accelerator produced ^{99m}Tc depends on different parameters such as the isotopic composition of the Mo target material, the bombarding proton energy and intensity, the target thickness and the irradiation time. Moreover, the final composition of the produced material is also dependent on post-irradiation processing methods and times (target transportation and chemistry, separation technique of technetium and radio labelling).

A comprehensive theoretical investigation related to accelerator produced ^{99m}Tc generated via the ^{100}Mo(p,x) reaction is therefore mandatory to establish the best irradiation conditions for accelerator produced ^{99m}Tc, as well as the estimation of in-target yields expected for all Tc nuclides from ^{100}Mo(p,x) reactions. Moreover, a careful evolution analysis post end of bombardment (EOB) of the most important parameters, namely the isotopic purity and the radionuclidic purity of the final accelerator produced Tc, taking into account the isotopic composition of ^{100}Mo-enriched molybdenum target material, is needed.

2.1. IRRADIATION FACILITIES

Variable or fixed energy high current cyclotrons are the most suitable accelerators for the direct production of ^{99m}Tc utilizing the ^{100}Mo(p,2n)^{99m}Tc reaction. A variety of cyclotrons available on the market or already deployed at research sites and in hospitals can be used for the direct production of ^{99m}Tc. The achievable yields, the specific activity and the purity level of the ^{99m}Tc are primarily determined by the cross-sections of the main and any side reactions involved in the whole production process.

2.2. TARGET MATERIAL REQUIREMENTS

Levels of ^{100}Mo enrichment at least as high as 99% are needed for good quality production of accelerator ^{99m}Tc. Any ^{100}Mo enriched material will contain minor amounts of the other lower mass stable isotopes (^{92,94,95,96,97,98}Mo) on which additional nuclear reactions are induced by the bombarding protons producing unwanted contaminating ^{9x}Tc, Ru, Nb and Zr radionuclides through separate reactions.

The presence of long lived Tc isotopes such as ^{99g}Tc, ^{98}Tc and ^{97g}Tc can influence the achievable specific activity of ^{99m}Tc but do not usually contribute seriously to the additional patient dose. The shorter lived Tc contaminants influence the specific activity as well as contributing to the patient dose. Owing to the decay characteristics of the contaminating technetium radionuclides and their half-lives, type and energy of the emitted radiations, the ^{93g}Tc, ^{94m}Tc, ^{94g}Tc, ^{95m}Tc, ^{95g}Tc, ^{96m}Tc and ^{96g}Tc isotopes could give rise to most of the additional patient dose. Utilizing bombarding proton energy not higher than 25 MeV, the contaminating Tc isotopes are only produced in (p,n), (p,2n) and (p,3n) reactions on different stable isotopes of the enriched molybdenum targets. To minimize the amount of the shorter lived contaminating Tc isotopes, the composition of the enriched target material should be chosen carefully, and the amount of ^{94}Mo, ^{95}Mo, ^{96}Mo and ^{97}Mo impurities of the target should be minimized. The actual value of the additional dose depends on the bombarding energy, target thickness, irradiation and time of use post separation (shelf life). Table 1 contains recommendation for the target isotopic composition. The columns represent the recommended maximal Mo-isotopic composition for the typical energy ranges that would be used in direct production of ^{99m}Tc. Also, the estimated impact on patient radiation dose due to the co-produced Tc isotopes under the respective irradiation conditions is listed.

TABLE 1. RECOMMENDED SPECIFICATIONS FOR ^{100}Mo TARGET

Isotope	Proposed % isotopic purity to maintain patient dose increase of ~10% compared with pure $^{99m}TcO_4$		
	≤20 MeV[a]	20–22 MeV[b]	22–24 MeV[c]
Mo-92	0.03	0.03	0.03
Mo-94	0.03	0.03	0.03
Mo-95	0.03	0.03	0.03
Mo-96	0.03	0.03	0.03
Mo-97	0.03	0.03	0.03
Mo-98	6.0	0.80	0.25

[a] Maximum increase in patient dose of 10.1% at 20 MeV, 18 h after EOB.
[b] Maximum increase in patient dose of 10.1% at 22 MeV, 18 h after EOB.
[c] Maximum increase in patient dose of 11.0% at 24 MeV, 18 h after EOB.

2.3. LIMITATION OF BOMBARDING ENERGIES AND BEAM INTENSITY

For production of good quality ^{99m}Tc, the bombarding energy should be accurately determined. The yield of ^{99m}Tc depends on the bombarding energy and irradiation time. Generally, a higher bombarding energy provides a larger yield, as shown in Fig. 1. However, the bombarding energy should be limited at an optimal value so as to minimize the co-production of radioactive contaminants.

Increasing either the irradiation time and bombarding energy increases the level of co-produced contaminating Tc and other radioisotopes, as shown in Figs 2 and 3. Since the amount of co-produced contaminating Tc isotopes depends on the composition of the target material, the optimal bombarding energy also depends on the enrichment level of the actual target material and the acceptable level of specific activity.

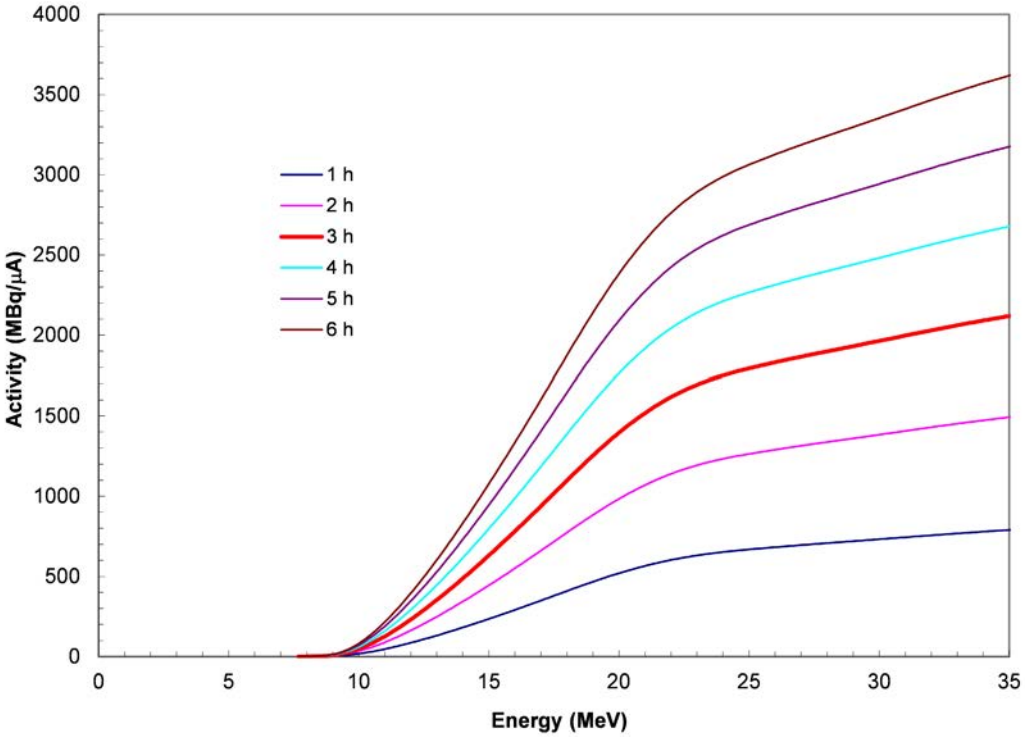

FIG. 1. EOB activity as a function of the bombarding energy and irradiation time.

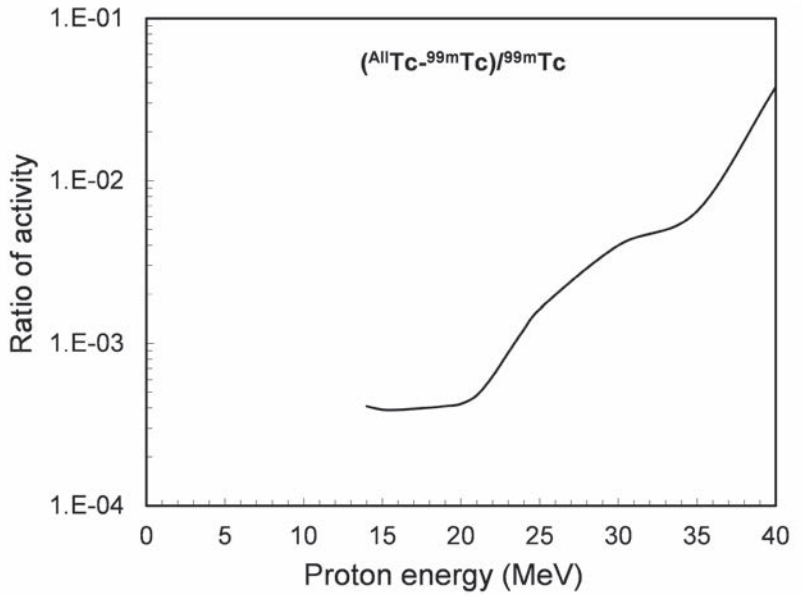

FIG. 2. Relative activity of contaminating Tc as a function of bombarding proton energy after a 3 h irradiation and a 2 h cooling time.

The beam intensity is limited only by the target construction and the beam performance of the cyclotron itself. Mo has good physical and chemical parameters and can withstand high power irradiation. However, targets prepared from enriched material can have different properties that mainly depend on the technology with which they are prepared. The target should be robust and cooled well enough to be able to withstand high power irradiation and should be capable of properly dissipating the power introduced by the bombarding beam.

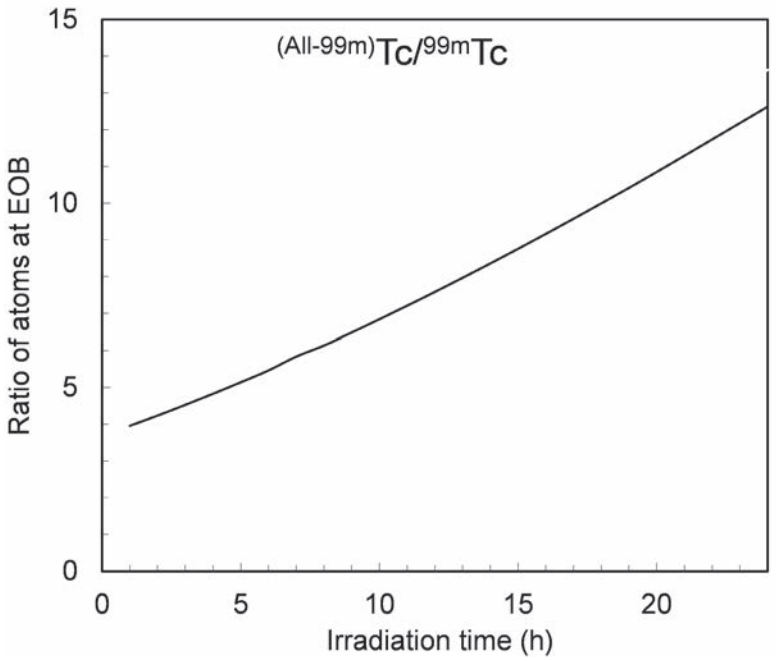

FIG. 3. Ratio of contaminating Tc atoms as a function of bombarding time for a 17 MeV irradiation after a 2 h cooling time.

2.4. NUCLEAR DATA

The predicted quality of accelerator produced ^{99m}Tc based on the ^{100}Mo(p,2n)^{99m}Tc reaction can be studied by calculating and comparing the yield of the main reaction with the combined yields of the side reactions. After collecting the available experimental cross-section data, acquired over 40 years for the ^{100}Mo(p,2n)^{99m}Tc reaction route, it was found that datasets showed large differences. A large disagreement of more than a factor of two may be observed between the lowest and the highest dataset values. Efforts were made to clarify the values by performing new experiments in which the excitation functions and thick target yields were measured for the two main reactions, namely ^{100}Mo(p,2n)^{99m}Tc and ^{100}Mo(p,x)^{99}Mo [7, 9].

Due to the relatively complex decay scheme of ^{99}Mo and ^{99m}Tc, the use of the proper decay branching ratios and gamma intensities is essential. The actual values of these data can vary for different evaluations. The early data are slightly different to the more recent data. A simplified decay scheme of ^{99}Mo and ^{99m}Tc is shown in Fig. 4. ^{99}Mo decays to ^{99g}Tc in 12.4% of the decay while 87.6% of the decay populates the higher laying isomer state ^{99m}Tc (E = 142 keV, $T_{1/2}$ = 6h). However, about 5.1% of the decaying ^{99}Mo directly populates the E = 140.5 keV

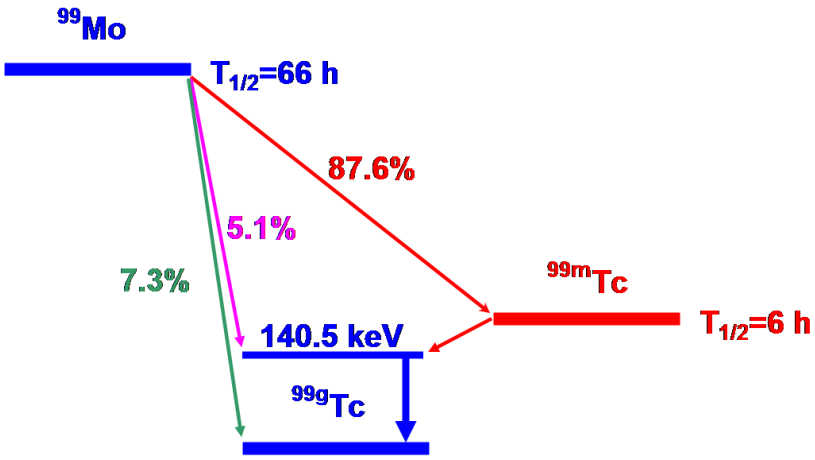

FIG. 4. Simplified decay scheme of ^{99}Mo and ^{99m}Tc.

energy level of ^{99}Tc, resulting in the emission of prompt E_γ = 140.5 keV gamma photons. The isomeric state, ^{99m}Tc, decays almost 100% (IT = 99.9963%, β^- = 0.0037%) to the E_γ = 140.5 keV energy level and then to the ground state of ^{99}Tc by emission of an E_γ = 140.5 keV gamma photon.

One of the most recent evaluations of gamma intensities was presented in 2004 by Bé et al. [10] and its results are collected in Table 2. The relatively complex decay of ^{99}Mo can partly explain the large differences that exist among the experimental cross-section datasets.

TABLE 2. INTENSITIES OF THE E_γ = 140.5 keV GAMMA PHOTONS EMITTED FROM DIFFERENT SOURCES USED IN Ref. [10]

Intensity of the E_γ = 140.5 keV gamma line from different sources	I_γ (%)
Prompt gamma intensity of the decaying ^{99}Mo	4.72
Radioactive equilibrium of the decaying ^{99}Mo and ^{99m}Tc	89.6
Decay of pure ^{99m}Tc (no decaying ^{99}Mo is present)	88.5

2.5. MEASUREMENTS OF THE CROSS-SECTION OF ^{100}Mo(p,2n)^{99m}Tc AND ^{100}Mo(p,x)^{99}Mo REACTIONS

Since the beginning of the CRP presented in this publication, several new, independent, experiments have been performed to determine the excitation function of the main reactions ^{100}Mo(p,2n)^{99m}Tc and ^{100}Mo(p,x)^{99}Mo [11–13]. Moreover, two other experiments were performed up to proton energy (E_p) = 16 MeV and E_p = 36.4 MeV, respectively. Additionally, results from one of the earlier experiments reported in 2003 [14] were re-evaluated using up to date nuclear decay data with the aim of improving the quality of the experimental datasets.

Cross-section values deduced in three independent experiments [12] using the latest evaluated decay data for the radionuclides involved provided datasets in very good agreement with each other indicating sound results of the cross-section of ^{100}Mo(p,2n)^{99m}Tc and ^{100}Mo(p,x)^{99}Mo reactions.

2.6. BENCHMARK EXPERIMENT

A benchmark experiment was carried out as part of the CRP to check and validate the deduced cross-section data. Experimental thick target yields of the ^{100}Mo(p,2n)^{99m}Tc and ^{100}Mo(p,pn)^{99}Mo reactions were determined by irradiating a thick Mo target and were compared with theoretical estimations based on the most recent cross-section data available. In this experiment, the decay of the irradiated Mo target was followed for several days, and about 100 measured activity points were compared with the values deduced by calculation based on the latest experimental cross-section data measured for both the ^{100}Mo(p,2n)^{99m}Tc and the ^{100}Mo(p,pn)^{99}Mo reaction. As shown in Fig. 5, excellent agreement was found between the experimental and calculated values confirming and validating the measured cross-section data of the ^{100}Mo(p,2n)^{99m}Tc and ^{100}Mo(p,pn)^{99}Mo reactions (Fig. 6).

When comparing the specific activity of the ^{99}Mo/^{99m}Tc generator produced ^{99m}Tc and the accelerator produced ^{99m}Tc, the decay characteristics of ^{99}Mo and the corresponding cross-section values for producing ^{99m}Tc, ^{99g}Tc and the lighter Tc radionuclides clearly indicate that the accelerator produced ^{99m}Tc product always has lower specific activity. However, by keeping the bombarding energy low and the irradiation time short, the difference can be kept at an acceptable level.

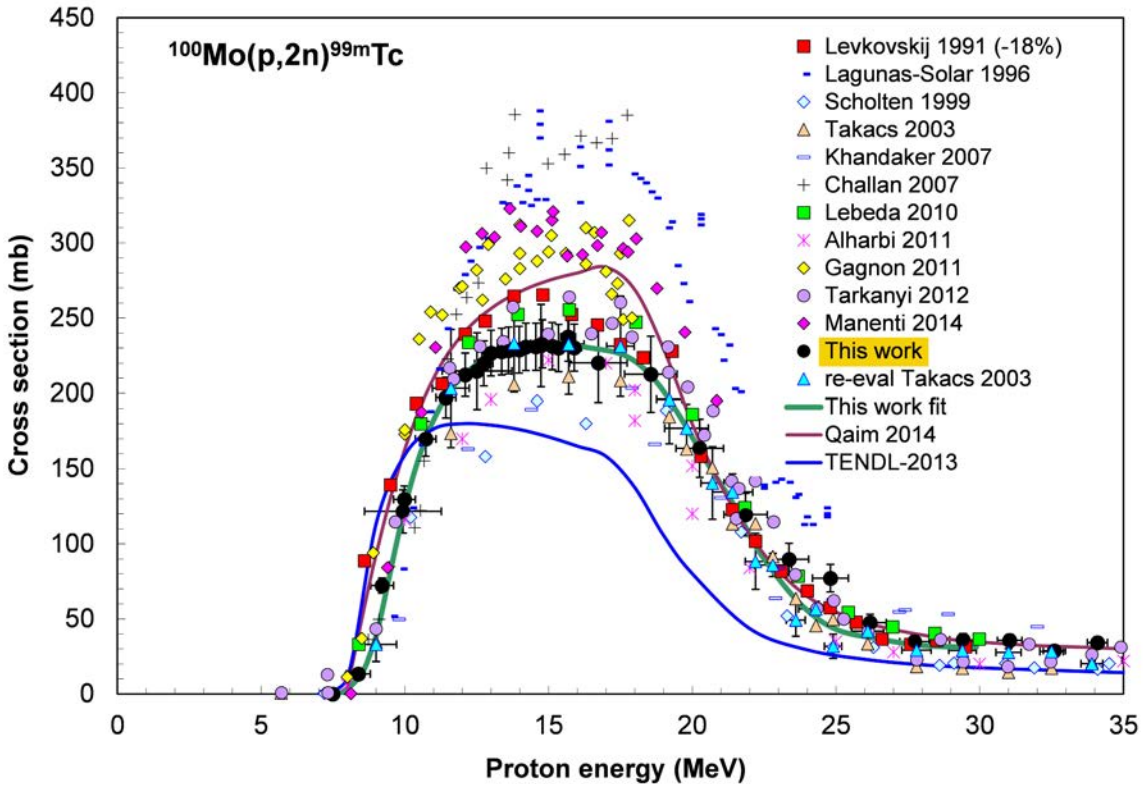

FIG. 5. Experimental cross-section data for the $^{100}Mo(p,2n)^{99m}Tc$ reaction. The newly measured experimental data are represented by the filled black dots.

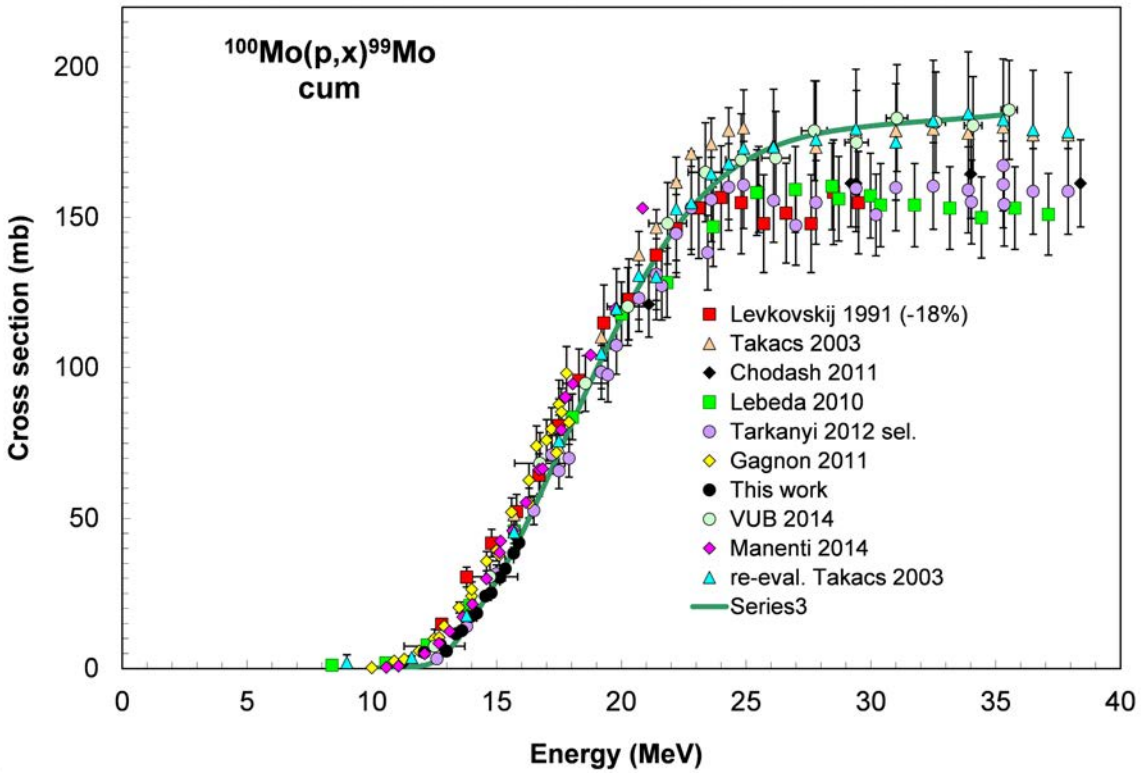

FIG. 6. Experimental cross-sections for the $^{100}Mo(p,x)^{99}Mo$ reaction. The newly measured experimental data are represented by the filled black dots.

2.7. GRAPHICAL USER INTERFACE FOR THE CALCULATION OF ACCELERATOR PRODUCED ^{99m}Tc QUALITY

Using basic nuclear data (cross-sections, gamma intensities and branching ratios) and the corresponding physical laws of activation and decay, the quality of accelerator produced ^{99m}Tc can be estimated by calculation. Considering actual irradiation circumstances, proton energy, beam intensity, irradiation time, target composition, irradiation geometry and target construction, the activity of the main radionuclides ^{99m}Tc and ^{99}Mo can be estimated, together with the amount of other possibly co-produced stable and radioisotopes of Tc, Ru, Mo, Nb and Zr, by using newly developed calculation tools.

For cyclotron production of ^{99m}Tc optimizing reaction conditions, it is crucial to maximize ^{99m}Tc production yield and minimize contributions from other radionuclides. In particular, target composition and thickness, the energy and intensity of the proton beam, irradiation time and radiation dose estimates to patients for different injection times must be determined.

A graphical user interface designed to estimate the characteristics of ^{99m}Tc cyclotron production was created by Hou et al. [15]. It can be used to estimate reaction yields, gamma emissions and doses for ^{99m}Tc and other reaction products [9]. Initial experience shows that theoretical estimates available from this interface allow the efficient analysis of gamma spectroscopy data from early cyclotron experiments, which assists with testing the method and optimizing production parameters. However, the main advantage of this interface will be at the later clinical stage when entering reaction parameters will allow the user to predict production yields and estimate radiation doses for each particular cyclotron run.

2.8. CO-PRODUCTION OF OTHER ISOTOPES

Depending on the target composition and bombarding beam energy, additional reaction channels can be opened that contribute to the production of Tc radionuclides other than ^{99}Tc as well as stable and/or radioactive isotopes of Mo, Nb, Zr and Ru. As examples, Figs 7–11 show the logarithm of the expected amount of different reaction products after a 3 h and 1 μA irradiation using a 99.5% enriched ^{100}Mo target material as a function of bombarding energy from 15 to 25 MeV.

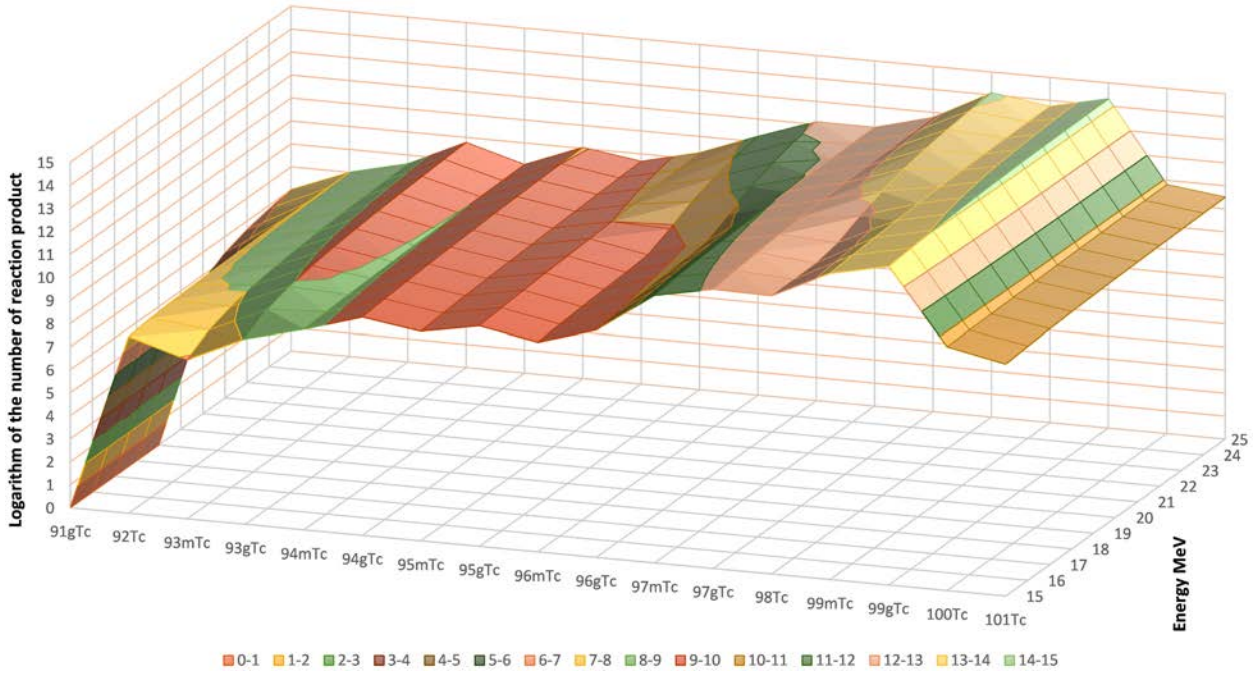

FIG. 7. Production of Tc nuclides as a function of bombarding energy for a 3 h 1 μA irradiation. The vertical axis represents the logarithm of the number of different Tc atoms present in the target at EOB.

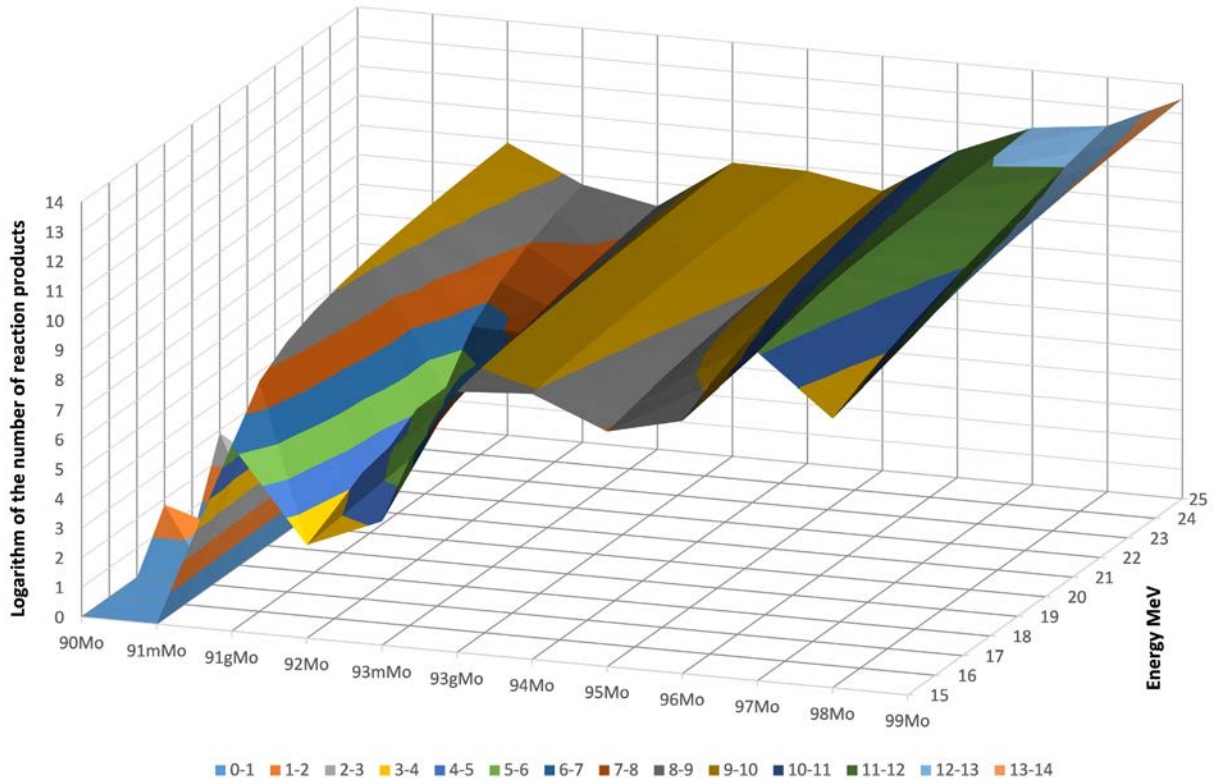

FIG. 8. Production of Mo nuclides as a function of bombarding energy for a 3 h 1 μA irradiation. The vertical axis represents the logarithm of the number of different Tc atoms present in the target at EOB.

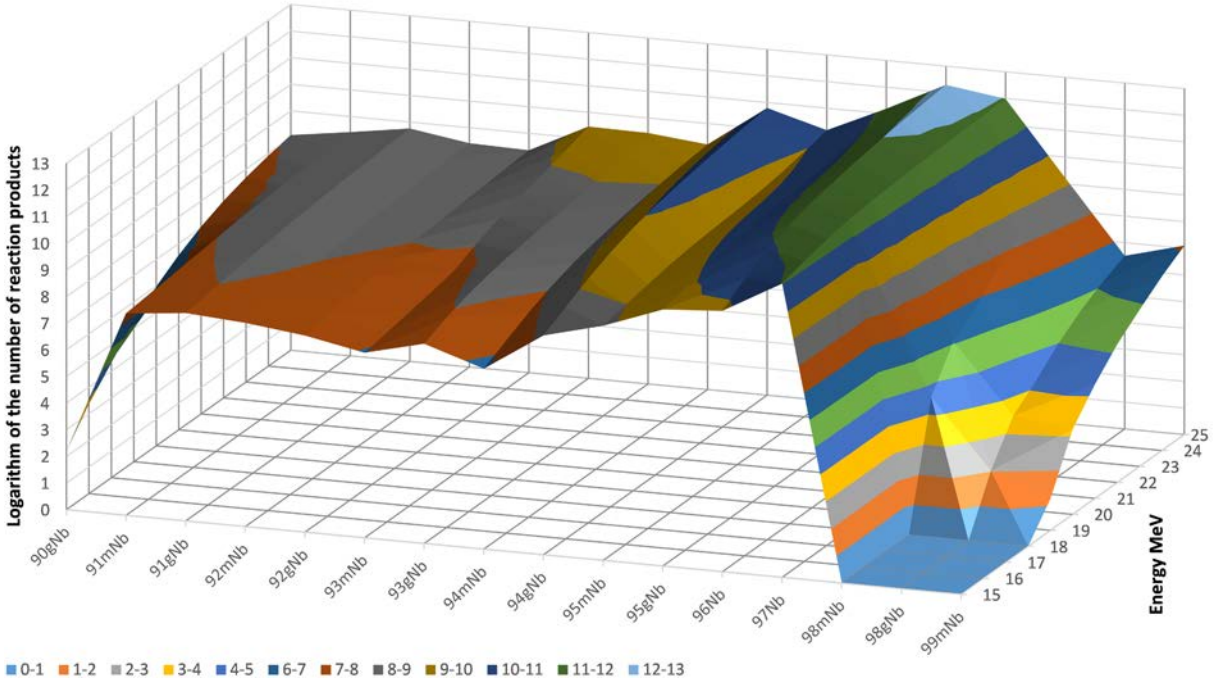

FIG. 9. Production of Nb nuclides as a function of bombarding energy for a 3 h 1 μA irradiation. The vertical axis represents the logarithm of the number of different Tc atoms present in the target at EOB.

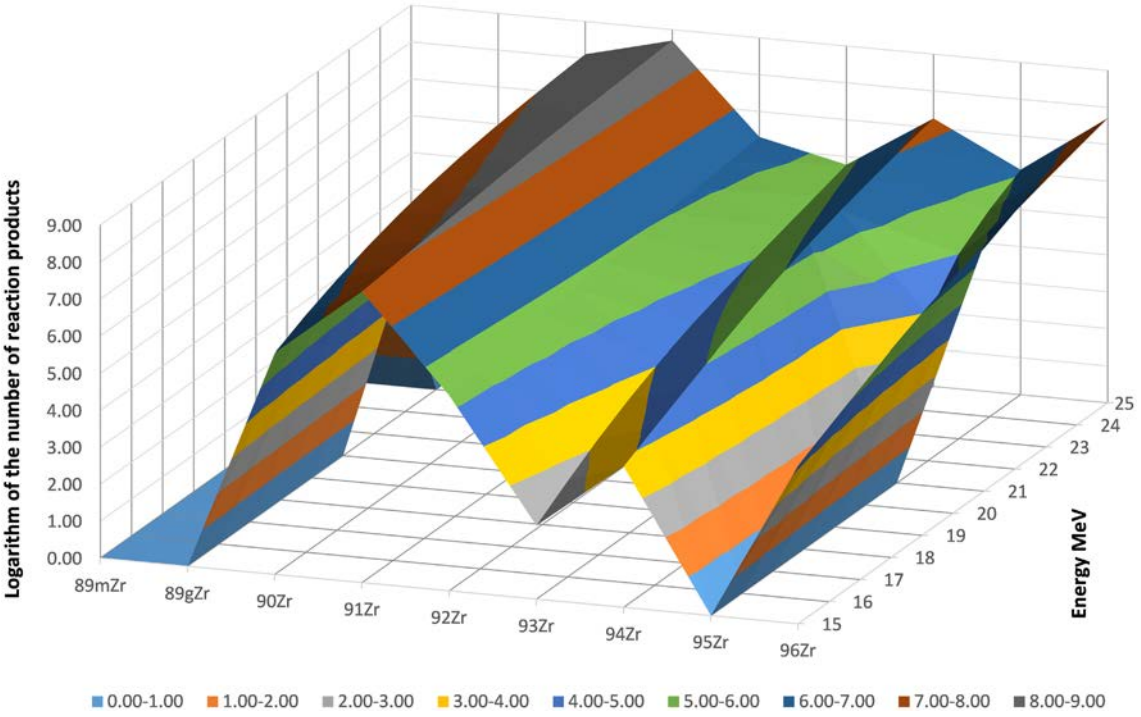

FIG. 10. Production of Zr nuclides as a function of bombarding energy for a 3 h 1 μA irradiation. The vertical axes represent the logarithm of the number of different Tc atoms present in the target at EOB.

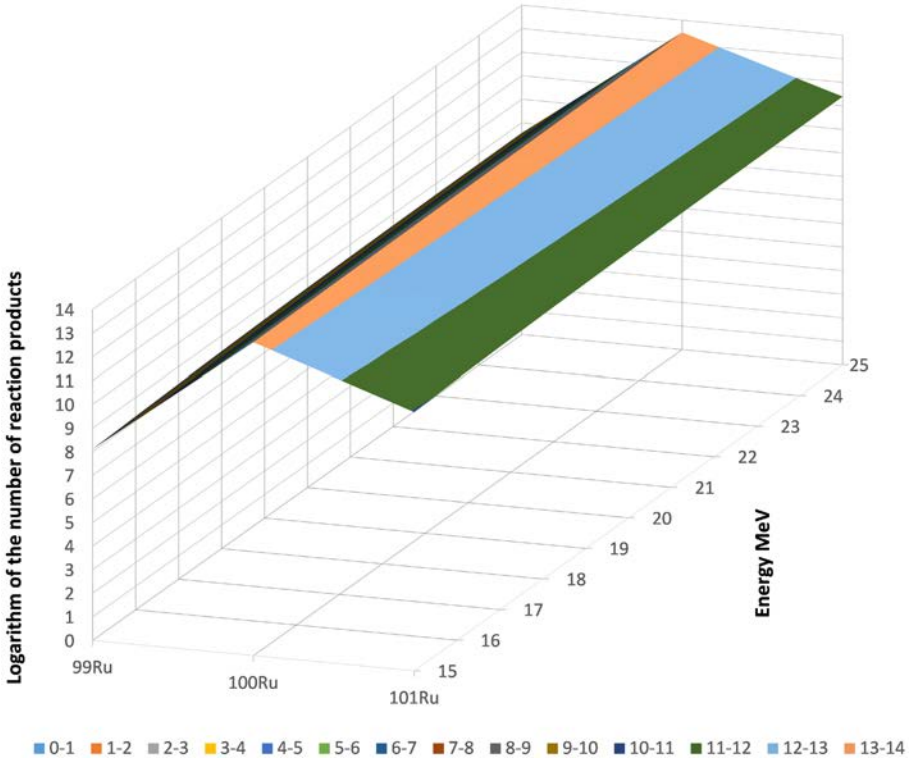

FIG. 11. Production of Ru nuclides as a function of bombarding energy for a 3 h 1 μA irradiation. The vertical axes represent the logarithm of the number of different Tc atoms present in the target at EOB.

Due to the different half-lives of the different Tc radionuclides, their ratio after EOB changes with time. The relative amount of the Tc radionuclides with half-lives shorter than the half-life of ^{99m}Tc decreases while the relative amounts of the Tc radionuclides with longer half-lives increase.

The time dependence of the relative amount of Tc radionuclides after EOB is shown in Fig. 12 for the 0–12 h following EOB.

At 17 MeV bombarding proton energy, the total amount of co-produced Tc nuclides is practically determined by ^{99g}Tc. Above 17 MeV, the threshold energy of the ^{100}Mo(p,3n)^{98}Tc reaction, a considerable amount of long lived ^{98}Tc is produced.

At a bombarding proton energy of 24 MeV, the amount of ^{98}Tc is almost equal to the amount of ^{99g}Tc (Fig. 13).

Below the threshold energy of 17 MeV in the ^{100}Mo(p,3n)^{98}Tc reaction, ^{99g}Tc is co-produced, contaminating additional Tc, while at a higher bombarding energy, a larger amount of other Tc isotopes, such as the long lived ^{98}Tc and ^{97g}Tc, is produced.

The relative activity (compared with the activity of ^{99m}Tc) of the co-produced Tc radionuclides is shown in Fig. 14 as a function of bombarding proton energy.

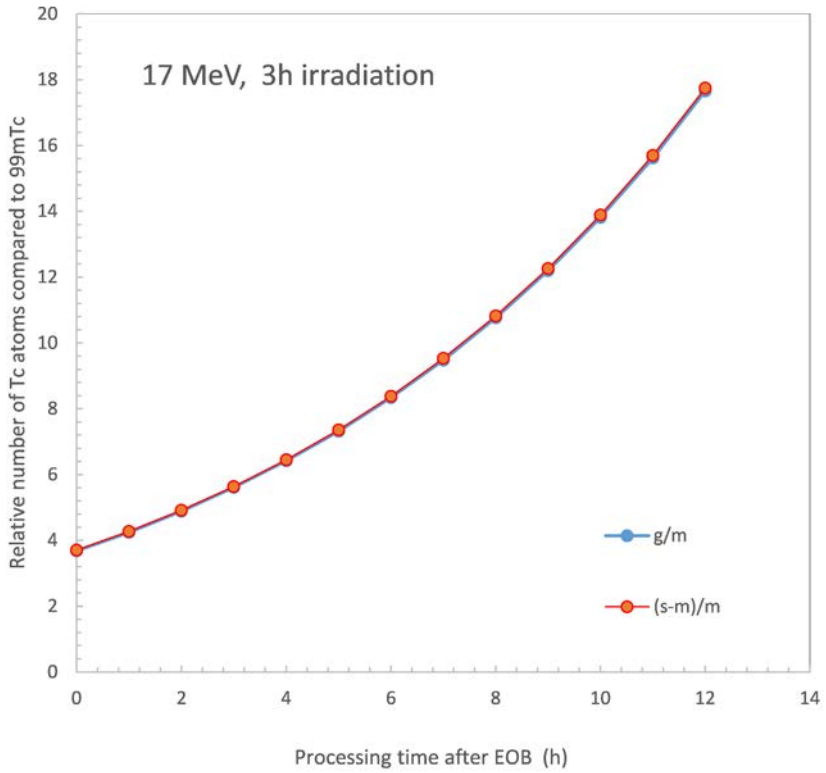

FIG. 12. Time dependence of the Tc radionuclides in the 0–12 h after EOB (g/m represents the ratio of ^{99g}Tc/^{99m}Tc while (s-m)/m represents (^{xx}Tc–^{99m}Tc)/^{99m}Tc for 17 MeV 3h irradiation).

2.9. A PRACTICAL APPROACH TO THE ACCELERATOR PRODUCTION OF ^{99m}Tc

To provide high quality accelerator produced ^{99m}Tc, each site should attempt to:

— Use a proton beam of suitable energy depending on the source material (see Table 1).
— Use the shortest irradiation time possible (to reduce radionuclidic impurities) while meeting the expected needs, taking decay time, labelling time and radiopharmaceutical distribution into account.
— Irradiate targets with the highest beam intensity possible.

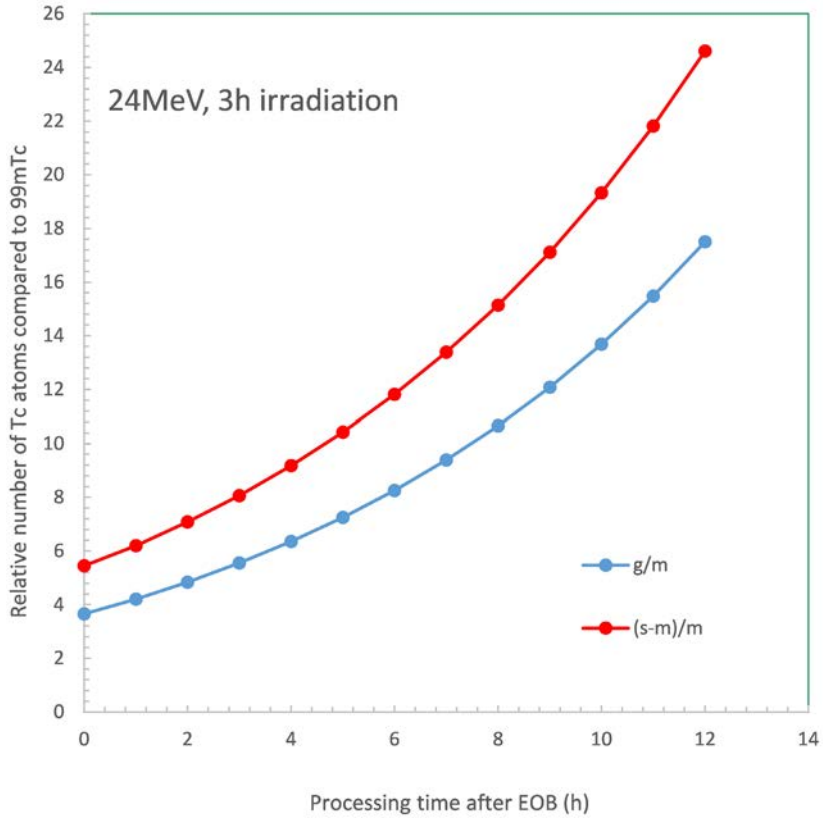

FIG. 13. Time dependence of the Tc radionuclides in the 0–12 h after EOB (g/m represents the ratio of ^{99g}Tc/^{99m}Tc while (s-m)/m represents (^{xx}Tc-^{99m}Tc)/^{99m}Tc for a 24 MeV 3 h irradiation).

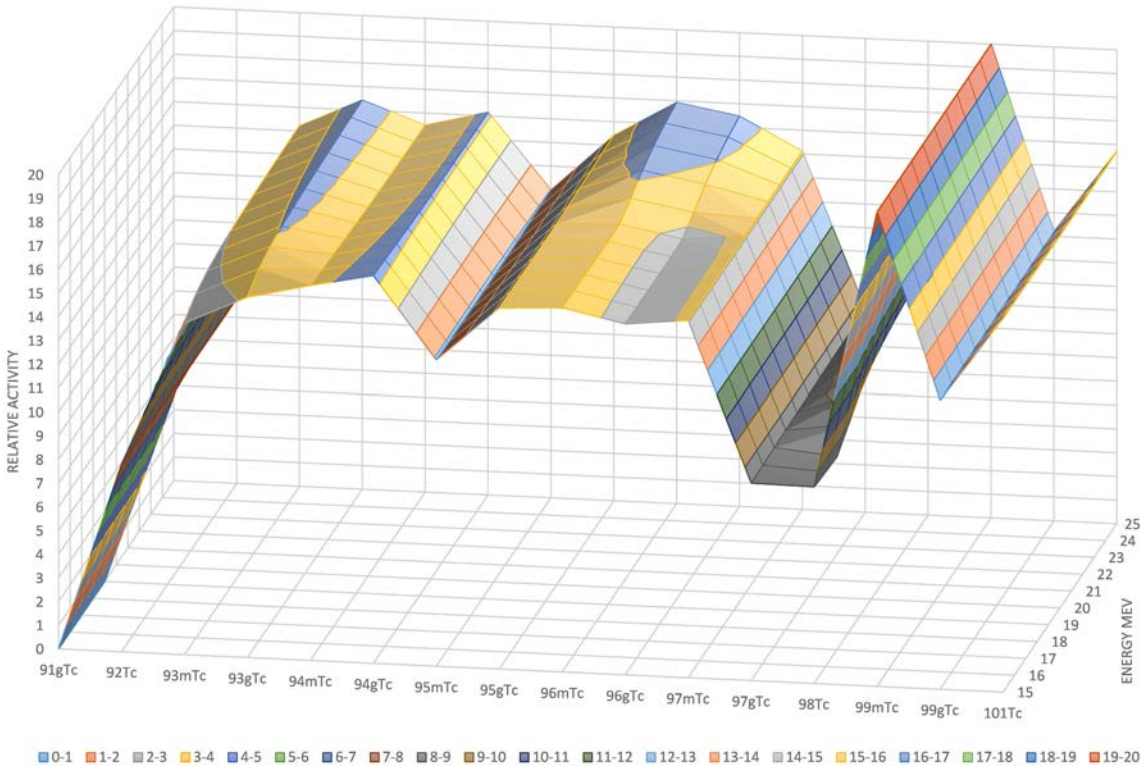

FIG. 14. The relative activity of other co-produced Tc radionuclides compared with ^{99m}Tc as a function of bombarding proton energy.

— Develop the shortest post irradiation processing time.
— As a target material, highly enriched ^{100}Mo is needed for the accelerator production of ^{99m}Tc to reduce the amount of contaminating technetium isotopes in the product.
— A target thickness that corresponds to the proton range from the bombarding energy down to E_p=7.8 MeV, the threshold energy of the ^{100}Mo(p,2n)^{99}Tc reaction, is known to minimize the amount of unwanted activity and minimize the amount of necessary target material. In this regard, an optimization process may be considered, taking into account the unwanted nuclide yield versus the beam penetration depth. Indeed, for beam energies larger than the threshold, but below around 10 MeV, the ^{99m}Tc production quickly drops off, as shown in Fig. 5 and reported in Esposito et al. [16]. The optimal target thickness may therefore depend on the incident proton energy.
— The bombarding energy should not be higher than E_p = 25 MeV since the numbers of contaminating Tc atoms, and other contaminants, increase rapidly with bombarding energy above that level.
— Calculations show that in any circumstances the total amount of contaminating Tc radionuclides in accelerator produced ^{99m}Tc is higher than in the same amount of generator produced ^{99m}Tc based on 24 h elution intervals. The higher contamination level may affect radiolabelling.
— A lower bombarding energy reduces the level of contaminating radioisotopes. A short irradiation with maximal beam intensity results in less radiocontamination of the ^{99m}Tc product.
— The expensive ^{100}Mo target material should be handled in such a manner that it is possible to recover and recycle for future irradiations. A proper recovery method should be developed to eliminate the chemical contaminations (Ru, Nb, Zr). Due to the 6.01 h half-life of the ^{99m}Tc, its fraction in the target decreases after EOB, therefore, relatively quick post irradiation processing is needed. Successive irradiations slowly change the composition of the original target material by changing the amount of initial Mo isotopes and reducing the amount of ^{100}Mo.
— The activity of ^{97}Nb can be significant due to the relatively high yield of the ^{100}Mo(p,α)^{97}Nb reaction. The largest relative change can be expected in the amount of ^{97}Mo isotope due to the decay of ^{97}Nb co-produced in relatively large amounts on the main target isotope ^{100}Mo.
— A change in target composition would slowly affect the isotopic composition, relative activity and relative dose of the final product. Successive irradiations may gradually build up the amount of Ru, Nb and Zr elements in the target up to 100 ppm levels which may require additional chemical treatments to purify the recycled target material unless the applied chemical processes (such as ion chromatography) can remove those potential contaminants.

3. TARGET PREPARATION

Molybdenum targets are generally preferred for high current bombardments owing to their higher thermal conductivity leading to more efficient heat removal. Several approaches to prepare Mo targets have been developed, including the use of foils, pressed/sintered powder, pressed powder with laser beam reinforcement, electrophoretic deposition and a vertical target with unsupported Mo powder. The use of an electroplating method has been attempted by several groups, and, despite successful electroplating with Mo of a maximum thickness of 20 μm [17], the thickness was insufficient for a full beam energy drop over the maximal production energy range and thus this target preparation method is no longer considered viable. Other target materials have also been developed, such as molybdenum oxide and molybdenum carbides (Table 3).

Additionally, the target angle with respect to the incoming beam is important for heat dissipation. The increased speed of the water on the back of the target plate and the decreased beam density when using a slanted target can allow for increased beam currents. Targets placed at 90° to the beam may develop ‘hot spots’ and are thus limited to lower beam currents and may not be suitable for high production targets.

This section also describes thermal modelling simulations carried out on a 30 degree slanted solid target, as well as a novel approach using cryogenic cooling on a target. Full details can be found in the separate country reports and the references contained therein.

TABLE 3. ^{100}Mo TARGET PREPARATION METHODS, DIMENSIONS AND MAXIMUM CURRENTS

Mo target type	Mo target size	Thickness	Mo mass	Max. current
Metallic foil	~	100 μm	1.6 g	500 μA (6 h)
Electrophoretic deposition method	~35–90 mm	50–100 μm	1–1.2 g	450 μA (6 h)
Pressed/sintered powder	6–16 mm ∅ 10 mm × 20 mm	~0.5 mm 0.25 mm	0.3–1.2 g 120	60 μA 60 μA
Mo oxide	10 mm ∅	2 mm	~1 g	n.a.
Mo carbide	10 mm ∅	64 mg/cm^2	50 mg	20 μA

3.1. ELECTROPLATING

The conditions for the electroplating of molybdenum onto a platinum (Pt) support from aqueous solution in a two-electrode electrochemical system (Pt-Pt) were investigated [18]. A thin multicoloured, shiny film was deposited on the platinum surface, covering the Pt and adhering well to it. However, the film was not conductive. It is assumed that the deposited layer consisted of molybdenum oxides at various oxidation states.

Two sets of molten salts were investigated for electroplating molybdenum: $ZnCl_2$-NaCl-KCl-$MoCl_3$ melted at 300°C, and LiCl-NaCl-KCl-$MoCl_3$ melted at 600°C. Molybdenum was fixed on Ni, Cu and Pt as a result of electrodeless deposition (no external current applied) and electroplating with current density in the range of 0.85–8.55 mA/cm^3. Mo or graphite rods were used as anodes. During the electrochemical process, the Mo anode dissolved providing additional molybdenum ions to the melts. The process was conducted in air or in argon flow. The influence of time, current density and addition of potassium fluoride (KF) on molybdenum deposit quality was studied in the CRP.

It was found that the use of $ZnCl_2$-NaCl-KCl-$MoCl_3$ and $ZnCl_2$-NaCl-KCl-$MoCl_3$-KF contributes to the deposition of zinc instead of Mo on the cathode. This was observed for both electrodeless Mo plating and electroplating using Mo or graphite rods as anodes. The thickness of electroplated Mo was definitely higher than that deposited in an electrodeless process (42.07% vs. 0.28 % of Mo normal weight determined by scanning electron microscope (SEM) studies). Applications of the argon flow in the electrochemical process prevent the deposition of MoO_3 (23.76% vs. 3.04% of oxygen normal weight determined by SEM studies. The addition of KF to the melts did not improve the quality of electroplated Mo. Generally, Mo layers obtained by electroplating from molten salts were sponges, and were weakly adhesive to the support, with low thickness; this method was also difficult to carry out.

3.2. MOLYBDENUM METAL FOIL TARGETS

Since enriched ^{100}Mo material is available in the powder form, to minimize the loss of the expensive isotopic material, it is necessary to transform the powder into rollable foil form. Several CRP research groups have reported on their preparation of thin Mo foils.

For example, the research group at the Legnaro National Laboratories' nuclear target laboratory prepared ^{100}Mo enriched foils with 20–25 μm ±2% nominal thickness and an isotopic composition of 0.08% ^{92}Mo, 0.05% ^{94}Mo, 0.1% ^{95}Mo, 0.11% ^{96}Mo, 0.07% ^{97}Mo, 0.54% ^{98}Mo and 99.05% ^{100}Mo using the melting–laminating process described below [19].

In this process, the powder isotopic material is first pelletized using a hydraulic press and then further melted into a droplet in a vacuum of ~10^{-6} mbar with an electron beam provided by an e-beam gun. The total material loss during the melting process was 15–18%. The produced droplet was then placed in a rolling pack between stainless steel sheets and passed through a rolling mill. In order to remove stresses from the rolled foils, they were annealed in a vacuum for 10–15 minutes at a temperature of around 1200°C. This procedure allowed for the production of

thin (10 μm) foils. The annealing process used for thin foils was not significantly helpful in the production of thick ones (400–600 μm).

To produce thick foils in a modified process, relatively big droplets of 6–7 mm diameter were flattened at a high temperature before rolling [19]. As molybdenum, an oxygen resistant metal at ambient temperature, oxidizes easily at temperatures above 600°C, to protect it from oxidation at high temperature, droplets were placed into a stainless steel packet under an argon gas atmosphere. The packet was then heated to a temperature of about 1100°C for 3–5 minutes and droplets were flattened with a hydraulic press; this was done quickly to preserve the high temperature. After cooling, the discs that had been produced were removed from the envelope and rolled down to the required thickness of a few hundred μm. In this experiment, the thinnest foil produced was of about 250 nm thick (thickness measured by an alpha particle energy loss method). Attempts to further reduce the foil thickness were not successful because below 250 nm the material starts sticking to the rolling pack [19].

To improve the purity of the starting material, and thus its malleability, in one approach the pellet was sintered under the above mentioned conditions and in another, the Mo powder was pretreated by heating in a reducing atmosphere (1 h at 1600°C under a H_2 atmosphere) to effectively remove any oxides present; however, in both cases, no improvement of the molybdenum malleability was observed [19].

3.3. PRESSED AND SINTERED MOLYBDENUM POWDER

The design and testing of a ^{100}Mo target using pressing and sintering technology for the TR19 cyclotron was developed during this CRP.

A method was developed to shape and press molybdenum powder and to then put it onto aluminium oxide and sinter it. The molybdenum powder was spread on a steel or tantalum plate, and pressed hydraulically to compress the powder at approximately 500 bar. The pressed powder was then transferred as a sheet onto the aluminium oxide plate for sintering. This process helped maintain targets of consistent quality and prevented the targets from bonding to the aluminium oxide. To prevent the introduction of contamination to the enriched molybdenum, the materials of the template and the bricks used for pressing need to be carefully controlled.

Critical parameters were optimized during the sintering process, including the type of atmosphere used, the temperature of the oven, the substrate on which the molybdenum was sintered and the pressure at which the molybdenum was pressed. The best results were obtained when molybdenum was sintered at 1600°C under a reducing atmosphere (5% H_2 in Ar) for 4 h, with the resulting molybdenum achieving a density of approximately 8.2 gcm^{-3}. Aluminium oxide was the substrate of choice due to its low activation and acceptable thermal properties.

Bonding ^{100}Mo to the substrate was a challenging process, and one that is still under optimization. Starting with natural abundance molybdenum, a method for preparing from powder foil-like pieces of rigid molybdenum of the desired dimensions (i.e. ~20 mm × 80 mm × 100 μm) was developed. Using a proprietary technology, a Mo density of higher than 10 g/cm^3 was obtained. The enriched ^{100}Mo targets showed similar characteristics compared with natural isotopic abundance Mo. Images showing the transition from the low current targets to the high current targets is shown in Fig. 15.

The ^{100}Mo targets were irradiated with typical beam currents of ~250 μA up to a maximum of 500 μA. Photographs of irradiated targets are shown in Fig. 16.

In another method, in order to increase durability, Mo powder was pressed into pellets that were then sintered. The mass of powdered Mo required for the manufacture of a pellet of 14 mm diameter and of about 0.700 mm in thickness was 730 mg. Pellets that were pressed for 60–90 minutes in a hydraulic press with a pressure of 800 MPa inside the matrix did not adhere to the stainless steel plates of the matrix and conducted electricity very well. Pellets pressed for a longer time were more mechanically resistant, however, even at the longest pressing time used in the study, a satisfactory mechanical stability was not achieved. This was due to the low density of pressed pellets of only 6.4 g/cm^3 (vs. of 10.26 g/cm^3 of the bulk density).

In order to improve the mechanical strength, the pressed Mo pellets were sintered in a hydrogen atmosphere at a temperature of 1600°C. As result of this process, the dimensions of the Mo pellets decreased — in diameter by 13%, thickness by 12%, weight by 1.5% and volume by 34% —while density increased by 50% to a value of 9.5 g/cm^3. These changes are due to the reduction of molybdenum oxide and the removal of oxygen from

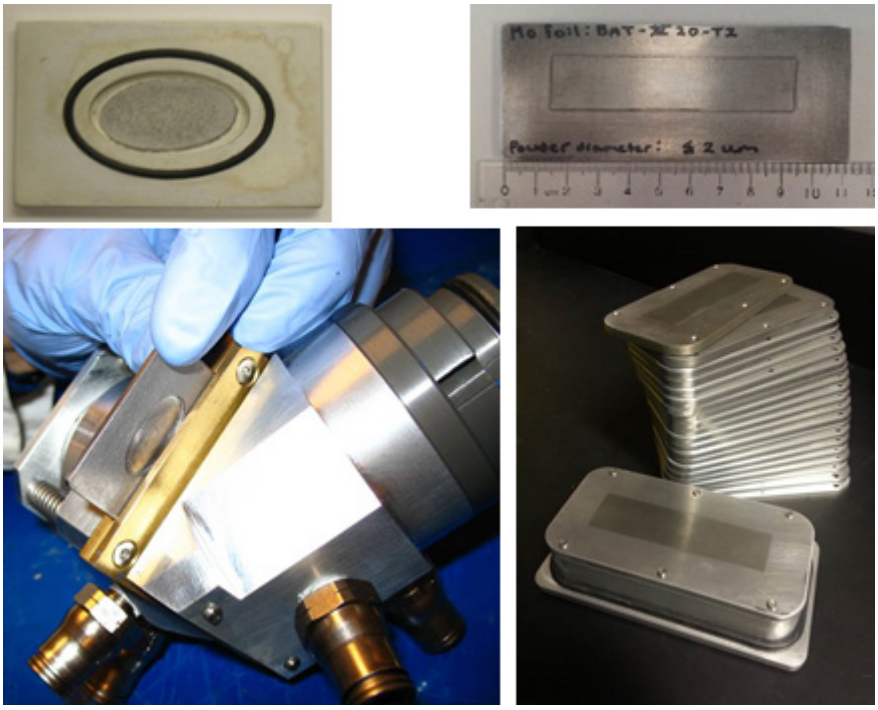

FIG. 15. Images of target transition: small low current targets (left, top and bottom), and initial preliminary foil studies (top right) and high current targets (bottom right).

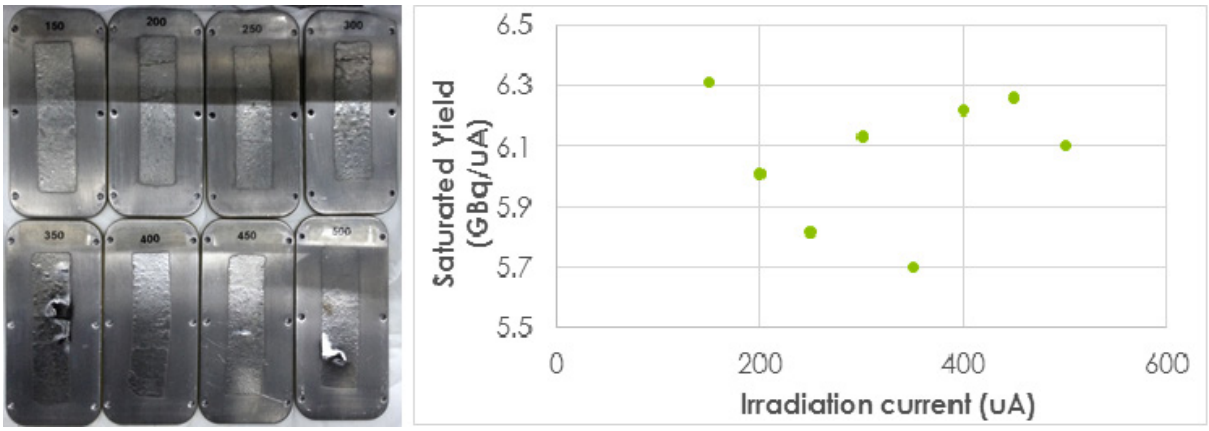

FIG. 16. Photographs of irradiated targets. The beam current (μA) is shown ranging from 150 μA to 500 μA at the top of each target (left). A plot of saturated yield against current is shown for the eight irradiated ^{100}Mo targets (right).

intermetallic space. This observation was confirmed in microscopic cross-sections of pellets before and after sintering (Fig. 17).

The nanohardness measurements revealed the hardness of sintered Mo pellets to be 5.02 GPa; this was similar across the pellet and significantly exceeded the value for similar sintered samples described in the literature [20]. After proton irradiation (6 μA, 16.5 MeV) the ^{100}Mo pellets remained unchanged and neither visible discolouration nor distortion were observed.

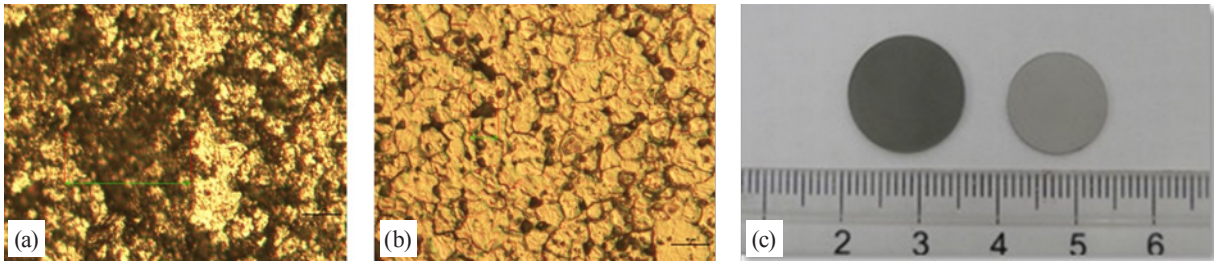

FIG. 17. Cross-sectional microscopy images of Mo pellets (a) before and (b) after sintering and (c) photograph of Mo pellets before (left) and after (right) sintering.

3.4. VACUUM SPUTTERED MOLYBDENUM

Vacuum sputtering of Mo on aluminium by cathodic arc was performed at an initial pressure of 7.5×10^{-7} mbar, as a multiple sputtering, alternating with intervals to enable cooling of the system. As a result of 6 min sputtering repeated every 15 min for 25 times, a 132.35 μm thick Mo layer was deposited on the Al. A cross-section investigation of the deposited layer by both an optical and a scanning microscope showed that the layer was of good quality, with high density, uniformity and tight coverage of the support. The described method is fast and simple; however, it caused a significant loss of the expensive enriched material during the preparation of target material.

3.5. ELECTROPHORETIC DEPOSITED AND SINTERED MOLYBDENUM

Electrophoretic deposition has also proved to be an efficient, reliable and fast method for coating quantities of 600–1200 mg of Mo powder onto tantalum backings. Losses of enriched isotope in the plating bath were negligible, typically of the order of a few mg, which could be recovered after evaporating the solvent. The deposits were uniform and adhered to the backing. However, the coatings were not sufficiently dense for immediate irradiation with proton beams. The sintering process for Mo follows standard industrial practices. The plates obtained from the electrophoretic deposition process were placed in alumina boats and sintered in a tube furnace under an ultra high pressure argon atmosphere. Optimum results were obtained by applying the following heating and cooling protocol: The temperature in the furnace was increased at a rate of 5°C/min between room temperature and 1300°C, then at 2°C/min between 1300 and 1700°C. The furnace temperature was maintained at 1700°C for 5 h and then allowed to cool to 1300°C at 5°C/min. The furnace was flushed with argon at 3 L/min throughout the entire cycle. A full sintering process took about 1 day [20].

The close control of process parameters was necessary to ensure reproducible results. The target plates that were manufactured according to this protocol were extremely robust. The Mo layer was scratch resistant and firmly bonded to the tantalum backing. A sinter density of approximately 70% of the bulk material could be achieved. The sintered layer retained sufficient porosity to facilitate the dissolution of the Mo after irradiation, which considerably reduced the time required for the separation and purification of the ^{99m}Tc. A target thus produced could be completely dissolved in hydrogen peroxide in less than 10 min. It was discovered that sintering in this temperature range also significantly increased both the tensile strength and hardness of the tantalum backing. Hence, the thickness of the backing plate could be further reduced, which consequently improved the heat transfer from the target to the cooling water during irradiation. Targets were irradiated on a PETtrace cyclotron with 16.5 MeV protons and beam currents of up to 130 μA (power density 1.1 kW/cm^3). Visual inspection after irradiation proved that all targets were perfectly intact [8].

For sintered targets, high mechanical strength and high thermal conductivity are desirable for effective evacuation of the heat produced during irradiation and for chemical inactivity. In terms of durability and chemical inactivity, niobium and titanium are suitable. The thermal conductivity of niobium is twice as good as that of titanium [21].

3.6. PRESSED POWDER AND LASER BEAM REINFORCED MOLYBDENUM

In this method, fine Mo powder is first compressed and then heated at a high temperature. In this process, the edges of powder grains melt and join and a quasi-solid structure is created. However, a tablet produced without additional processing does not have enough durability and may disintegrate in the target set-up area or during the removal from the target system after the irradiation [21].

In one of the CRP participating laboratories [21], a tablet surface burning method was developed with the aim of increasing mechanical durability. A solid state focused laser beam with the following specifications was used:

— Impulse energy: 250 MJ;
— Wavelength: 1.6 μm;
— Impulse repetition frequency: 40 Hz;
— Impulse duration: 200 μsec.

For this experiment, a special laser apparatus was developed in which the laser beam is focused on a Mo tablet by a lens with a focal distance of $F = 150$ mm after passing through a beam expander. The diameter of the light spot in the focused area varied within the range of 150–300 μm. The Mo powder in the path of the laser was melted, creating a solid strip of Mo of a few hundred μm width. Figure 18 shows a Mo tablet after orthogonal processing with the above mentioned laser beam [21].

During the laser processing of a Mo tablet the temperature at the surface will reach more than 2700°C for a very short time. Under these conditions, Mo could be oxidized to MoO_3 (Mo starts to be oxidized in air at $T > 600$°C). To check the potential oxidation, a special airtight box filled with inert neon gas was added to the laser processing system. Three identical tablets were prepared; one was simply pressed without any laser processing, the second was laser processed in an air atmosphere and the third tablet was processed using the same laser procedure in a neon atmosphere. In addition, a pure MoO_3 powder sample was used as a calibration point. All four samples were investigated under X ray phase analysis. The results showed that Mo did not transform into MoO_3 during laser processing, neither in the air nor in the neon atmosphere. The reason for this could be the very short presence and interaction timing of the high temperature, which is not enough for the slow chemical oxidizing process [21].

The results of this experiment showed that the mechanical strength of the tablet's surface increased by more than 1.5 times after laser treatment. The technique developed for the laser treatment of the compressed Mo tablet surface was used to make solid targets for irradiation by a cyclotron proton beam. Figure 19 shows a target disk with laser pressed Mo treatment. To increase the surface strength of the Mo pressed in the centre of the target disk, its surface was treated with similar parameters.

However, the Mo powder pressed into the target disk may fall out during transportation to the hot cell after irradiation due to insufficient adhesion to the disk. Therefore, to provide sufficient adhesion, additional treatment with a laser beam was performed at four diametrically opposite points, as shown in Fig. 20.

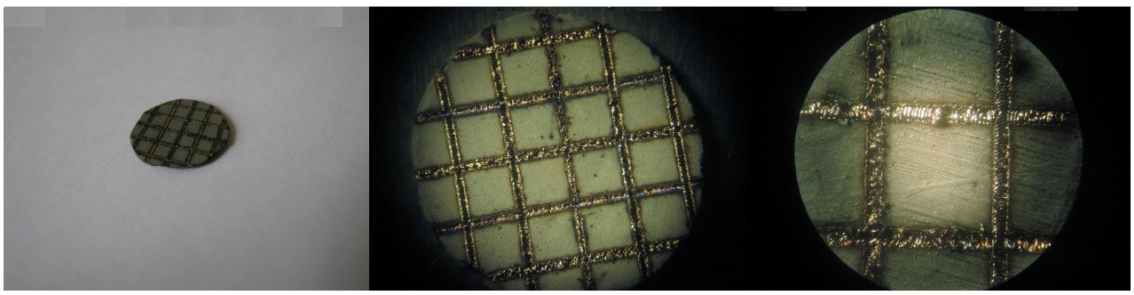

FIG. 18. Mo tablet processed by a laser beam at different magnifications: (a) general view; (b) 20 × magnification under optical microscope; (c) 42 × magnification [21].

FIG. 19. The target disk with laser pressed Mo treatment (left), with 40× magnification (right) [21].

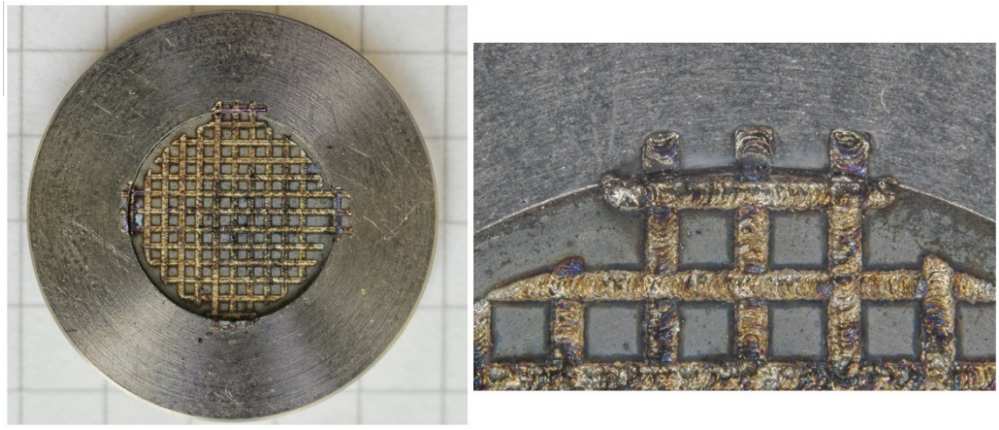

FIG. 20. The target disc with Mo after the additional strengthened adhesion at four points (left) and at 30× magnification (right) [21].

3.7. NON-COMPACTED POWDER MOLYBDENUM: VERTICAL TARGET

An alternative method using ^{100}Mo powder as purchased by employing a vertical irradiation technique was also developed. Figure 21 shows a target vessel that was developed based on a previous study [22] for a vertical irradiation method that can properly hold almost any form of target material, including powders or low-melting-point materials, on the beam trajectory. The target vessel was made of a ceramic, silicon carbide (SiC), which has favourable properties, i.e., it practically never melts, has fair thermal conductivity and excellent chemical resistance. In this study, 500 mg of ^{100}Mo powder was prepared in the SiC target vessel and sealed with a 25 μm Nb foil. The target was placed at the beam port to be irradiated.

The SiC vessel has two connectors through which the solution, pressure gas and exhaust can pass freely, thus the target ^{100}Mo was dissolved in situ, and the dissolved ^{100}Mo solution was transferred to the hot cell by means of gas pressure without using any robotic devices.

3.8. MOLYBDENUM OXIDE IN-TARGET PRECIPITATION

A low cost and easy to operate system for molybdenum oxide exists that may also be complementary to other methods for initial trials. In this CRP, an automated production system was developed for remote target preparation and recovery (Fig. 22) as well as separation and purification of ^{99m}Tc. In this method, an oxide target that can be readily dissolved in appropriate solvents was developed.

The vessel has a stair-like structure upon which remotely introduced $^{100}MoO_3$ solution precipitates during heating under a high flow of N_2.

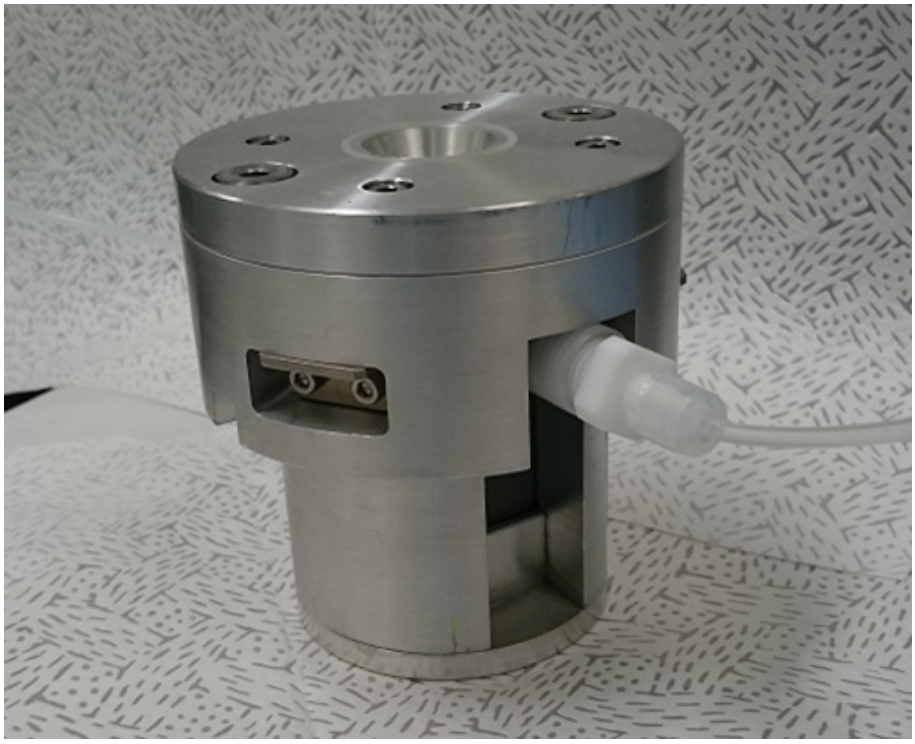

FIG. 21. Developed target vessel made of SiC and its holder for a vertical irradiation system.

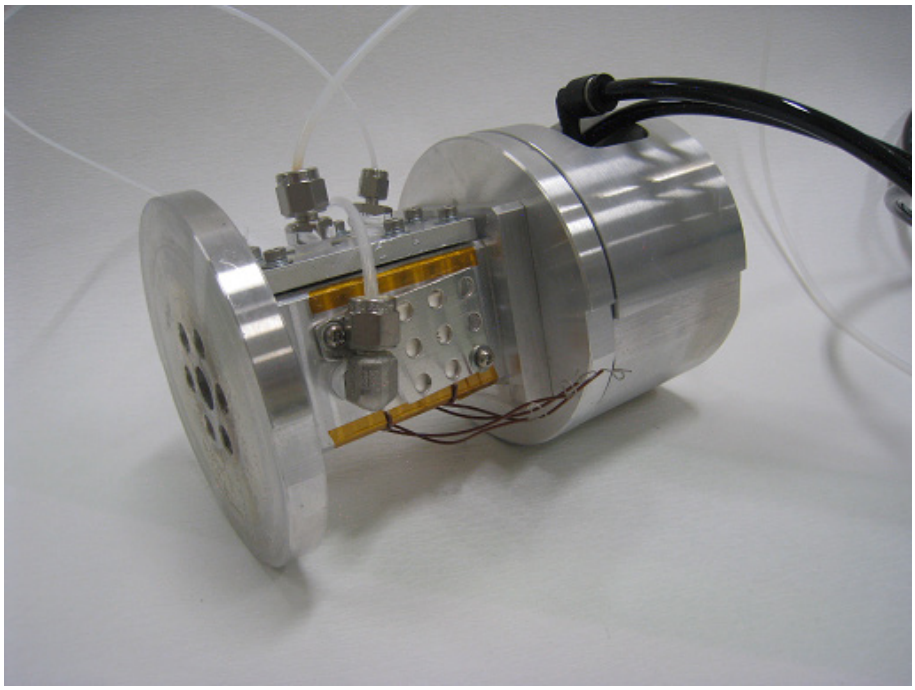

FIG. 22. Developed target vessel for $^{100}MoO_3$.

The target material $^{100}MoO_4^{2-}$/ H_2O_2 solution was loaded into a target vessel at a speed of 300 μL/min by means of a syringe pump. On the way to the target vessel, the loaded solution was mixed with a relatively large amount of N_2 (+1 L/min) in ordinal polyetheretherketone tubing (0.75 mm diameter). Consequently, the ^{100}Mo solution splashed into the target vessel through a painting air brush. The spread mist of ^{100}Mo solution was immediately dried and precipitated onto an appropriate area inside the target vessel, which was heated to 130–150°C by an

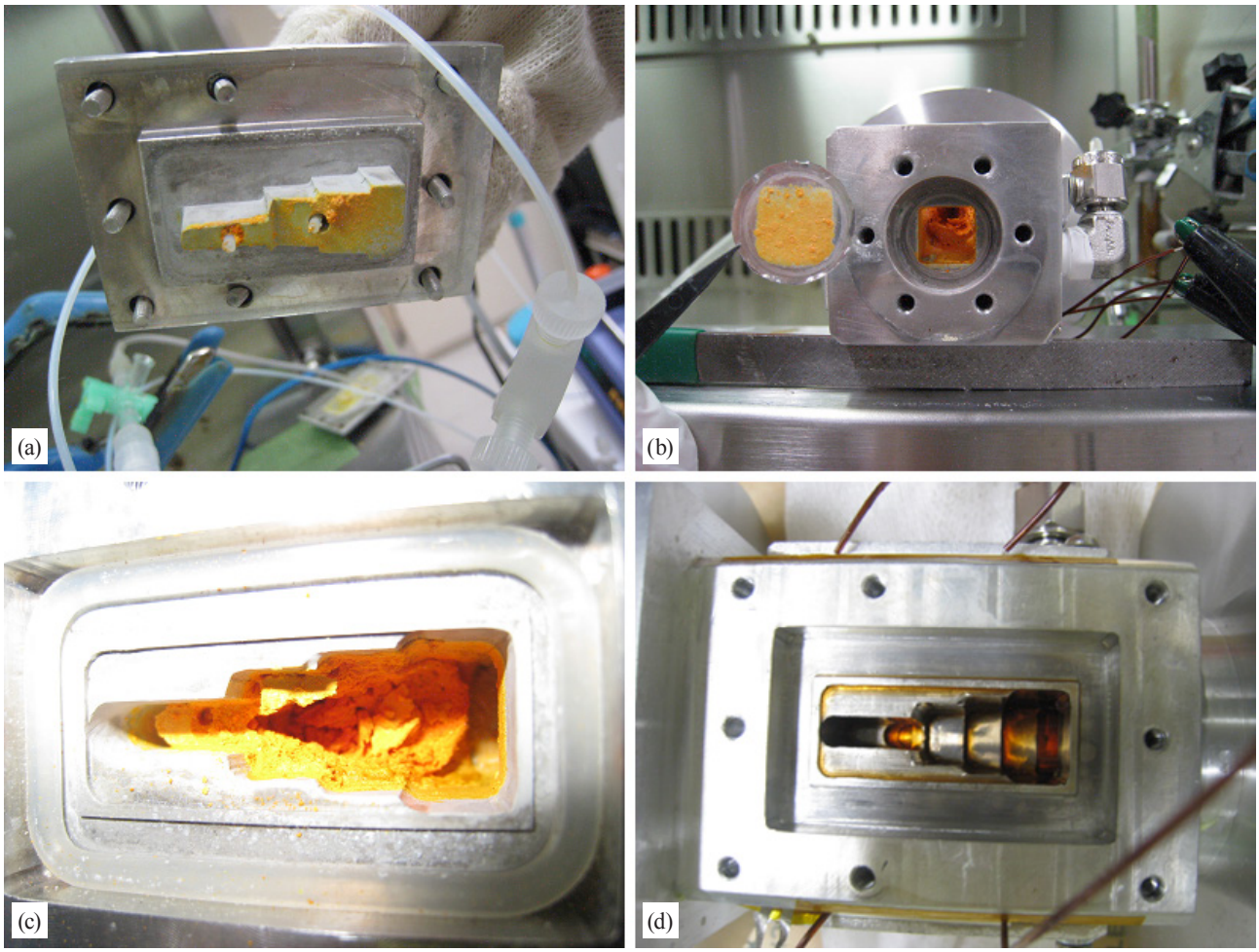

FIG. 23. Prepared target and post-processed vessel: (a) top cover; (b) front foil (Nb, 25 µm) as beam entrance; (c) stair-like body (beam enters from right side); (d) after target solution discharged.

electric heater; this left a 3–5 mm thick ^{100}Mo oxide layer on a stair-style vessel (Fig. 23 (a)). In this study, 1500 mg of ^{100}Mo (as elemental weight) in 10 mL of H_2O_2 was prepared in 1.5 h.[1]

3.9. MOLYBDENUM CARBIDE

Molybdenum carbide was also investigated as a target material. This compound was synthesized via an ammonium heptamolybdate (HMT) complex and then heated under an argon atmosphere at elevated temperatures [23]. Targets were pressed and sintered under vacuum prior to irradiation. While not suitable for very high currents, targets prepared using this material are easily amenable to thermochromatography and can be recycled from the resulting Mo oxide. The chemistry developed for the Mo carbide targets is also suitable for synthesis of tungsten carbide targets for the cyclotron production of ^{186}Re [24].

3.10. THERMAL MODELLING

Although increasing the beam current may improve the radionuclide production yields, the thermal performance of target materials often dictates the maximum beam current on the target. This limitation is

[1] The detailed process has been described in Evaluation of the ^{99m}Tc Remote Production by Proton Bombardment on ^{100}Mo Target on the accompanying CD-ROM (Nagatsu et al.).

commonly observed for solid targets as these materials often demonstrate low melting points and poor thermal conductivities. In relation to this topic, a participant in the CRP research group focused on improving the power handling capability of ^{100}Mo solid targets through the choice of the target substrate, the shape and location of the cooling channels on the back of the substrate and the optimization of the water flow rate. The use of finite element analysis to model both heat transfer and turbulent flow, followed by experimental validation, was investigated.

To validate the model, a target plate with simplistic geometry equipped with a thermocouple to perform real time measurements during irradiation was used (Fig. 24). Target plates made of copper and zirconium were tested because of their significantly different thermal properties (copper with a thermal conductivity, k, of 401 $W \cdot m^{-1} \cdot K^{-1}$ (at 300 K) is an excellent thermal conductor, while zirconium with a value of k equal to 22.6 $W \cdot m^{-1} \cdot K^{-1}$ (at 300 K) is a relatively poor thermal conductor). Irradiations were performed with cyclotron proton beam currents of up to 80 μA (17.5 MeV) for the copper plate and 50 μA (15.5 MeV) for zirconium.

For modelling the 3-D heat transfer and turbulent flow of the cooling water, the COMSOL Multiphysics (v.3.5a.) software for steady state general heat transfer and for k-epsilon turbulence models were used, respectively. A sample proton beam profile was obtained experimentally using radiochromic film and the cooling water temperature, cooling water flow rate and target plate/cooling water channel geometry were used as experimental input parameters to the model. The temperature dependent material properties (thermal conductivity, density, heat capacity, etc.) were defined using COMSOL's built-in material library [25].

The experimental measurements performed in this study allowed the selection of a convective heat transfer model that is capable of accurately predicting the target plate temperature for plates made of materials with widely varying thermal properties.

3.11. CRYOGENIC COOLING

Typical solid target technology provides target cooling by a helium flow on the front side and water stream on the back side during irradiation. Such an arrangement provides around 500 W thermal power dissipation. Thus, for a beam energy E_p = 18 MeV, the maximum intensity would be $I_p \sim 30$ μA. Nevertheless, several cyclotrons

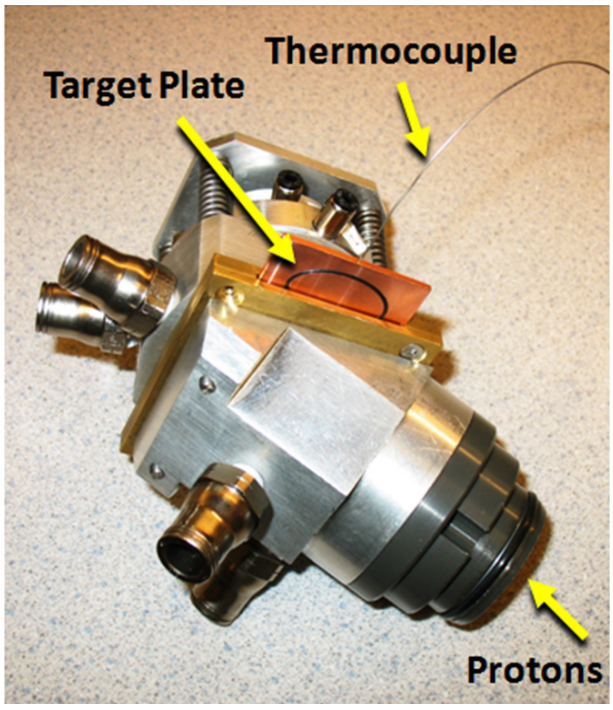

FIG. 24. Target system used to measure thermal characteristics of a cyclotron solid target.

could provide up to 100 μA. One of the ways to increase the cooling efficiency is to decrease the temperature of the cooling element dramatically — e.g. down to the temperature of liquid nitrogen.

The thermal stream is the equivalent of the electric current in Ohm's law. The task is to increase the thermal stream for better cooling and there are only two ways of doing this, namely increasing the thermal conductivity, or increasing the temperature difference between the warm and cold parts of the target. Because the development of thermal conductivity is limited due to the consistency of the powder, the only remaining option is to increase the temperature difference between the heated target and the cooling element. Liquid nitrogen was proposed as an alternative to simple water cooling.

This idea has been tested with a layout that was mounted using a solid state continuous wave laser with wavelength of 1.06 μm. As shown in Fig. 25, the laser beam, with a maximum power of 50 W, was directed to the front face of the target, which was prepared from Mo pressed powder. The temperature of the target face was measured by infrared thermometer (pyrometer) that was preliminarily calibrated for correct measurement in the green spectrum of light.

The results of several experiments performed in this study show:

— Without cooling, the face temperature of the target under laser heating rises with time and achieves a plateau with a value of 500°C.
— When liquid nitrogen cooling is applied to a target face, the temperature of the target under laser heating rises with time and achieves a plateau of 320°C (Fig. 26 shows the experimental set-up at this stage in the experiment).
— This simple qualitative test showed that cryogenic cooling could work in general.
— The effective cooling decreases the temperature of the target front by 180°C (from 500°C to 320°C).
— The simulation of heating by means of a laser beam is not exactly equivalent because during irradiation with a proton beam the evolution of heat takes place along the beam direction on the whole length, while under irradiation with a laser beam it happens only on the very thick slice of target. The thermal stream is much longer in the second case and the total thermal resistance is higher. This suggests that during irradiation with a proton beam, the efficiency of cryogenic cooling would be better than in the simulation.

A preliminary estimation shows that for target cooling, 5–7 litres of liquid nitrogen per hour will be needed, which is acceptable and cost effective for extra cooling leading to an increased output of the final product. These investigations can be continued under CO_2 laser beam with a maximum beam power of 500 W.

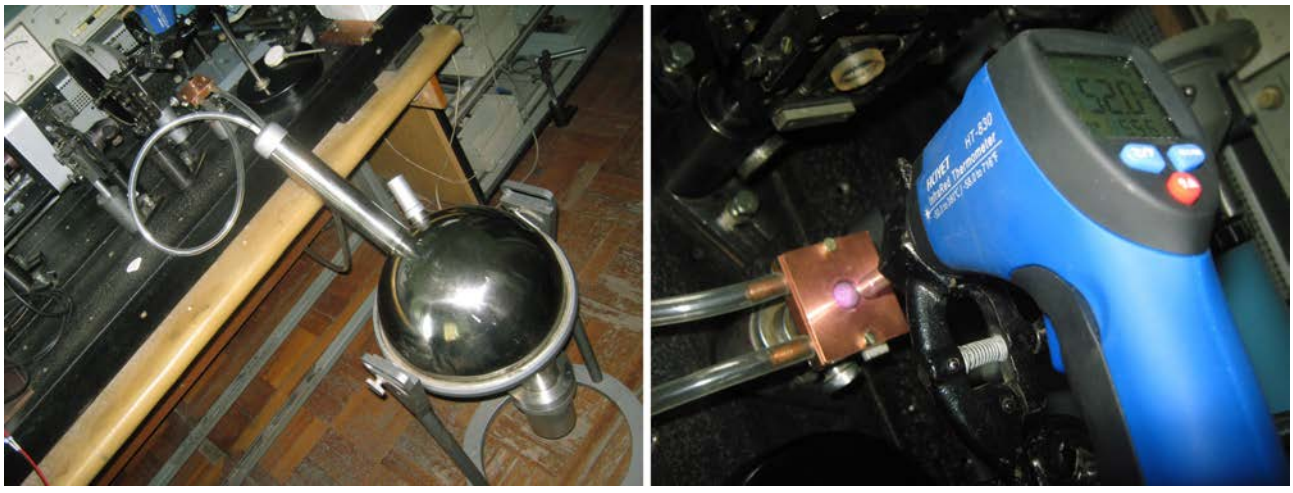

FIG. 25. Laser system for heating simulation and the testing of a cryogenic cooling system. In the right picture, the red spot that can be seen in the centre of the target is infrared radiation from the heated target.

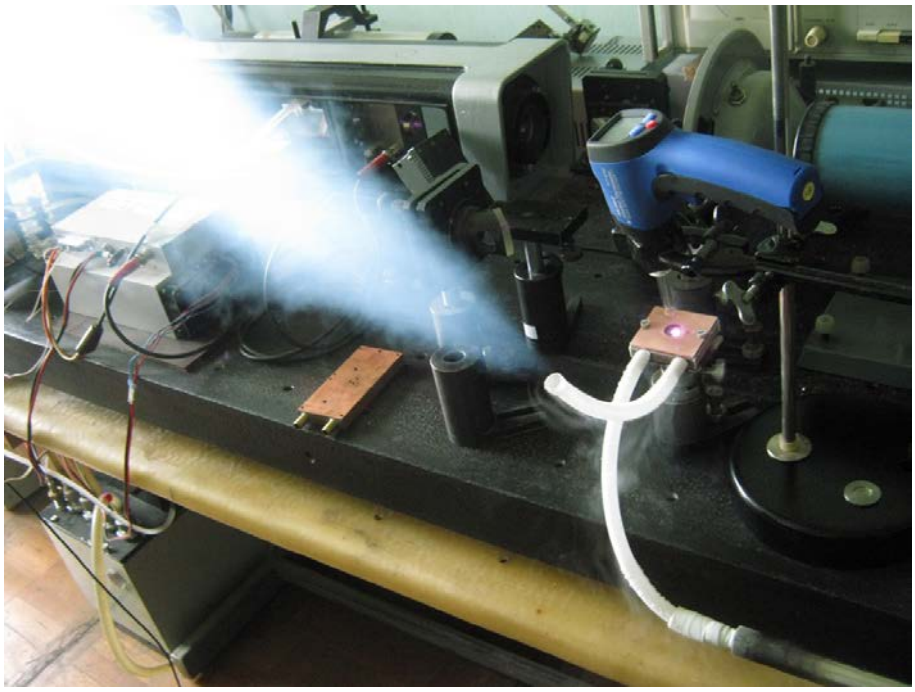

FIG. 26. Laser beam heating and liquid nitrogen cooling test.

4. TARGET DISSOLUTION AND SEPARATION

The efficient and timely dissolution of the $^{99m}Tc/^{100}Mo$ target is the first of the two critical chemistry steps in the separation process; the second step is the isolation and purification of the ^{99m}Tc product. Owing to the significant amount of radioactivity present following irradiation, this dissolution must be performed within a hot cell.

4.1. CHEMICAL DISSOLUTION

In an alkaline medium, the dissolution is performed through following reactions:

$$Mo + 3\ H_2O_2 \rightarrow MoO_3 + 3H_2O$$
$$MoO_3 + 2\ NaOH \rightarrow Na_2MoO_4 + H_2O$$

In the work performed in the CRP, the Mo used for dissolution was in the form of either powder (100 μm) or foil (1 mm thick). Mo powder dissolves in 1M NaOH using a twofold excess of the basic solution and a 25% excess of H_2O_2 at the temperature of 70°C after 30 min. Mo as a foil does not dissolve in these conditions. To achieve complete dissolution within 30 min, it was necessary to use a sevenfold excess of H_2O_2. Mo foils were digested in acid (in different acids and at different concentrations), in a base (NaOH at different concentrations with or without H_2O_2) and finally with only H_2O_2 and heat.

Dissolution testing using a statistical screening design was performed to determine the critical factors in the dissolution process (Table 4). Some of the variables tested included the porosity of the ^{100}Mo target (annealed and unannealed), dissolution temperatures and varying concentrations of the hydrogen peroxide solvent. Both the time needed for the complete dissolution of the target and the amount of leftover hydrogen peroxide were measured. The concentration, volume and temperature of the H_2O_2 were found to be major factors impacting the dissolution time. At present, the dissolution of annealed, bonded and irradiated Mo targets can be achieved in ≤40 minutes. Automation or remote operation of the dissolution process is essential for minimizing radiation exposure to personnel and for ensuring process reliability and reproducibility.

TABLE 4. DISSOLUTION RESULTS

Dissolution approach	Results
HNO_3 at different concentrations	Fast reaction
HCl at different concentrations	Medium
NaOH 6N	No reaction
NaOH 6N with H_2O_2 at different concentrations	Passivation
H_2O_2 30% cold	No reaction
H_2O_2 30% and heating	Fast reaction

4.2. ELECTROCHEMICAL DISSOLUTION

For the electrochemical dissolution of Mo, a galvanostatic method was selected. In order to optimize parameters of Mo dissolution, a two-electrode system was used. Pressed and sintered Mo pellets were used as the anode and platinum gauze served as the cathode. The electrolyte solutions contained 1–5M potassium hydroxide (KOH) with a volume of 13–20 mL. It was observed that the mass of Mo used in the experiments appeared to be the most essential parameter influencing the rate and effectiveness of the dissolution. When using a current of 100 mA, a Mo anode with a mass of 60 mg dissolved completely in 3M KOH after 1 h. In the same conditions, the efficiency of dissolving 702 mg of Mo was only 23 %. Moreover, the effects of current density and electrolyte concentration on Mo electrochemical dissolution were observed. It was found that the rate of electrochemical dissolution is increased by the addition of 30% H_2O_2 and that this effect is greater for more concentrated solutions of KOH. The efficiency of the described process was improved by increasing the temperature of the electrolyte solution from 25 to 50°C. However, a higher temperature could not be applied for the electrochemical dissolution of Mo in mixtures of KOH and 30% H_2O_2 due to the violent chemical reaction and the foaming of the solution, which caused rapid leaps of voltage between the electrodes. The highest yield of 80% was achieved by the electrochemical dissolution of Mo in 5M KOH at a temperature of 50°C, whereas a yield of 72% was reached for a mixture of 5M KOH and 30% H_2O_2 at ambient temperature. Seventy min was required for the complete dissolution of the target material.

4.3. SEPARATION TECHNIQUES

Several techniques are known to separate Tc from Mo. Among the most commonly used techniques are the aqueous biphasic extraction chromatography (ABEC) technique, Chattopadhyay's method with ion exchanger cartridges (Dowex-1 × 8) [26], and the thermochromatography and solvent extraction method with methyl ethyl ketone (MEK).

4.3.1. Solvent extraction

The traditional MEK extraction process offers several advantages. This technique is relatively economical, rapid and lends itself to the development of automation procedures. It provides a high extraction yield of high quality ^{99m}Tc from Mo targets. The high level of efficiency of this extraction technique is due to the affinity of the bi-negative molybdate (MoO_4^{2-}) for the aqueous phase and to the selective affinity of the pertechnetate ($^{99m}TcO_4^-$) for MEK.

The results of preliminary experimental studies show that the solvent extraction technique is one of the most efficient separation methods. It generally involves the following steps:

(1) Digestion of the irradiated target: The irradiated Mo is oxidized in H_2O_2 and then dissolved in KOH, NaOH or ammonium carbonate to ensure that the pH is >7.5. In the next step, liquid MEK is added to that solution. The ^{99m}Tc dissolves in MEK while Mo dissolves in KOH; the result is a mixture of two solutions with very different densities.

(2) Extraction of ^{99m}Tc from the aqueous alkaline solution of Mo into the organic phase (MEK): The final product can be easily purified from organic solvents and molybdate residuals by passage through silica and alumina columns. Finally, $[^{99m}TcO_4]^-$ is collected from the alumina column with saline. The upper organic layer containing the Tc radionuclides is collected with a pipette and passed through a basic alumina column to trap any Mo impurity present in the extracted organic layer. The compound is washed with 5M of NaOH and then sodium sulphate is added and the product filtrated. The product was evaporated to dryness and 0.9% of NaCl was added (to dissolve the pertechnetate) before final purification using an alumina column. The aqueous layer containing the Mo target material is preserved for the recovery of Mo. The final products will comply with pharmacopoeia protocols in terms of radionuclide purity. At this stage in the process, the solution is relatively pure apart from the presence of other Tc isotopes such as ^{97}Tc, ^{96}Tc and ground state Tc, and ^{95}Nb and ^{96}Nb as contamination. Results are improved in automatic productions, with purification on alumina removing all impurities except Tc isotopes.

Several research groups have reported the automation of this process; further details are given in the reports on the accompanying CD-ROM. For example, in one of the laboratories participating in the CRP, Legnaro National Laboratories (Italy), a semi-automatic module using this technique has been developed, which is able to recover about 80% of the initial activity in 35 min. The measured purity values of the final pertechnetate saline solution complied with pharmacopoeia values set for the generator based ^{99m}Tc product. To ensure the optimal operator radioprotection and consistent reproducibility of the process, an extraction prototype system was then completely automated and initiated by remote control assembled using commercially available modular units (Fig. 27).

The components of the module are: a programmable logic controller; a PC with modular lab software; helium and nitrogen lines; three modular units with two- and three-way valves; a heater for reactor housing; a Waters Sep-Pak Cartridge silica column; an acidic alumina column; tubing; fittings; a separation column; vials for reagents, solvents and washing; and two vials for waste and the end product solution. In order to test the efficiency of the system, six Mo metal foils enriched in ^{100}Mo (99.05%) that had been irradiated with a proton beam in a stacked foil configuration were treated with the automatic procedure and the ^{99m}Tc was extracted.

The organic solution containing the ^{99m}Tc pertechnetate, after the separation of the phases, was placed at the top of the vial. The solution was then transferred through silica and alumina columns to the waste vial, leaving the aqueous phase in the bottom of the separation column vial. The $^{99m}TcO_4^-$ adsorbed on the alumina column was

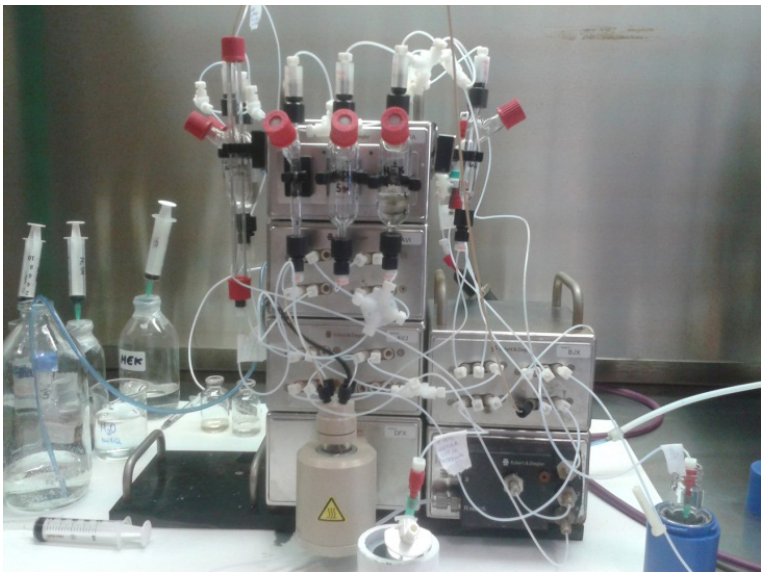

FIG. 27. An automatic and remote controlled ^{99m}Tc solvent extraction module.

eluted with saline and collected in the final vial. In 70 min, the module was able to recover more than 90% of the initial activity. In order to determine isotopic impurity, Mo breakthrough and percentage of organic solution, a detailed quality control analysis of the final pertechnetate solution was performed (Table 5).

TABLE 5. QUALITY CONTROL ANALYSIS OF THE FINAL PERTECHNETATE SOLUTION

Radionuclidic purity	^{xx}Nb in final eluate	Below minimum detectable activity
	^{xx}Mo in final eluate	Below minimum detectable activity
	^{99m}Tc	>99%
	pH	4.5–5
Chemical purity	Mo	<5 ppm
	Al	<5 ppm
	MEK	<0.0004% (v/v)
Radiochemical purity	$^{99m}TcO_4^-$	>99%

Another automated system has been developed by one of the CRP participants for the chemistry of separation and recovery of ^{99m}Tc from Mo using the MEK solvent extraction technique; this system is known as a TCM-AUTOSOLEX (technetium automated solvent extraction) generator and has been widely tested for the separation of ^{99m}Tc from (n,γ) ^{99}Mo (Figs 28 and 29) [27]. In this system, a precise separation of the aqueous phase from the organic phase was achieved through control with an indigenously developed conductivity detector. The evaporation of the organic phase was carried out in a temperature controlled water bath to prevent charring.

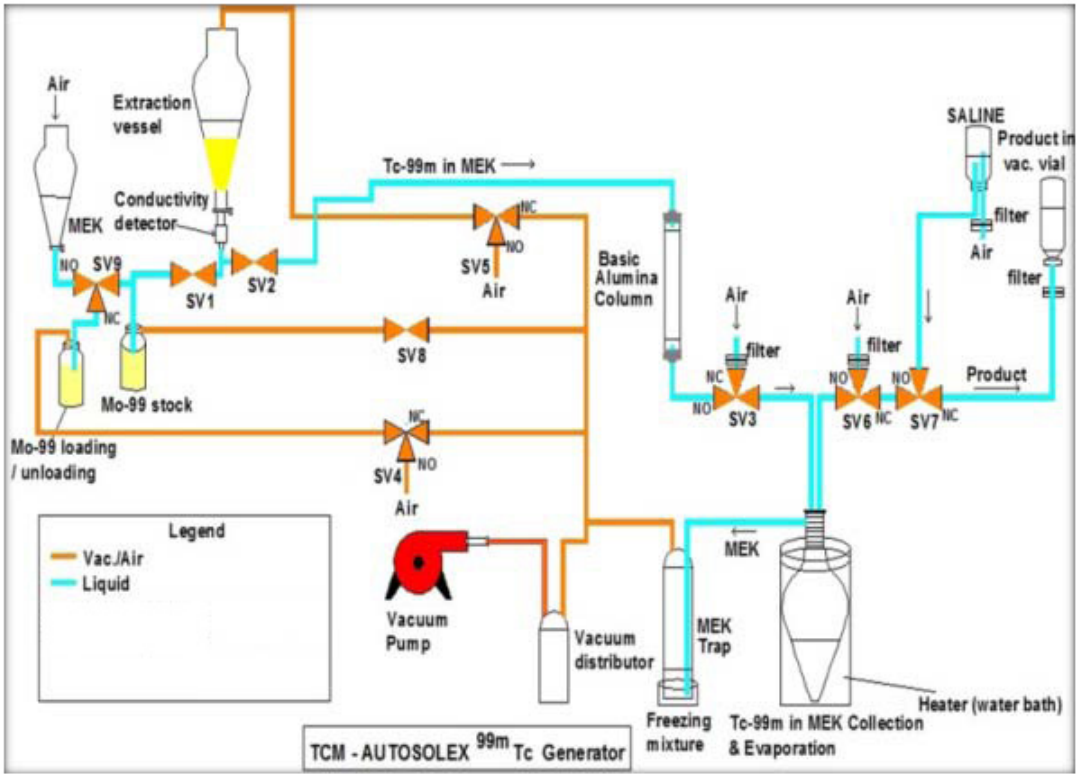

FIG. 28. Process diagram of TCM-Autosolex generator. (NO — normally opened; NC — normally closed.)

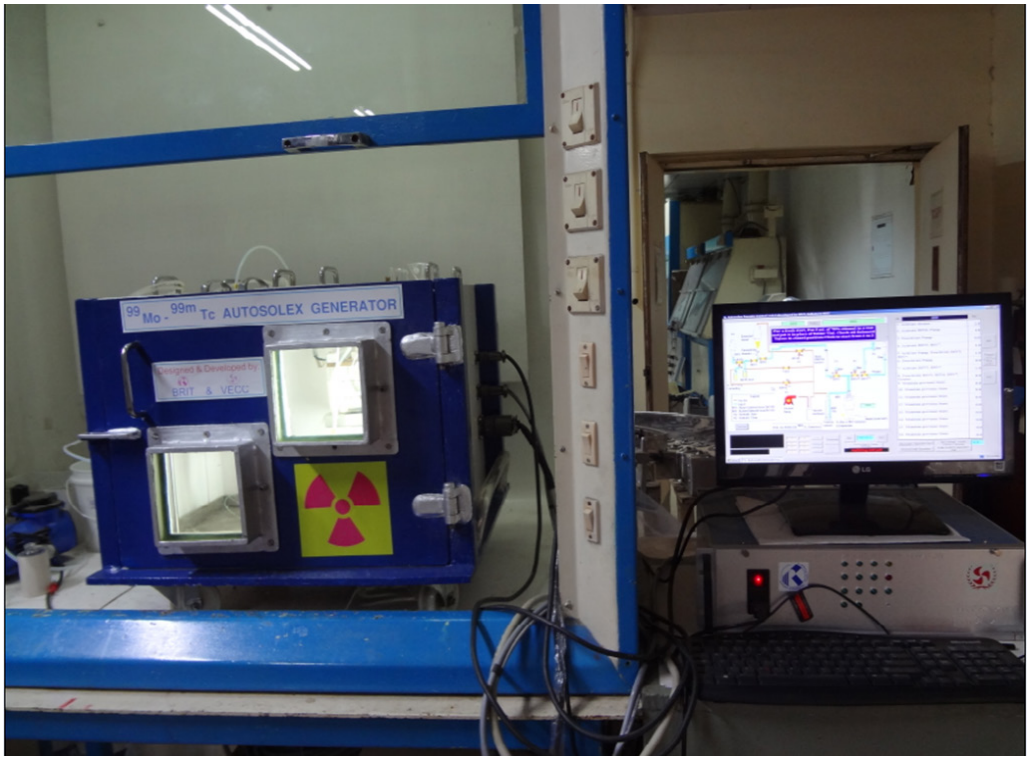

FIG. 29. TCM-AUTOSOLEX separation module.

A similar method for the direct extraction of ^{99m}Tc from the irradiated material using a centrifuge extractor with MEK solvent technology has also been reported. This technology has been successfully used for many years in the Russian Federation [28]. The centrifuge extractor was designed at the A.N. Frumkin Institute of Physical Chemistry and Electrochemistry in Moscow and allows the separation of the two elements to achieve a high purity, followed by the separation of the ^{99m}Tc from MEK by evaporation [29]. The complete automated system, obtained from the Moscow Federal Center of Nuclear Medicine Projects Design and Development, developed by a commercial Russian Federation company, was installed in a hot cell as shown in Fig. 30. It was tested with MoO_3 irradiated under electron beam from LUE20 and showed good results [30]. It will also be used for the extraction of ^{99m}Tc from proton irradiated Mo targets.

4.3.2. Column chromatography

An alternative to solvent extraction is the separation of metal ions by direct contact of the aqueous sample with a sorbent, usually using a column chromatographic technique. Different ion exchange resins were used, including Dowex-1, a polyethylene glycol (PEG) coated C-18 SPE cartridge, TEVA resin, OASIS HLB Plus-PEG-2000 and AnaLigRTc-02 resins.

Several commercial reversed phase resins have been evaluated for their potential of separating pertechnetate from molybdate. Pertechnetate adsorbed strongly on the RP-SPE cartridge Chromabond HR-P (Macherey-Nagel); however, none of the solvents used (H_2O, MeCN, DCM and DMSO) were successful in desorbing the pertechnetate. In addition, 0.4% of the ^{99}Mo was adsorbed on the HR-P cartridge. Oasis HLB (Waters) was successful in retaining pertechnetate but acetonitrile was needed for desorption. It was, however, encouraging that no [^{99}Mo]molybdate breakthrough to the Tc fraction was observed. The resins Waters tC18 plus and Phenomenex Strata C18-U did not successfully retain pertechnetate.

As part of the work in the CRP, the synthesis of PS-DVB-PEG resin was also carried out. In short, a 500 mL, three-necked round-bottom flask with magnetic stirrer and condenser was capped with a drying tube. It was put into an oil bath on a heat/stir plate and was equipped with a thermometer. Chloromethylated polystyrene 1% divinylbenzene copolymer beads (3.0–3.5 g) were pre-swelled in diethylene glycol dimethyl ether (anhydrous, 99.5%, 40 mL) or tetrahydrofuran (THF) (anhydrous, with inhibitor, ≥99.9%, 60 mL) by stirring for

FIG. 30. Main part of the centrifuge extractor system.

15 min at room temperature. Polyethyleneglycol methyl ether (average molecular weight 2000 or 5000, 20–25 g) was added to the system, and NaH (600 mg) was slowly added over 30 min. The oil bath was then heated to 70°C (gentle reflux for THF) for 17 h. The NaH was quenched with isopropanol (IPA, ≥99.5%) until no reaction could be observed. The resin was then washed once with IPA and twice with deionized water and filtered using a Buchner funnel. The total synthesis time was 20 h, and the yield of the synthesis was over 2.5 g PS-DVB-PEG resin per g of polystyrene starting material. Elemental analysis indicated a carbon content of 69–76%. Recovery of ^{99m}Tc was 82 ± 9 % (n = 5). The PEG resins produced in-house showed similar adsorption characteristics to ABEC resin from Eichrom Technologies; however, elution profiles of the pertechnetate were more variable between batches of the in-house synthesized resin. These interesting differences could not be attributed to synthesis or resin analysis (elemental analysis). To determine the adsorption due to PEG grafted on the beads, PS-DVB-Cl and PS-DVB-OH were included in the study. As expected, pertechnetate did not adsorb on the resins. The PEG resins all exhibited very low ^{99}Mo retention and thus low breakthrough to the Tc fraction. The highest breakthrough observed was 0.08% for the PS-DVB-PEG resin.

PEG coated C-18 cartridges were also examined. In the aqueous biphasic extraction chromatography method, a C-18 (OASIS HB) column coated with PEG as extractant was used. C-18 cartridges containing 3 g of resin were coated by pouring PEG3000 solution through the cartridge and then washing with deionized water. The PEG concentration in the final product was evaluated by iodine visualization in thin layer chromatography (TLC). The PEG3000 concentration in the final product was below the limit of detection for the TLC spot test (0.1 mg/mL), the pH was 6 and the product was clear and colourless. The mixture of ammonium molybdate and about 2 MBq of ^{99}Mo in 10 mL of 3M ammonium carbonate solution was loaded on the column. ^{99m}Tc was eluted with around 50 mL of water. The effect of the molecular mass of PEG being in a range of 2000–6000 on the ^{99m}Tc elution yield and content of polyethylene glycol in the ^{99m}Tc fraction was studied. Using the C-18 column modified in-house with polyethylene glycol, ^{99m}Tc was allowed to separate from excess Mo with a yield of over 80%. The highest elution yield of ^{99m}Tc (>80%) was obtained for polyethylene glycol with low molecular weight (PEG-2000 and PEG-3000). With increasing PEG molecular weight, elution yields of ^{99m}Tc drop to around 70% for PEG-6000. The PEG contamination in ^{99m}Tc solution was lower than 0.005% and significantly decreased with increasing PEG molecular weight. The contamination of ^{99m}Tc with ^{99}Mo was lower than 0.01% for all experiments. More than

99.5% of the ^{99}Mo was present in the load with wash fractions (n = 2), thus allowing for minimal losses in terms of recycling enriched ^{100}Mo [31].

Tentagel N-OH (Rapp Polymere) was also identified, tested and found to give high yields (i.e. >98%). As with the other resins tested, Tentagel N-OH was not originally designed for the separation of ^{99m}Tc (rather, it is used for peptide synthesis), but its properties were such that results were observed using this resin that were superior to those that had been observed with ABEC. As product quality is imperative, and in accordance with guidelines from Health Canada, the International Conference on Harmonisation of Technical Requirements for Pharmaceuticals for Human Use, the European Medicines Agency and the United States Food and Drug Administration, a process development approach was used. To date, an 8-factor, 16-run D-optimal design using the Tentagel N-OH resin has been implemented to assess critical process parameters in the production of ^{99m}Tc. Factors assessed include load molarity, load temperature, load time, resin mass, SPE column diameter, wash molarity, elution temperature and elution speed. Further optimization studies are under way. Investigators are focused on moving forward with the Tentagel N-OH resin for commercial-scale production of cyclotron based ^{99m}Tc.

Process automation is imperative for minimizing radiation exposure to personnel, and for the purpose of ensuring process reliability and reproducibility. Furthermore, automation also allows for digital process trending of system parameters (e.g. pressure, flow rate), thus facilitating optimization and troubleshooting. With regards to the automation of the chemistry for extracting ^{99m}Tc from the irradiated and dissolved ^{100}Mo target material, numerous separation units have been evaluated. As none of the commercial units are traditionally used for ^{99m}Tc extraction, there was a need for reprogramming and reconfiguring the chemistry unit to suit the processing scheme. With a strong focus on commercial level production, a cassette based automated system has therefore been employed by the studies carried out in the framework of the CRP since the beginning of the study for ease of scale-up and regulatory approval. An initial cyclotron test using the optimized dissolution and separation conditions together with complete automation yielded 106 GBq (decay corrected to EOB) of [^{99m}Tc]TcO_4^-.

Separation can be successfully implemented with Dowex-1 resin. In order to separate ^{99m}Tc from ^{99}Mo using Dowex-1 × 8, a solution of Na_2MoO_4 containing 10 MBq of ^{99m}Tc was introduced onto the column and molybdate anions were retained. ^{99m}Tc was eluted with 5 mL of tetrabutylammonium bromide solution in CH_2Cl_2. Variable volumes of resin and variable flow rates were used for the best recovery of ^{99m}Tc. In four experimental runs, the ^{99m}Tc yield was 77.5%, 78.6%, 78.5% and 79.1%, respectively. Almost total retention of ^{99m}Tc was achieved with a flow rate of 0.6 mL/min. Increasing the flow rate to 2 mL/min during column loading and elution resulted in a more than 10% decrease in the elution yield. The elution was fastest at the beginning and more than 90% of ^{99m}Tc was eluted in the first 5 mL of tetrabutylammonium bromide solution. Maximum ^{99m}Tc yield was obtained after about 10 min of tetrabutylammonium bromide solution contact with Dowex resin (Fig. 31).

Another approach was proposed in this CRP using HNO_3. A resin column immobilized the pertechnetate and allowed the molybdate to flow. The Mo line and the resin column were washed with 1 mL of water and the water was also collected in the Mo collection vial after washing. The resin column was then washed with 5 mL of water and the water was collected in the waste collection vial. 4 mL of 4M HNO_3 was passed through the resin column to elute ^{99m}Tc into the evaporation vial. The HNO_3 line and the resin column were washed with 1 mL water and the water was collected in an evaporation vial. The evaporation vial was then heated while a flow of air was passed through the HNO_3 acid line. HNO_3 was thus evaporated out completely and the evaporated HNO_3 was trapped in a NaOH bath. The evaporation vial was then cooled and the requisite volume (10 mL) of saline was added. Sodium pertechnetate in saline thus obtained was passed through a small acidic alumina column (1.5 g), a Millipore filter (0.22 μm) and then collected in a vacuum vial. The chemistry of separation and purification of ^{99m}Tc based on the Dowex-1 resin and HNO_3 method has been automated and named TCM-AUTODOWNA (Fig. 32 and Fig. 33). It utilizes available ^{99}Mo produced by the (n,γ) reaction at the Bhabha Atomic Research Centre, India, and is also compatible with cyclotron produced ^{99m}Tc using enriched ^{100}Mo. In the new Dowex-1 resin and HNO_3 method, pertechnetate was bound efficiently (95%) and eluted from the resin with a very high yield (90%). ^{99}Mo along with the non-radioactive Mo target material ended up in the waste stream. The overall yield of ^{99m}Tc in this separation method was found to be about 80%.

Another type of resin is TEVA, which was also applied in some systems used in the work carried out in this CRP to separate ^{99m}Tc from Mo. The resulting solution is evaporated to dryness and then the residue containing ^{100}Mo, ^{nat}Cu, ^{99m}Tc and ^{65}Zn is re-dissolved in nitric acid (0.1N). This solution was loaded on the preconditioned TEVA cartridge. All the ^{99m}Tc and a trace of enriched Mo were retained by the TEVA cartridge after rinsing with nitric acid (1N). The solution containing ^{100}Mo, ^{nat}Cu and ^{65}Zn was stored to recover high costly enriched Mo.

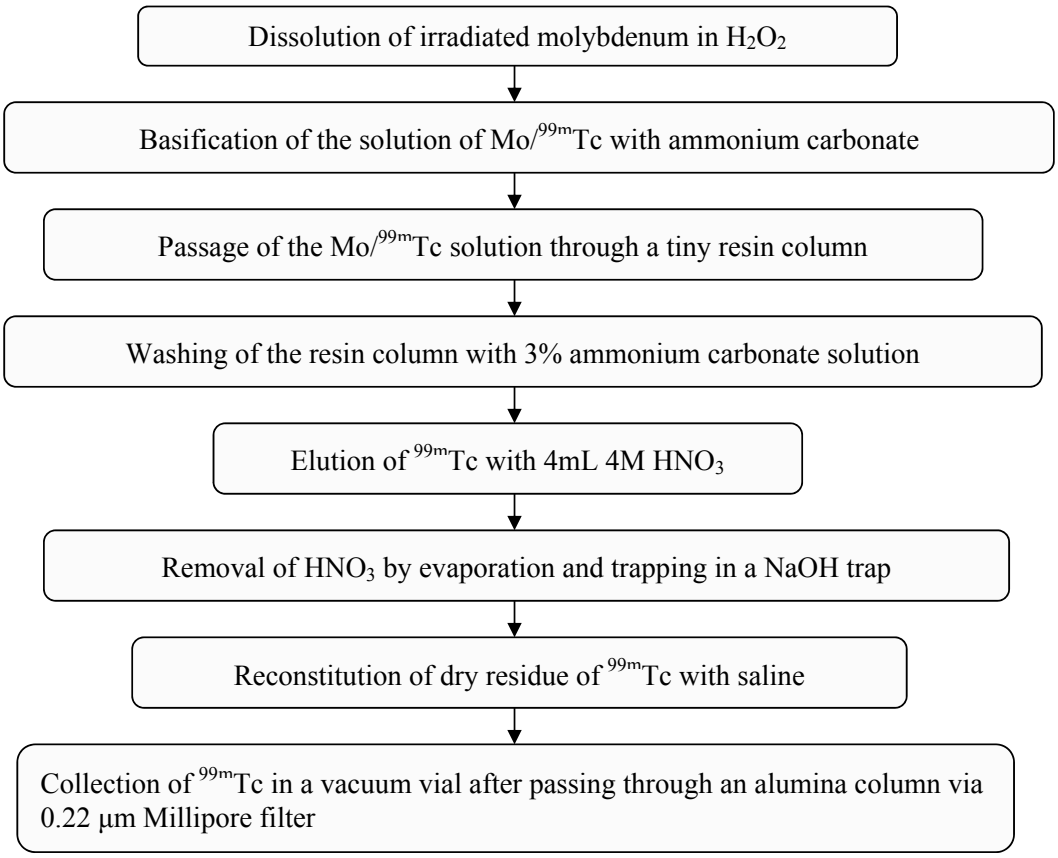

FIG. 31. Separation and purification of ^{99m}Tc from the irradiated Mo target using Dowex-1 column.

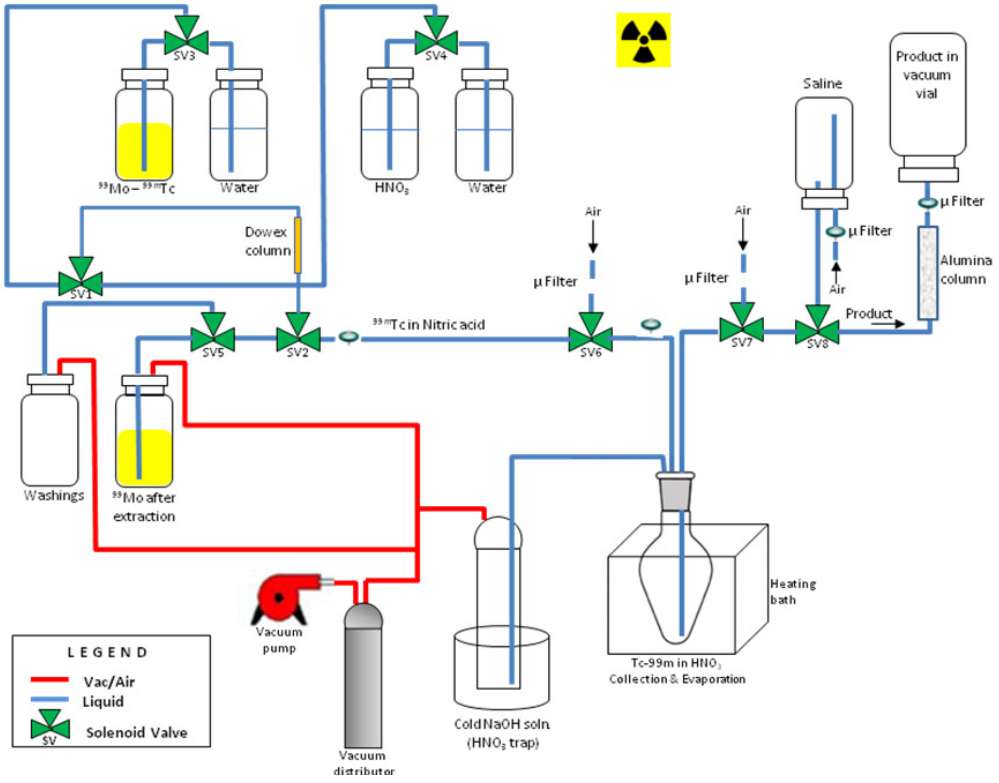

FIG. 32. Process diagram of TCM-AUTODOWNA.

FIG. 33. ^{99m}Tc-TCM-AUTODOWNA module.

^{99m}Tc was eluted from a TEVA cartridge by HNO_3 (8N). The resulting solution was evaporated to dryness and sodium chloride 0.9% and 2 drops of hydrogen peroxide (30%) were added. This solution was passed through the preconditioned alumina column to remove any trace of enriched Mo from the final produced bulk.

The tandem column system is necessary to obtain a high quality of ^{99m}Tc in terms of radionuclidic, radiochemical and chemical purity. Another option is based on a connection TEVA cartridge with AnaLig. Specifically, 30% H_2O_2 (5 mL) was introduced into the target vessel and allowed to dissolve the target material for 10 min. Subsequently, 15% H_2O_2 (10 mL) and 2 × 6.3% NH_3 aqueous solution were introduced in series to complete the dissolving reaction (10 min each). The liquefied target was then collected into an interim reservoir.

The collected ^{99m}Tc/^{100}Mo in about 30 mL of H_2O_2 and H_3 media was transferred to a Tc-selective disposable column (TEVA, Eichrom Technologies) to isolate ^{99m}Tc (specifically, TcO_4^-) not only from the ^{100}Mo target but also from the H_2O_2. (During long distance transfer of solution containing H_2O_2 in narrow tubing, H_2O_2 generates considerable bubbles that absorb applied pressure. Consequently, the target solution will be unstable, likely causing clogging that should be avoided. Therefore, elimination of H_2O_2 before transfer is essential.) After washing the TEVA column with solutions (0.1N NH_3 aq (12 mL), 1.5N HNO_3 (12 mL)), the ^{99m}Tc trapped onto the TEVA column was stripped off by 8N HNO_3 (6 mL), and the eluted solution was led to a mixing vessel containing 2N NaOH (24 mL). The two solutions were well mixed by bubbling N_2 for 5 min, and the solution was then remotely transferred to the hot cell through Teflon tubing (~15 m), as would be done for a typical liquid target. In this way, a low cost, solid target remote production was achieved without using any robotic devices.

Table 6 shows typical data for the quality control tests of $Na^{99m}TcO_4$ prepared in cyclotron and from an alumina column generator.

The use of molecular recognition technology products is a different approach that has many advantages over ion exchange resins that are routinely used. Advanced sorbents are produced by preparing molecularly imprinted polymers, which enable highly selective recognition and separation of specific ions even in the presence of a large excess of similar species. For the ^{99m}Tc separation from ^{99}Mo using AnaLig Tc-02 resin, a mixture of Na_2MoO_4 solution in 2M NaOH and tracers of ^{99}Mo (80–100 kBq) or $^{99m}TcO_4^{-1}$ (170–240 MBq) was delivered to the column using a peristaltic pump with a flow rate of 0.2 mL/min; 5–10 mL of water was used as an eluent. The recovered ^{99m}Tc amounted to 85%. This method, followed by purification of ^{99m}Tc using using 3 columns connected in series containing AnaLig, Dionex and alumina beds resins for the separation of ^{99m}Tc from the irradiated ^{100}Mo target. The ^{99m}Tc recovery yields amounted to 76.3% and losses were 8.2%, 13.2% and 2.3% at each column, respectively. The ^{99m}Tc solution was free of Mo.

TABLE 6. DATA FROM QUALITY CONTROL TESTS OF $Na^{99m}TcO_4$ PREPARED IN A CYCLOTRON AND FROM AN ALUMINA COLUMN GENERATOR

Quality control parameter	TcO_4^- obtained from a cyclotron by		TcO_4^- obtained from generator
	Dowex-1 method	MEK method	
Clarity	Clear	Clear	Clear
pH	6–7	6–7	6–7
^{99}Mo breakthrough	$<10^{-4}$ %	$<10^{-4}$ %	$<10^{-4}$ %
Radiochemical purity	>99 %	>99 %	>99 %
Chemical purity: Al and Mo	<10 ppm	<10 ppm	<10 ppm
Nitrate	<10 ppm	—	—
Peroxide level	<5 ppm	<5 ppm	—
MEK content	—	<0.1% (v/v)	—

The fine separation and preparation steps were carried out using another Tc-selective disposable column (AnaLig Tc-02, GL Sciences) in the hot cell. The ^{99m}Tc was dissolved in nearly 1.4N $NaNO_3$ (35 mL) solution delivered from the target room and was loaded into the AnaLig column to trap ^{99m}Tc and isolate from impurities at a speed of 1 mL/min. The AnaLig column used in this process has a unique property that traps TcO_4^- quantitatively where Na^+ ionic strength of passing media is 0.1M or higher. According to information about the eluents, solutions at temperatures between 50–70°C will strip the trapped Tc from the column. Meanwhile, mixing both solutions of ^{99m}Tc/HNO_3 and NaOH generates neutralization heat that may negatively affect the trapping efficiency. Therefore, the mixed solution was transferred via a long tube from the target room to the hot cell to cool the solution for reliable trapping without a separate cooling period. After loading crude ^{99m}Tc solution, the column was washed with saline (10 mL), and ^{99m}Tc as the final product was stripped off by loading 10 mL of pure water. Figure 34 shows a diagram and an apparatus developed for the ^{99m}Tc remote production system in this CRP.

Another combination of more than one resin was also proposed. The solution is transferred from the target vessel and further prepared by drying and dissolving it in 4N NaOH base before adding it to a PEGylated ion column where the pertechnetate is trapped, allowing Mo and other ions to pass through to the waste. The pertechnetate is eluted with water [32]. The eluted pertechnetate is trapped on an alumina column that will trap any molybdate. Following elution with saline, a chemically pure Tc product was produced. Colorimetric assays determined the levels of alumina and Mo. The isotopic composition of the Mo target material will dictate the Tc isotopic impurities as indicated above. The molybdate in the waste solution can be purified via ion exchange and reduced to a powder suitable for introduction into the electrophoretic plating system by temperature stepped hydrogen reduction. To date, a recovery efficiency of 93% with a range of 91–95% has been demonstrated. A commercial chemistry system using disposable units as illustrated in Fig. 35 has been implemented.

The components typically used for an automated purification system are shown in Fig. 35. Two syringes at the top are initially filled with water (H_2O) and sodium hydroxide 4N NaOH. The raw target dissolution is loaded via the Luer taper connector labelled ‘Tc+Mo’. The ChemMatrix resin (C) is in a standard solid phase separation reservoir. Nitrogen is connected to one end of the kit (N_2). The two waste vessels are indicated as W1 (molybdate recovery) and W2. The strong cation exchange resin (SCX), the sodium chloride vial (NaCl) and the alumina column (A) complete the system. The product is eluted at location ‘P’, normally through a 0.22 μm filter. The processing time is less than 90 min with an efficiency of 92.7 ± 1.1%. The resulting radiochemical purity is >99.99% as TcO_4^-. Analysis for trace impurities indicate that <10 Bq ^{99}Mo and <5 ppm of Al^{3+} are present. There is no evidence of non-Tc impurities. The fluid path is disposable, consistent with GMP.

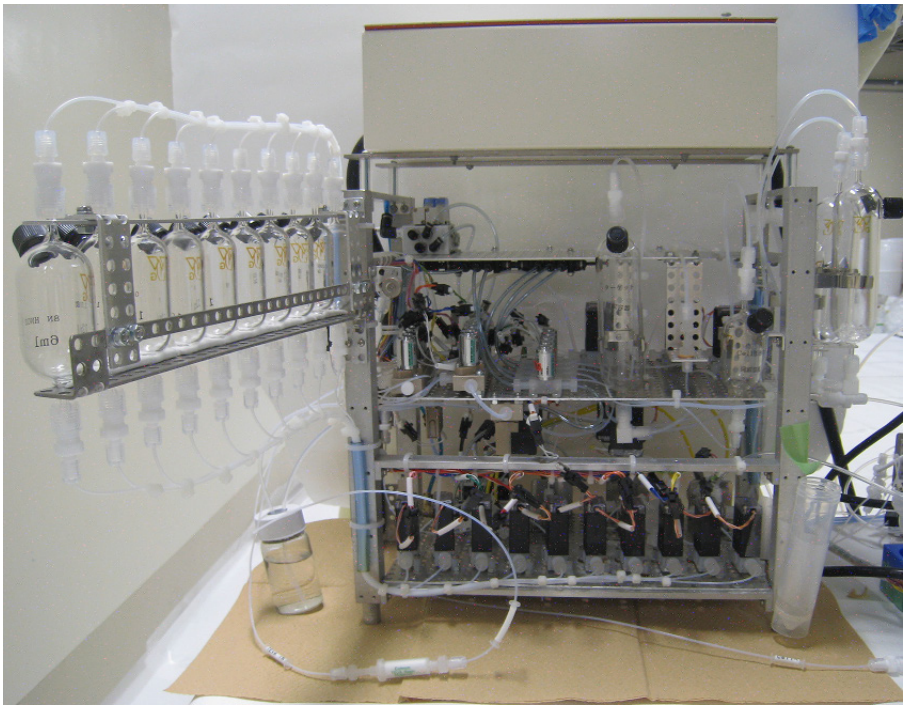

FIG. 34. A remote ^{99m}Tc production system developed in this CRP. The device and process is described in the final report of the CRP on the attached CD-ROM by Nagatsu et al.

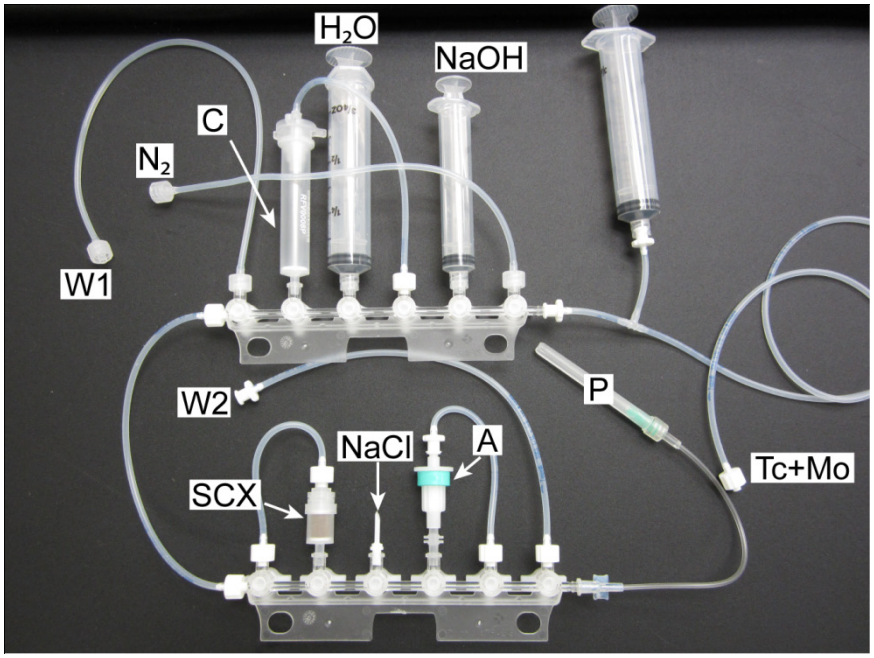

FIG. 35. An example of a disposable reagent kit for the separation and isolation of ^{99m}Tc (courtesy of M. Vuckovic, BC Cancer Agency, Vancouver, Canada).

4.3.3. Thermochromatography

The thermochromatography technique is also recommended for use with separation cyclotron produced $^{99m}TcO_4^-$. The whole process of the separation can be carried out in one step, which is convenient. One research group in the CRP employed a sublimation method for extracting the ^{99m}Tc from the irradiated target material, as

described by Vleck et al. [33]. For the separation, custom quartz glassware based on the design of Rösch et al. was used [34, 35]. Figure 36 shows the individual pieces of the apparatus used for processing the irradiated target materials. The assembled glassware system with the irradiated target in its target holder was transferred into an 850°C preheated furnace. Moist air obtained by pumping air through a water filled bubbling tube was pumped into the apparatus, via the spout-like opening on tube B. Heating continued for 20 min under these conditions and the ^{100}Mo and ^{99m}Tc compounds were deposited in tubes C and D (~ 250°C), respectively. This deposition process is temperature dependent, thus ^{100}Mo deposits in the lower part of tube C in a higher temperature zone (~500°C). Continued heating under these conditions converts the $^{100}Mo_2C$ to $^{100}MoO_3$.

In Mo target processing by thermal chromatography using moist air, hot yellowish $^{100}MoO_3$ was deposited in tube C below the constriction, and ^{99m}Tc as pertechnetate ($^{99m}TcO_4$) was deposited in tube D. After the processing, Tube D was washed with 8 mL of ~100°C 1.0×10^{-4} M NaOH [23]. After thermochromatography, the yield of ^{99m}Tc deposited in tube D was confirmed using a dose calibrator. As Fig. 36 indicates, the depth to which the thermochromatography apparatus was lowered into the vertical furnace was 15 cm. This ensured the maximum possible deposition of ^{99m}Tc in tube D; washing tube D with hot (~100°C) NaOH resulted in a near quantitative recovery of ^{99m}Tc. With 20 min needed for the thermal chromatography process, the total target processing time can typically be less than 45 min.

In order to evaluate the recovery efficiency of the chromatography process techniques, complete dissolution of similar irradiated targets using 30% H_2O_2 after bombardment was performed and the activities obtained were compared to recovered values obtained through thermochromatography techniques. Calculated activities for H_2O_2 processed targets and activities obtained from thermal chromatography processed targets were in good agreement with one another, indicating near quantitative recovery [23].

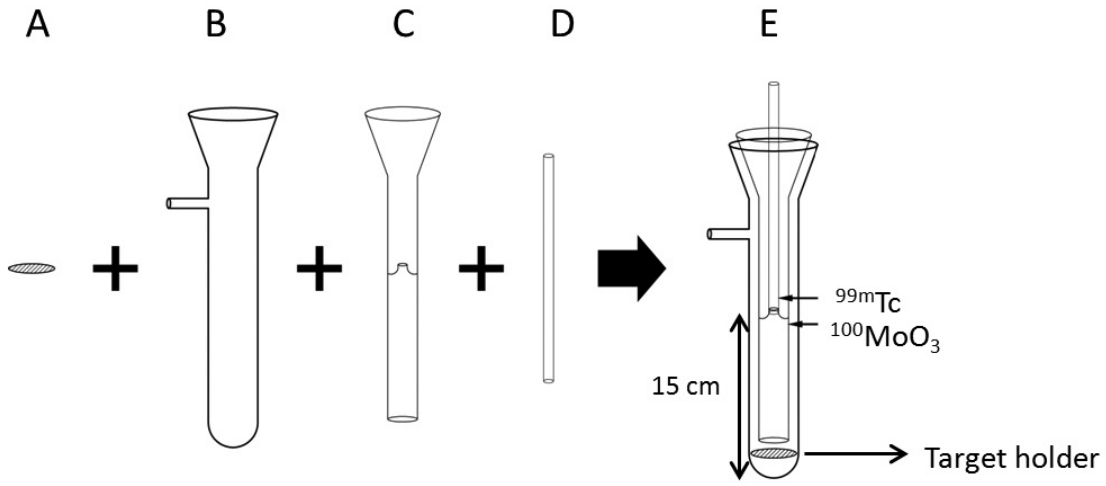

FIG. 36. A diagram of the apparatus used for target processing [23], platinum target holder (A), outer (B), middle (C) and inner (D) quartz tubes, and the assembled apparatus (E).

4.3.4. Chemical precipitation

Chemical precipitation is a less popular method that is nonetheless worthy of consideration. The method is based on the precipitation of insoluble heteropoly acid salt ammonium Mo phosphate hydrate (AMP) and the obtained results were more promising. In the first step, the Mo target was dissolved in 3.5 M HNO_3. Next, triammonium phosphate was added and Mo was precipitated from the solution according to the reaction:

$$(NH_4)_3PO_4 \cdot 3H_2O + 12MoO_4^{2-} + 24H^+ \rightarrow (NH_4)_3P(Mo_3O_{10})_4\downarrow + 15H_2O$$

Based on the experiments performed in the framework of the CRP, the following parameters of AMP precipitation were selected: for 25 mg of Mo target dissolved in 1 mL 3.5M HNO_3, exactly 0.3 mmol of $(NH_4)_3PO_4$ and 0.16 mmol of NH_4NO_3 should be added. The precipitate can be separated by filtration. Possible co-precipitation of ^{99m}Tc with AMP was also studied. After the separation process, 99.6% of total ^{99m}Tc activity is in the filtrate solution. From the studies that have been performed, it can be concluded that the proposed process is promising and allows the fast separation of macro amounts of Mo from the solution without co-precipitation of ^{99m}Tc. Ninety-nine per cent of Mo is bound in the precipitate, from which it will be recovered. After filtration, the solution contains about 0.3 mg/mL Mo. Because the accepted value for Mo in ^{99m}Tc cannot exceed 10 pmm, an additional purification process is needed. In order to remove the Mo residue, a PEGylated C-18 column is used. Molybdate and pertechnetate anions are adsorbed from highly saline solutions (2.5M NH_4NO_3 or 4M NaOH) and TcO_4^- anions are selectively eluted using pure water. C-18 cartridges (Oasis HLB Plus 225 mg) were coated with 5 mL PEG-2000 solution (0.25M), through the cartridge, followed by washing with 50 mL deionized water. An initial separation experiment was performed using generator eluted [^{99m}Tc]TcO_4^- and a solution containing 300 mg/L Mo (after separation of AMP) with 8M NaOH (1:1, volume). After loading, the column was washed with 5 mL NaOH (4M). The [^{99m}Tc]TcO_4^- was eluted using 50 mL water. Recovery of ^{99m}Tc was greater than 99 % [31]. It is necessary to concentrate the solution, owing to the high volume of eluate. In the first step, solution with pertechnetate should be passed over a cation exchange resin to remove sodium anions. In the next step, $^{99m}TcO_4^-$ can be eluted from a small alumina column in 5 mL of 0.9 % NaCl.

Although a number of separation methods have been demonstrated, the potential of using an automated system for both steps is particularly attractive for routine use in a GMP regulatory environment.

5. QUALITY CONTROL

One of the goals of this CRP was to provide broad guidelines to assist in the development of appropriate quality control procedures and release specifications that could be used by a Member State's health regulatory agency as part of their review process. This section has been organized bearing in mind the following constraints: (1) safety and efficacy, where safety can be monitored by pre-release tests, appropriate standard operating procedures and validated post-release tests; (2) an assessment of radionuclidic impurities and method(s) to address their reduction; and (3) an assessment of the impact of cyclotron produced Tc isotopes on patient radiation dosimetry.

Methods and tests that are typically used for confirmation of the pharmaceutical quality of the cyclotron produced ^{99m}Tc, such as the appearance of the solution, pH, sterility and bacterial endotoxins, are not discussed here, since these parameters are assessed by approved pharmacopoeia based methods.

The specification of locally produced ^{99m}Tc in a cyclotron should take into account the methods used for its separation, since the impurity profile is method dependent. Some examples of final product specifications are summarized in tables in the following sections.

5.1. RADIONUCLIDIC PURITY

Radionuclidic purity can be assessed by gamma ray spectroscopy where the spectrum should be identical to that of a pre-qualified ^{99m}Tc standard that exhibits a major photopeak with an energy of 140 keV and/or 6.02 h half-life.

Radionuclidic purity may include an assessment for non-technetium as well as technetium radioisotopes. For non-technetium radioisotopes, the European Union Pharmacopoeia mentions possible contamination of generator derived ^{99m}Tc with ^{99}Mo and other radioisotopes. In addition, and depending on the quality of the ^{100}Mo target, cyclotron produced ^{99m}Tc might be contaminated by the following radioisotopes:

— ^{91}Zr;
— ^{91g}Nb, ^{93g}Nb, ^{94g}Nb, ^{95m}Nb, ^{95g}Nb, ^{96}Nb, ^{97}Nb;

— ^{91g}Mo, ^{93g}Mo, ^{94}Mo, ^{95}Mo, ^{96}Mo, ^{97}Mo, ^{98}Mo, ^{99}Mo;
— ^{99}Ru, ^{100}Ru, ^{101}Ru.

A precise analysis using gamma spectroscopy is needed for their identification and quantification.

Contamination with technetium isotopes other than ^{99m}Tc arises during the enrichment process used to create the ^{100}Mo target material (small abundance of other Mo isotopes); their abundance is also affected by the proton beam energy. Possible contaminants are $^{(90–100)}$Tc, mainly ^{99g}Tc. The ratio of ^{99g}Tc/^{99m}Tc of around 5 at 2–3 h after EOB is rather constant with a bombardment energy of up to 25 MeV, but it is also time dependent. This might affect the labelling efficiency in the preparation of some kits. On a daily basis, other Tc and non-Tc isotopes with higher energy gamma rays could be monitored with a combination of a suitable dose calibrator with a lead shield or a gamma spectrometer with a lead shield. In both cases, the lead shield should be sufficient to absorb the 140 keV gamma rays from ^{99m}Tc.

The following post-release method is considered to be suitable if the same batch of ^{100}Mo is used under the same irradiation conditions. The preparation is allowed to decay for 4–6 weeks and the gamma ray spectrum is examined for the presence of other gamma-ray-emitting impurities. These impurities are identified and quantified, and related to the expiry time for the product (^{99m}Tc-pertechnetate).

5.2. THE RADIOCHEMICAL PURITY OF PERTECHNETATE

Radiochemical purity can be performed by the well-established technique of paper chromatography using methanol/water (85:15 v/v) as the solvent as described in the European Pharmacopoeia and the United States Pharmacopeia to determine the radiochemical purity of the ^{99m}Tc pertechnetate produced. The ^{99m}Tc-pertechnetate anion migrates with a retention (Rf) value of 0.6. More than 99% of the measured radioactivity corresponds to an Rf of 0.6; less than 1% was detected at the start. ^{99m}Tc-pertechnetate migrates with the solvent (saline) front; reduced, hydrolysed activity remains at the start. All reported results show that more than 99% of radiochemical purity is obtained. Modifications of the above method can be used if validated against pharmacopoeia methods.

5.3. THE CHEMICAL PURITY OF PERTECHNETATE

An anodic stripping voltammetry system has been developed that can be used for trace metal analysis in the bulk of produced ^{99m}Tc. This system uses a working electrode (static mercury dropped electrode), a reference electrode (Ag/AgCl/KCl (3 mol)) and an auxiliary platinum electrode. Aluminium and Mo content can also be determined by a colorimetric spot test. The amount of aluminium and Mo in the final product was found to be less than 10 ppm using this method.

In certain methods that use MEK as solvent for extraction, the content of this solvent in the final product can be determined by a spot test. The amount of MEK in the final product was found to be less than 0.1% (v/v). In the other method, in which nitric acid is used for separation and purification, the amount of nitrate ions (as an impurity) should be determined. Nitrate can be determined using colorimetric test strips. This test strip measures the nitrate ion concentration semi-quantitatively by a visual comparison of the reaction zone of the test strip with the colour scale. The content of nitrate was found to be less than 10 mg/L. Similarly, the presence of hydrogen peroxide in the final radioactive TcO_4^- solutions can be measured using colorimetric test strips. The content of hydrogen peroxide was found to be less than 5 ppm MEK. Mo and aluminium contents in the final radioactive TcO_4^- solution can be determined by turbidity and colour tests using iodoform, potassium thiocyanate and chromazural-s tests, respectively [27].

(a) *MEK content test:* 200 μL of 1N NaOH, 200 μL of 0.1N I_2, 50 μL of the test solution and 150 μL distilled water were combined in a test tube. The turbidity produced in the sample was compared with that of the standard (0.1% v/v).
(b) *Mo content test:* 50 μL of the test sample, 50 μL of 10% potassium thiocyanate (KCNS) and 10% $SnCl_2$ were taken in a test tube. The orange-red colour produced in the sample was compared with that of the standard (10 ppm).

(c) *Aluminium content test*: 10 µL of the test sample, 30 µL of acetate buffer (0.1M sodium acetate and 0.1M acetic acid, pH = 4.6) and 10 µL of chromazural-s (2.7 mM) were taken in a test tube. The reddish pink colour produced in the sample was compared with that of the standard (10 ppm) [27].

(d) *Nitrate (NO_3^-) content test:* The level of nitrate ion in the final radioactive TcO_4^- solutions was measured using colorimetric test strips. These test strips measure the nitrate ion concentration semi-quantitatively by visual comparison of the reaction zone of the test strip with the fields of a colour scale that can measure 10–500 mg/L of NO_3^-.

(e) *Hydrogen peroxide (H_2O_2) content test:* The presence of hydrogen peroxide in the final radioactive TcO_4^- solutions was measured using colorimetric test strips. These test strips measure the peroxide concentration semi-quantitatively by visual comparison of the reaction zone of the test strip with the fields of a colour scale that can measure 0.5–25 mg/L of peroxide.

Table 7 shows acceptance limits and procedures to control the radionuclide identity, radionuclidic purity, radiochemical identity, radiochemical purity and chemical purity of ^{99m}Tc.

TABLE 7. ACCEPTANCE LIMITS AND PROCEDURES TO CONTROL THE RADIONUCLIDIC AND CHEMICAL PURITY OF ^{99m}Tc

	Acceptance limits	Determined by	Procedure
Radionuclide identity	Half-life between 5.72 and 6.32 h	Half-life determination	United States Pharmacopeia <821>
	Main emission peaks: 0.141 MeV	Gamma spectrometry	European Pharmacopoeia
Radionuclidic purity	Proposed: Radioisotopic purity >99.5%	Gamma ray spectrometry	
	No gamma ray peaks at 569 keV (^{96}Nb), 658 keV (^{97}Nb), 739 keV (^{99}Mo) are detected		
	Isotopes other than ^{99m}Tc contribute an emission rate of less than 6 000 emissions per second per MBq of ^{99m}Tc	Modified Mo shield assay	
	Not more than: 0.005 % ^{99}Mo 0.005% ^{96}Nb 0.005% ^{97}Nb 0.01% ^{93m}Tc 0.04% ^{93}Tc; ^{94}Tc 0.02% ^{94m}Tc 0.07% ^{95}Tc 0.07% ^{96}Tc 0.05% ^{95m}Tc 0.01% ^{97m}Tc 0.02% of other gamma impurities	Gamma spectrometry	European Pharmacopoeia (draft version)
	Rf = 0.8–1.0	TLC-radiometric	
	Rf > 0.7	TLC	
	Rf = 0.8	Ascending paper chromatography	
	≥95%	TLC-radiometric	
	>95%	Ascending paper chromatography	
	Aluminium content < 10 µg/mL of solution (10 ppm)	Colorimetric assay	

TABLE 7. ACCEPTANCE LIMITS AND PROCEDURES TO CONTROL THE RADIONUCLIDIC AND CHEMICAL PURITY OF ^{99m}Tc (cont.)

	Acceptance limits	Determined by	Procedure
	Mo content < 30 µg/mL of solution (30 ppm)	Photometric assay	
	Hydrogen peroxide content < 50 µL/mL of solution (50 ppm)	Colorimetric assay	
	Aluminium ≤ 5,000 ppm Ethanol ≤ 5,000 ppm	USP monograph on residual solvents	
	Not more than: 5 µg/ml Pb, Al, Ba, Ni 10 µg/ml B, Zn 20 µg/ml Si, Mg, Ca	Spectrometry ICP-OES in-house method	

6. RECYCLING

Due to the very high cost of enriched ^{100}Mo, it should be recovered after irradiation and ^{99m}Tc extraction. Several methods have been developed to accomplish this.

6.1. HYDROGEN SULPHATE (H_2S) METHOD

A recycling flow chart for a recovery method using hydrogen sulphate is shown in Fig. 37. In this technique, the use of a combination of processes for Mo recovery after the extraction of ^{99m}Tc from irradiated Mo was selected and the chemistry processing was optimized as described below.

First step: recovery of MoS_3 from K_2MoO_4 solution; second step: transformation of MoS_3 to MoO_3; and third step: recovery of metallic Mo from MoO_3.

In the first step, the following reaction is carried out. The hydrogen sulphide is put into an alkaline solution.

$$KMoO_4 + 4H_2S \rightarrow MoS_3 + K_2S + 4H_2O$$

To produce hydrogen sulphide, a laboratory method based on the action of 20–30% hydrochloric acid for the iron sulphide was used in the work carried out in the framework of this CRP. This method should be carried out under a hood. The method is based on the reaction:

$$FeS + 2HCl \rightarrow FeCl_2 + H2S\uparrow$$

In an alkaline environment, molybdenum sulphide precipitates to form soluble potassium thiomolybdate:

$$MoS_3 + K_2S \rightarrow K_2MoS_4$$

A neutralization of the alkaline solution of hydrochloric acid should then be carried out by the following reaction:

$$K_2MoS_4 + 2HCl \rightarrow MoS_3\downarrow + HCl + H_2S$$

Mo sulphide precipitates as an amorphous black/brown flock.

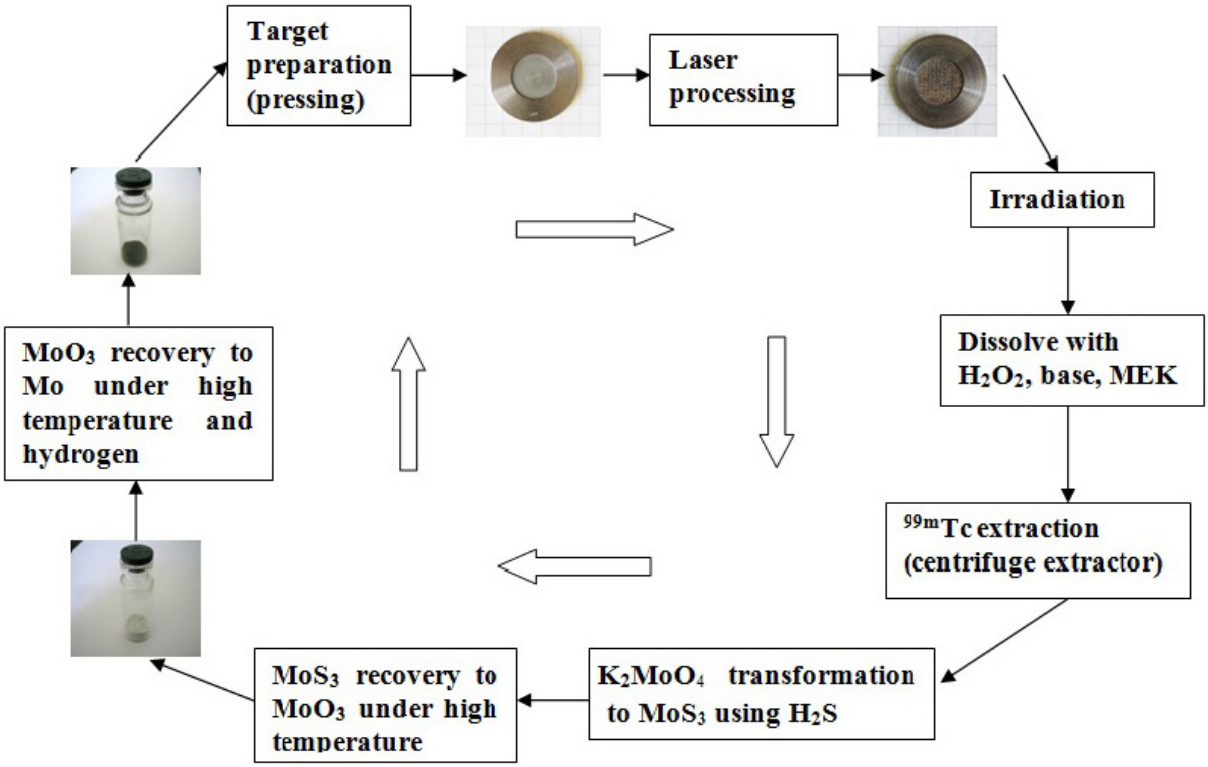

FIG. 37. A recycling flow chart of ^{99m}Tc production.

The precipitate was washed with distilled water from the chloride ions. The washed precipitate was annealed in a muffle furnace feeding for two modes of air:

$MoS_3 \rightarrow MoS_2 + S$ by T = 250–300°C
$2MoS_2 + 7O_2 \rightarrow 2MoO_3 + 4SO_2$ by T = 500–600°C

Parallel reactions can take place:

$MoS_2 + 6MoO_3 \rightarrow 7MoO_2 + 2SO_2$
$2MoO_2 + O_2 \rightarrow 2MoO_3$

The resulting white-grey pitch is crushed to a powder. The recycling apparatus is shown in Fig. 38.

The final state recovery of Mo from MoO_3 is carried out via hydrogen reduction at a temperature of 700°C in a special furnace by the following reaction:

$MoO_3 + 3H_2 \rightarrow Mo + 3H_2O\uparrow$

6.2. HMT METHOD

In what is known as the HMT method, recovered $^{100}MoO_3$ was dissolved 28% NH_3(aq) and this ammonia solution was stored for further use in the synthesis of $(NH_4)_6Mo_7O_{24}\cdot 4H_2O$ [21]. MoO_3 was converted to Mo_2C as described in Section 2.2 with an average efficiency of 85%. In the synthesis of $(NH_4)_6Mo_7O_{24}\cdot 4H_2O$ using recovered $^{100}MoO_3$, heating to 50°C was necessary for complete dissolution. On using $^{100}Mo_2C$ obtained from recycled $^{100}MoO_3$, activities were identical to those obtained using fresh $^{100}MoO_3$ (Fig. 39 and Fig. 40) [23].

FIG. 38. Exhaust hood with Mo recycling trial layout.

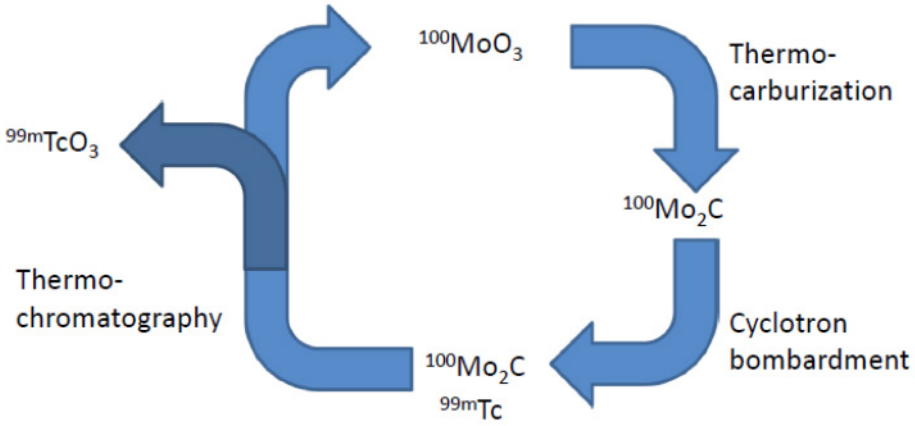

FIG. 39. Life cycle of MoO_3 in the $^{100}Mo(p,2n)^{99m}Tc$ reaction production method [23].

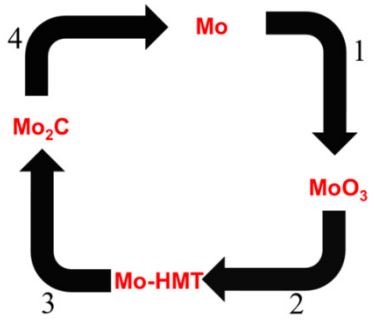

FIG. 40. Life cycle of Mo metal targets in the $^{100}Mo(p,2n)^{99m}Tc$ reaction production method with thermochromatography purification [23]; (1) thermochromatography: $Mo + 1.5O_2 \rightarrow MoO_3$, (2) complex formation: $(NH_4)_4((CH_2)_6N_4)_2Mo_7O_{24}$, (3) thermocarburization: Mo_2C; (4) decarburization: Mo.

Using a similar technique, experiments were also conducted using Mo metal targets. These experiments illustrated that Mo metal was also amenable to the thermochromatographic method of separation and that Mo metal can be efficiently recycled under low reducing conditions (4% H_2 in argon).

6.3. AMMONIUM MOLYBDATE METHOD

6.3.1. Recovery of Mo from the irradiated target

The aqueous fraction containing ammonium molybdate obtained after solvent extraction with MEK or the eluate obtained after passing the load solution through the resin column in the Dowex-1 resin and HNO_3 method can be used to recover the enriched target material. In order to standardize Mo recovery, 500 mg of Mo was dissolved and 200 μCi of ^{99}Mo was added to this solution. From this solution the ^{99m}Tc and ^{99}Mo fractions were then separated by the two separation methods described in Sections 6.1 and 6.2. The total ^{99}Mo activities in the solution before separation and in the Mo fraction obtained after separation were estimated. In the Mo fraction, Mo was present as ammonium molybdate. This fraction also contained some ammonium carbonate that was used during the Mo dissolution step.

6.3.2. Conversion of molybdate to MoO_3

The Mo fraction obtained in each separation process was separately heated in a small vial. Care was taken to avoid any loss of this solution during heating. When all the solvent had evaporated, the dry residue obtained was heated for 1 h at about 700°C. The residue turned light yellow in colour after this heating step. On cooling, the colour of the residue turned grey. The weight of the dry powder obtained was recorded. It was also noted that commercial MoO_3 also turned yellow on heating. The recovery yield of Mo was estimated to be more than 94.5% as MoO_3 (n = 3).

6.3.3. Reduction of natural ammonium molybdate to Mo with hydrogen at high temperature

The reduction method of ammonium molybdate to Mo is a three step process. In the first step, ammonium molybdate is converted into molybdenum oxide at 600°C for about 4 h under atmospheric conditions. In the second step, the molybdenum oxide produced in the first step is reduced in a 100% hydrogen atmosphere with a continuous flow rate of 0.5 L/min at 1050°C for 6 h. Flushing of the furnace with nitrogen gas is essential before the introduction of hydrogen to remove all air from the furnace. Finally, in the third step, the reduced metal produced in the second step is heated at 200°C in a vacuum furnace for about 2 h to remove traces of adsorbed moisture.

Alternatively, the fraction containing ^{100}Mo-molybdate in aqueous sodium hydroxide can be passed through a cation exchange column (Dowex 50W-X8, H^+ form, 80 mL) to quantitatively remove sodium as well as trace cations from the solution [19]. The slightly acidic eluate (pH ~ 6) contains various hydrates of molybdenum trioxide (molybdic acids), which are isolated by evaporation to dryness. Upon further heating, the molybdic acids decompose to water and $^{100}MoO_3$.

The $^{100}MoO_3$ is converted back to Mo in a two step reduction process similar to the methods described previously using a tube furnace and hydrogen gas [36]. MoO_3 was first reduced to MoO_2 in an argon and hydrogen atmosphere (2% H_2, 3 L/min) at 700–800°C (ramp rate 5°C/min). After 30 min, the process gas was changed to 100 % H_2 (3 L/min) and the temperature gradually increased at 5°C/min to 1100°C and held for 30 min. The furnace was then allowed to cool down to room temperature at a rate of 5°C/min.

6.4. ACID PRECIPITATION METHOD

A typical waste solution following purification of ^{99m}Tc yields approximately 70 mL of waste solution containing approximately 0.8–1.5 g ^{100}Mo in 4M sodium hydroxide. The recycling process involves a sequence of batch processes:

(a) *Concentration:* The molybdate is concentrated, preferably by evaporation of water, to obtain a minimum of 30 g Mo/L, and preferably more than 50 g/L. The subsequent ammonia precipitation exploits solubility equilibrium; less concentrated solutions result in larger losses.

(b) *Ammonia precipitation*:
   (i) A source of ammonia is introduced. Ammonium hydroxide suffices and is relatively inexpensive; additionally, its use allows for a simple reactor design. Excess ammonia is needed to ensure a complete reaction; a 4/1 molar ratio of ammonia/molybdate has been shown to provide satisfactory results.
   (ii) The solution is heated using a hot plate, water jacketed reactor or other means to bring the temperature above 75°C, preferably between 85–95°C. The pH is adjusted to 2.5–3, preferably with nitric acid. The elevated temperature is maintained and the solution is agitated while precipitating. It is precipitated for 45–180 min, preferably 90–150 min, or longer if the concentration of Mo is low. A white precipitate (hydrated ammonium molybdate: $MoO_3(NH_3)2(H_2O)x$) begins to form within 5 min of pH adjustment; this formation will take longer if the concentration of Mo is low.
   (iii) The precipitate needs to be immediately filtered while hot and washed with a small quantity of hot (85–95°C) diluted acid, preferably nitric acid, with a pH adjusted to 3.

(c) *Calcination:* The ammonium molybdate is decomposed by calcination at 265–500°C, preferably 425–475°C, leaving molybdenum trioxide (MoO_3).

(d) *Hydrogen reduction:*
   (i) Molybdenum trioxide is reduced to molybdenum dioxide by hydrogen reduction at a temperature between 400–700°C. It is reported that at temperatures beyond 550°C, MoO_3 sublimes appreciably. 1–10% hydrogen in argon (or in another inert gas) is used since the reduction is exothermic and the lower hydrogen content helps to prevent thermal runaway. It may be desired to include a condenser or filter on the furnace exit stream to capture small quantities of Mo/Mo compounds which may, over time, amount to a recoverable quantity.
   (ii) The molybdenum dioxide is reduced to Mo powder at 800–1100°C with hydrogen. 100% hydrogen gas may be used in this step to reduce reaction times. Reduction rates are dependent on sample size, temperature and gas flow rates. Thin layers (<4 mm) are desired for complete hydrogen penetration. High gas flow rates can blow the Mo out of the furnace.

6.5. AMMONIUM ISOPOLYMOLYBDATE PRECIPITATION METHOD

Following MEK separation, Mo oxide solution was acidified to pH2 using nitric acid 8M, then ammonium isopolymolybdate was precipitated with the addition of 1M solution of NH_4OH (pH4). The volume of the solution was reduced by half using mild heating and the solution was kept overnight. After filtration of the ammonium salt with a filter without ashes the product was calcinated at about 500°C to obtain Mo.

7. PRECLINICAL AND CLINICAL STUDIES

Imaging and biodistribution information on cyclotron produced ^{99m}Tc radiopharmaceuticals versus their counterparts derived from conventional reactor based [^{99m}Tc] is summarized in this section to demonstrate their equivalence. Phantom, animal and clinical studies for several ^{99m}Tc-labelled radiopharmaceuticals are presented.

7.1. PHANTOM STUDIES

In order to determine the impact of higher energy photons associated with Tc-isotope impurities, phantom studies were performed. The point-spread function was determined from line sources imaged with a standard clinical single-photon emission computed tomography (SPECT) camera. The line sources were filled with equivalent quantities of ^{99m}Tc derived from a clinical ^{99}Mo/^{99m}Tc generator and from cyclotron production using a target composed of high purity ^{100}Mo.

The profiles were measured on two separate days to emphasize the possible influence of longer lived Tc isotopes produced in the cyclotron derived batch that emit higher (>500 keV) energy photons. There was no measurable difference between generator ^{99m}Tc and cyclotron ^{99m}Tc, even after a 24 h decay time (Fig. 41).

Image definition and contrast were evaluated using a capillary and a Jaszczak phantom (Fig. 42) [37]. For the capillary phantom at 10 cm from the gamma camera collimator, the planar image resolution at full width half maximum was 6.82 ± 0.04 mm for the generator eluted ^{99m}Tc and 6.83 ± 0.09 for the cyclotron produced (cyclotron energy, E_{in} = 24 MeV, 2 h irradiation, 99.815% ^{100}Mo). Planar images acquired using the Jaszczak phantom were of comparable quality without significant loss in spatial resolution (Fig. 42). On average, the contrast of images acquired using cyclotron produced ^{99m}Tc up to 17 h post-EOB (n = 7) was 1.16 ± 0.02 with a contrast-to-noise ratio of 10.47 ± 0.26, which compares favourably with the best of two values obtained for generator eluted ^{99m}Tc: 1.14 (contrast) and 10.28 (contrast-to-noise ratio). The potential dose increase to patients compared with pure (theoretical) ^{99m}Tc was below 4% at the end of the product shelf life (tentatively 12 h post-synthesis).

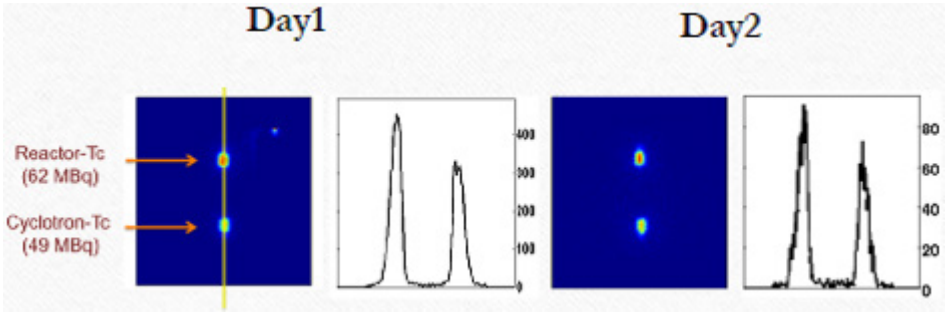

FIG. 41. Line source comparison between reactor produced and cyclotron produced ^{99m}Tc.

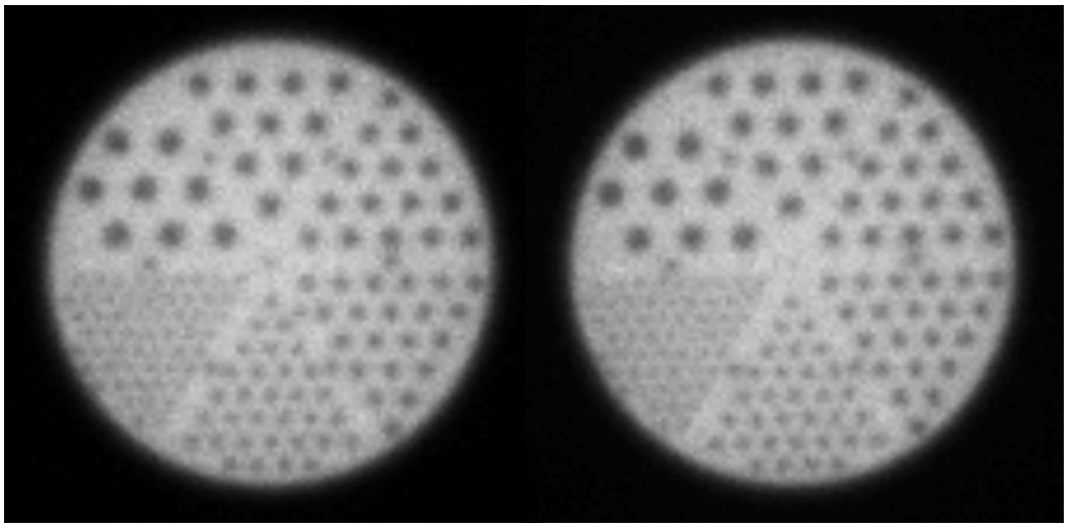

FIG. 42. Planar Jaszczak phantom images acquired with generator eluted (left) and cyclotron produced (right) ^{99m}Tc-pertechnetate in a standard 130–151 keV energy window for ^{99m}Tc clinical scans.

7.2. ANIMAL STUDIES

Several groups participating in the CRP have studied different ^{99m}Tc-labelled radiopharmaceuticals in animals in preparation for clinical studies. All animal experiments in these trials were carried out in accordance with the guidelines in force in the State where they took place. Presented here are several representative studies.

7.2.1. Biodistribution studies using ^{99m}Tc-MDP

Biodistribution studies were performed by the CRP participant group from the Syrian Arab Republic in healthy Wistar rats (male, 160–220 g). In one study, 0.3 mL technetium methylene diphosphonate (^{99m}Tc-MDP) or ^{99m}Tc-pertechnetate (both 2.2–3.7 MBq) in saline was administered to rats intravenously via the tail vein. The animals were anaesthetized and sacrificed, usually 1 h post-intravenous injection, and selected tissues were collected. The radioactivity of samples from the femur, liver, kidneys and blood were measured using a Gamma Counter CE/SN: 03L 504. The uptake in the different organs expressed as %ID of ^{99m}Tc-MDP is shown in Fig. 43.

The results of the biodistribution studies for both ^{99m}TC-MDP prepared from cyclotron produced ^{99m}Tc-MDP and ^{99m}Tc-MDP from ^{99m}Tc produced by a commercially available ^{99}Mo/^{99m}Tc generator were similar and revealed significant bone uptake within 1 h post-injection (Fig. 43). The femur was taken to be representative of the skeleton; the observed uptake in the femur was 1.22% and 1.18% for ^{99m}Tc-MDP (^{99}Mo/^{99m}Tc generator produced ^{99m}Tc) and ^{99m}TC-MDP (cyclotron produced ^{99m}Tc), respectively. Some radioactivity is also seen in the liver and kidney. Most of the radioactivity (54%) was excreted through the bladder.

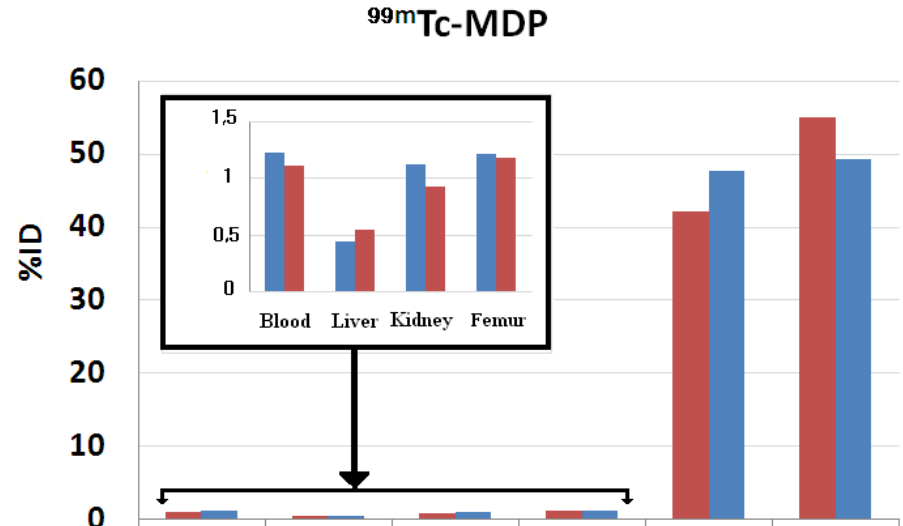

	Blood	Liver	Kidney	Femur	Body	Urine
Cyclotron	1,11	0,55	0,93	1,18	42,18	54,97
Generator	1,22	0,45	1,12	1,21	47,7	49,3

FIG. 43. Biodistribution pattern of the ^{99m}TC-MDP complex in Wistar rats.

7.2.2. Imaging study using ^{99m}Tc-MDP

A comparison of MDP labelling using ^{99m}Tc from a generator with ^{99m}Tc produced from the irradiation of recycled ^{100}Mo metal showed similar chromatography results with <1% colloid for both generator Tc and cyclotron Tc. Free pertechnetate was <1% for generator Tc, and <3% for cyclotron Tc. Using the imaging parameters described above, Fig. 44 shows MDP images obtained with ^{99m}Tc from the two different production methods. Images are displayed using the default window and level settings (i.e. upper and lower limits set to the maximum and minimum pixel intensities, respectively, for each image). Qualitatively, there is no significant difference in the biodistribution of the two radiopharmaceuticals.

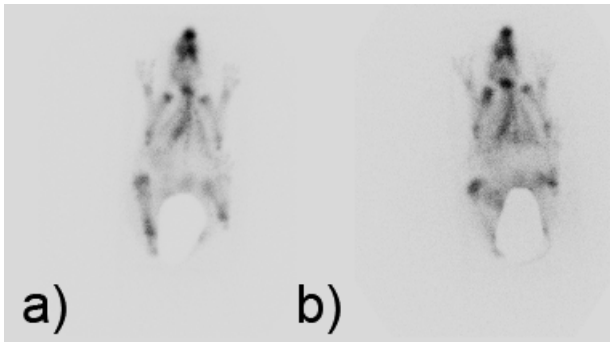

FIG. 44. 40 MBq [^{99m}Tc]MDP uptake 2 hr post-injection for: (a) ^{99m}Tc from a generator, and (b) ^{99m}Tc obtained from cyclotron irradiation of recycled ^{100}Mo. The same rabbit was used for both images, which were separated by 6 d.

7.2.3. Biodistribution studies using [^{99m}Tc]disofenin

In one study in the framework of the CRP to compare biodistribution patterns of [^{99m}Tc]disofenin in rabbits, the substance was diluted to 200 MBq/mL with 0.9% NaCl solution, of which 0.2 mL (i.e. 40 MBq) was then injected intravenously into the ear vein of a rabbit using a 26G needle. Planar images were acquired between 5 and 10 min post-injection on a Symbia T16 SPECT/CT system. Comparison of the images obtained using cyclotron produced [^{99m}Tc]disofenin and those obtained using generator based [^{99m}Tc]disofenin was performed qualitatively through visual inspection of the images.

Due to the fast dynamics associated with this particular radiopharmaceutical, and the fact that the vivarium (i.e. injection location) and the gamma camera used in this study were separated by three floors, imaging at identical time points post-injection was not straightforward. Nevertheless, similar qualitative distributions were generally noted. However, further repeated uptake studies would be beneficial.

7.2.4. Biodistribution studies [^{99m}Tc]TcO_4^-

In a study in the framework of this CRP, the [^{99m}Tc]TcO_4^- was diluted to 200 MBq/mL with 0.9% NaCl solution, of which 0.2 mL (i.e. 40 MBq) was then injected intravenously into the ear vein of a rabbit using a 26G needle. Image acquisition was started at 8 and 23 min post-injection for the cyclotron and generator [^{99m}Tc]TcO_4^-, respectively. A 50 min dynamic image acquisition was performed (1 min frames) on an ADAC Argus single head gamma camera with a low energy general purpose collimator. A qualitative comparison of the cyclotron and generator based images was performed through visual inspection of the images, as well as a comparison of uptake trends in the thyroid, heart, liver and kidneys. Trends were determined by segmenting the respective organs in the summed image dataset, extending these regions of interest to all 50 images, and then calculating the average background subtracted pixel intensity for each region.

The rabbit images taken were initially prepared using window and level settings that spanned the maximum and minimum pixel intensities; however, this resulted in images which revealed little tissue uptake other than in the tissues of the bladder. Overall, similar distributions are noted between the generator and cyclotron sources of ^{99m}Tc; however, as noted above for [^{99m}Tc]disofenin, these results are qualitative and analysis would benefit from further repeated uptake studies.

7.2.5. Biodistribution studies using [^{99m}Tc]HMPAO (Ceretec) and [^{99m}Tc]tetrofosmin (Myoview)

In vivo multimodality imaging studies (SPECT-CT) were performed using generator and accelerator produced ^{99m}Tc pertechnetate and the labelled radiopharmaceuticals: (^{99m}Tc) exametazime HMPAO (hexamethylpropyleneamine oxime) (CERETC) and tetrofosmin (Myoview). Anaesthetized Wistar rats were injected in the jugular vein with either generator or cyclotron ^{99m}Tc pertechnetate, and HMPAO or tetrofosmine. All the experimental procedures were carried out strictly following the current regulations in the State where they took place. Whole body SPECT-CT biodistribution studies were carried out with the hybrid YAP(S)PET-CT small animal scanner. In vivo SPECT-CT preclinical imaging studies in a rat animal model using a high resolution small

animal scanner confirmed equivalent uptake in the heart and brain perfusion of ^{99m}Tc-radiopharmaceuticals labelled with cyclotron compared with generator produced Tc.

7.3. CLINICAL IMAGING

In the framework of this CRP, several groups have studied different ^{99m}Tc-labelled radiopharmaceuticals as part of a clinical study. All clinical trials were carried out in accordance with the appropriate State's guidelines. This section presents several representative examples.

One study was performed by the Canadian reseach group in the University of Alberta using [^{99m}Tc]TcO_4^- from a TR19 cyclotron, and included case matched patients imaged with reactor based [^{99m}Tc]TcO_4^- (Fig. 45). A blinded case control comparison showed that uptake, clearance and biodistribution patterns were identical for the two sources of ^{99m}Tc. No haematological or biochemical toxicity was associated with the cyclotron based injections.

A second trial with ^{99m}Tc produced using a TR24 cyclotron at 24 MeV was performed. The recruitment of patients receiving cyclotron produced [^{99m}Tc]TcO_4^- was completed in April 2015. Preliminary whole body scans obtained showed that the five case matched patients had identical biodistribution patterns for the cyclotron and generator produced radiotracers (Fig. 46). Image definition and contrast were equivalent and there were no particular features allowing discrimination between the Tc production methods. No adverse effects were observed.

In another trial, ^{99m}Tc-MDP was prepared by adding ^{99m}Tc-pertechnetate produced by cyclotron to an MDP kit. The prepared radiopharmaceutical was injected into a patient 15 min post-preparation. Figure 47 shows the bone scan peformed using ^{99m}Tc-MDP in this study.

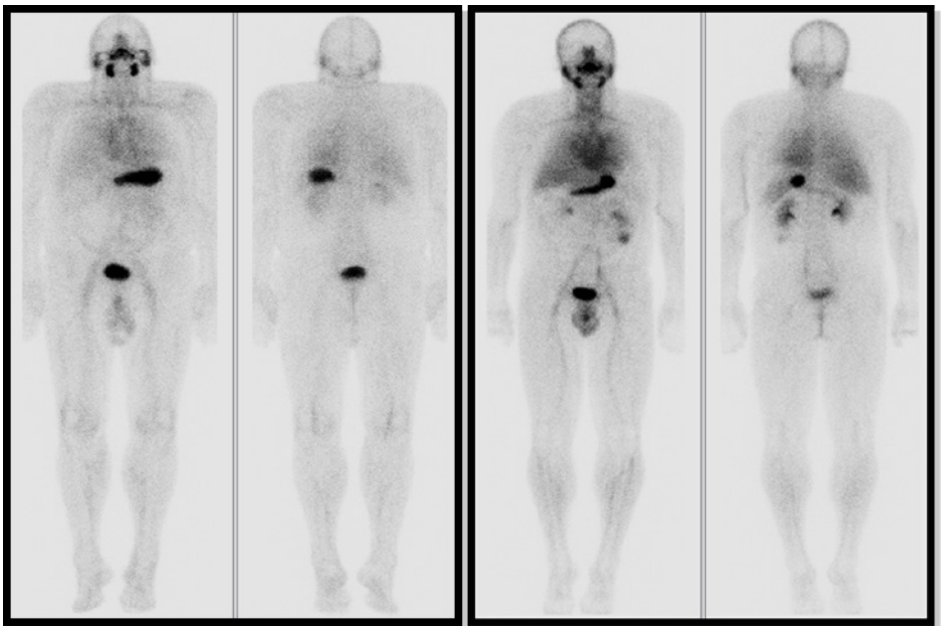

FIG. 45. Comparison of cyclotron based (left) and reactor based (right) ^{99m}Tc pertechnetate (cancer thyroid patients imaged post-thyroidectomy).

7.3.1. ^{99m}Tc-ethylenedicysteine

^{99m}Tc-ethylenedicysteine (^{99m}Tc-EC) was prepared by adding ^{99m}Tc-pertechnetate produced by the cyclotron to an EC kit. The prepared radiopharmaceutical was injected into a patient 15 min post-preparation. Dynamic imaging was carried out for 20 min post-injection. Figure 48 shows the images of a renal scan study of a 5 year old male child.

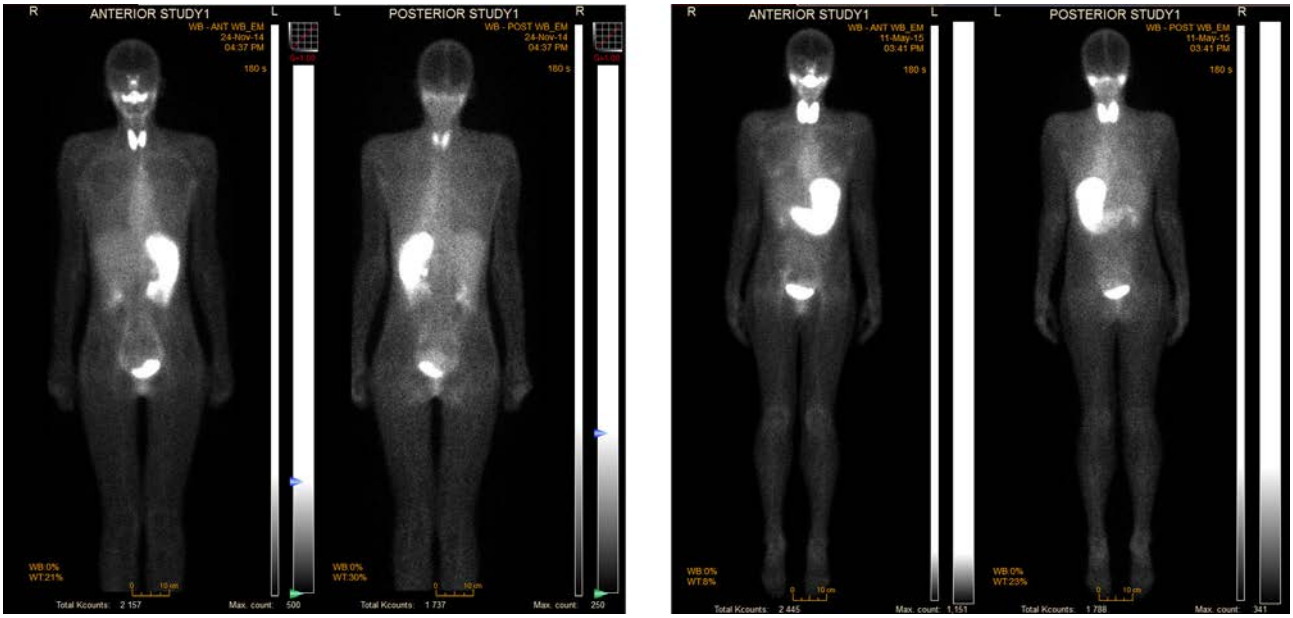

FIG. 46. Whole body scans obtained using cyclotron produced (left) and reactor produced (right) ^{99m}Tc-pertechnetate as part of a clinical trial (Graves' disease was suspected in both patients, note thyroid uptake).

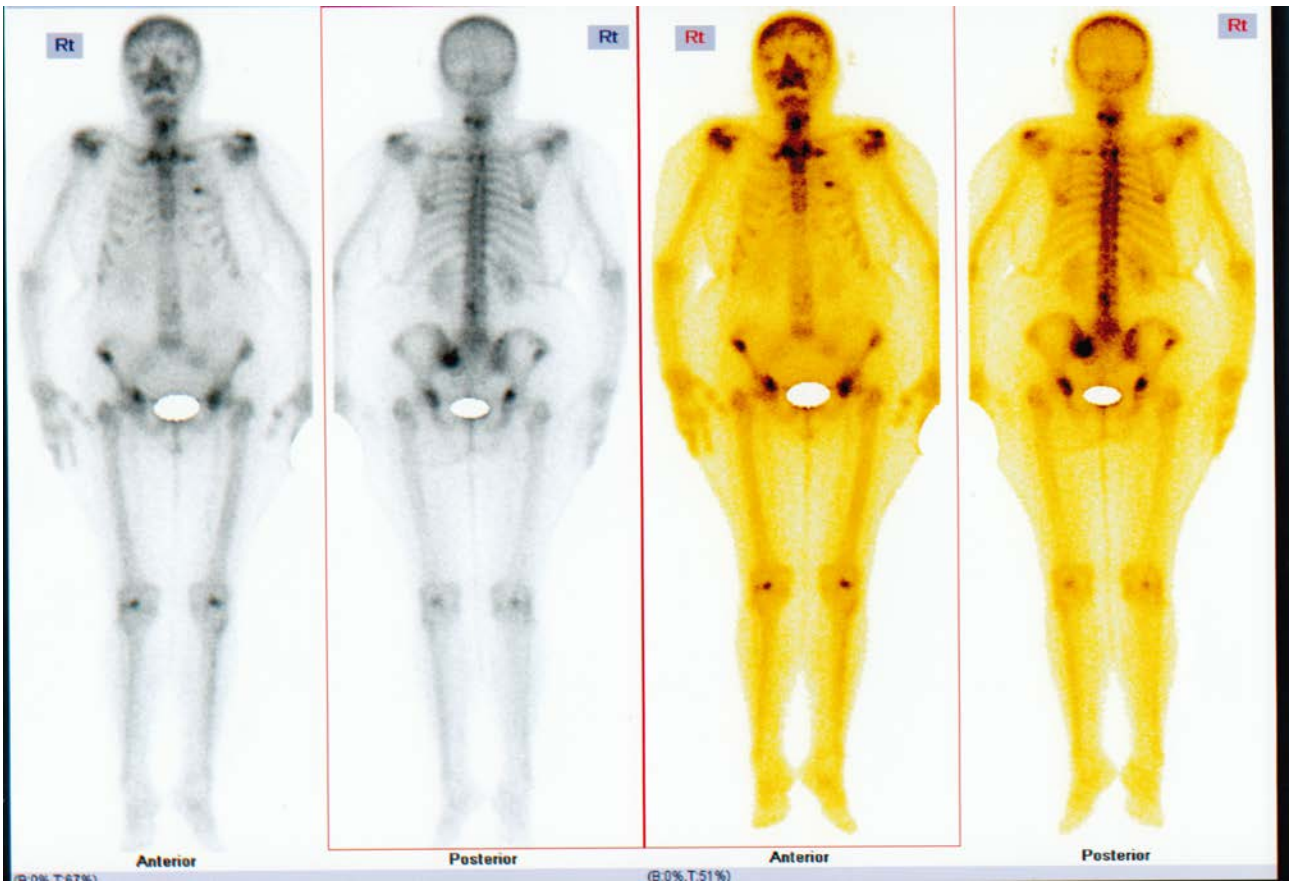

FIG. 47. Bone scans of a 72 year old woman performed using ^{99m}Tc-MDP.

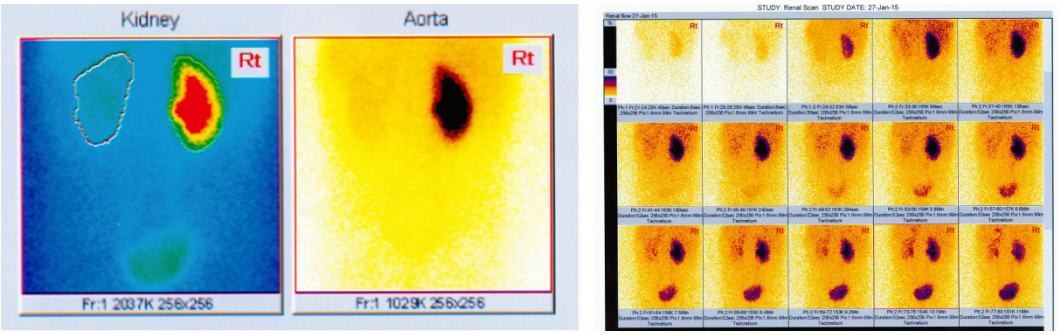

FIG. 48. ^{99m}Tc-EC image showing uniform biodistribution in the right kidney and evidence of failure in the left kidney (image courtesy of Damascus Hospital).

8. GMP

Cyclotron produced ^{99m}Tc in the form of sodium pertechnetate will be used for the same clinical indications as generator produced [^{99m}Tc]TcO_4^-. Hence, the GMP requirements that currently apply to ^{99m}Tc radiopharmaceutical manufacturing will apply whether using ^{99m}Tc from cyclotron derived or from reactor derived sources. Based on existing regulations that provide guidelines on the GMP requirements for ^{99m}Tc radiopharmaceutical manufacturing [38], the minimum quality requirements for cyclotron derived [^{99m}Tc]TcO_4^- are expected to be specified in the forthcoming European Pharmacopoeia monograph. Implementation of these regulations with regard to chemical and pharmaceutical characterization may be modified based on a Member State's national regulatory authorities.

For non-approved medicinal products used in clinical trials, European regulation requests characterization according to the guidelines included in the investigational medicinal product dossier or based on basic requirements for active substances used as starting materials for preparation of medicinal products [39].

9. CONCLUSION

Cyclotron production of ^{99m}Tc by the proton bombardment of enriched ^{100}Mo has been demonstrated in a number of Member States. Several Member States are moving towards clinical trials and it is anticipated that cyclotron produced ^{99m}Tc will be used in clinical applications within the next few years.

To achieve this, significant progress has been made in the development of target systems that can be operated remotely, if not automatically, including solution targets and targets based on the use of oxides of Mo or other salt forms. Production yields for high beam currents and 6 h irradiations have yielded more than 1.2 TBq of ^{99m}Tc, indicating that single cyclotrons can potentially meet the needs of a local community or region. Comparable chemistry systems for the isolation of ^{99m}Tc from the ^{100}Mo target matrix have been explored with approaches that are based on established literature for liquid–liquid extraction, dry distillation and ion chromatography. Efficient recovery procedures have been established that result in >90% recovery of the target material in usable forms for preparing targets for future irradiation.

The labelling of radiopharmaceutical kits indicate that standard radiopharmaceuticals can be prepared that meet quality control requirements for use in humans. Theoretical calculations have been performed for the estimated co-production of other Tc isotopes. These results are in agreement with experimental results and have been used to predict radiation dosimetry for clinical studies. Depending upon irradiation conditions and target composition, it appears that cyclotron produced ^{99m}Tc can be used with less than a 10% increase in patient dose when compared with fission based ^{99m}Tc from a generator.

The next stage will see the implementation of the processes described in this report to begin preclinical imaging and clinical trials, with the aim of establishing a regulatory framework for implementing this approach in order to provide cyclotron produced ^{99m}Tc for nuclear medicine.

REFERENCES

[1] INTERNATIONAL ATOMIC ENERGY AGENCY, Non-HEU Production Technologies for Molybdenum-99 and Technetium-99m, IAEA Nuclear Energy Series No. NF-T-5.4, IAEA, Vienna (2013).

[2] INTERNATIONAL ATOMIC ENERGY AGENCY, Technetium-99m Radiopharmaceuticals: Status and Trends, IAEA Radioisotopes and Radiopharmaceuticals Series No. 1, IAEA, Vienna (2009).

[3] OECD NUCLEAR ENERGY AGENCY, The Supply of Medical Radioisotopes: Market Impact of Converting to Low-Enriched Uranium Targets for Medical Isotope Production, OECD Publishing, Paris (2012).

[4] NATIONAL RESEARCH COUNCIL, Medical Isotope Production without Highly Enriched Uranium, National Academies Press, Washington, DC (2009).

[5] BENARD, F., et al., Implementation of multi-curie production of (99m)Tc by conventional medical cyclotrons, J. Nucl. Med. **55** 6 (2014) 1017–1022.

[6] OECD NUCLEAR ENERGY AGENCY, The Supply of Medical Radioisotopes: Review of Potential Molybdenum-99/ Technetium-99m Production Technologies, OECD Publishing, Paris (2010).

[7] CELLER, A., et al., Theoretical modeling of yields for proton-induced reactions on natural and enriched molybdenum targets, Phys. Med. Biol. **56** (2011) 5469–5484.

[8] MORLEY, T.J., et al., An automated module for the separation and purification of cyclotron-produced (TcO4-)-Tc-99m, Nucl. Med. Biol. **39** 4 (2012) 551–559.

[9] TAKACS, S., et al., Reexamination of cross sections of the Mo-100(p,2n)Tc-99m reaction, Nucl. Instrum. Meth. B **347** (2015) 26–38.

[10] BÉ, M.-M., et al., Table of Radionuclides, Vol. 1 - A=1 to 150, Monographie BIPM-5, Bureau International des Poids et Mesures, Sèvres, France (2004).

[11] GAGNON, K., et al., Cyclotron production of (99m)Tc: experimental measurement of the (100)Mo(p,x)(99)Mo, (99m)Tc and (99g)Tc excitation functions from 8 to 18 MeV, Nucl. Med. Biol. **38** 6 (2011) 907–916.

[12] TARKANYI, F., et al., Investigation of activation cross-sections of proton induced nuclear reactions on Mo-nat up to 40 MeV: New data and evaluation, Nucl. Instrum. Meth. B **280** (2012) 45–73.

[13] MANENTI, S., et al., The excitation functions of Mo-100(p,x)Mo-99 and Mo-100(p,2n)Tc-99m, Appl. Radiat. Isotopes **94** (2014) 344–348.

[14] TAKACS, S., et al., Evaluation of proton induced reactions on Mo-100: New cross sections for produ ction of Tc-99m and Mo-99, J. Radioanal. Nucl. Chem. **257** 1 (2003) 195–201.

[15] HOU, X., et al., Graphical user interface for yield and dose estimations for cyclotron-produced technetium, Phys. Med. Biol. **59** 13 (2014) 3337–3352.

[16] ESPOSITO, J., et al., Evaluation of Mo-99 and Tc-99m productions based on a high-performance cyclotron, Sci. Technol. Nucl. Instrum. **2013** (2013) 1–14.

[17] HANEMAAYER, V., et al., Solid targets for Tc-99m production on medical cyclotrons, J. Radioanal. Nucl. Chem. **299** 2 (2014) 1007–1011.

[18] MORLEY, T.J., et al.,The deposition of smooth metallic molybdenum from aqueous electrolytes containing molybdate ions, Electrochem. Commun. **15** 1 (2012) 78–80.

[19] STOLARZ, A., et al., Molybdenum targets produced by mechanical reshaping, J. Radioanal. Nucl. Chem. **305** 3 (2015) 947–952.

[20] SRIVATSAN, T.S., et al., The microstructure and hardness of molybdenum powders consolidated by plasma pressure compaction, Powder Technol. **114** 1–3 (2001) 136–144.

[21] AVETISYAN, A., et. al., The powdered molybdenum target preparation technology for ^{99m}Tc production on C-18 cyclotron, Int. J. Eng. Sci. Innov. Technol. **4** 3 (2015) 37–44.

[22] NAGATSU, K., et al., An alumina ceramic target vessel for the remote production of metallic radionuclides by in situ target dissolution, Nucl. Med. Biol. **39** 8 (2012) 1281–1285.

[23] RICHARDS, V.N., et al., Cyclotron production of (99m)Tc using (100)Mo2C targets, Nucl. Med. Biol. **40** 7 (2013) 939–945.

[24] RICHARDS, V.N., et al., Production and separation of Re-186g from proton bombardment of (WC)-W-186, Nucl. Med. Biol. **42** 6 (2015) 530–535.

[25] AVILA-RODRIGUEZ, M.A., et al., The use of radiochromic films to measure and analyze the beam profile of charged particle accelerators, Appl. Radiat. Isotopes **67** 11 (2009) 2025–2028.

[26] CHATTOPADHYAY, S., et al., Recovery of 99mTc from Na2[99Mo]MoO4 solution obtained from reactor-produced (n,gamma) 99Mo using a tiny Dowex-1 column in tandem with a small alumina column, Appl. Radiat. Isot. **66** 12 (2008) 1814–1817.

[27] CHATTOPADHYAY, S., et al., Pharmaceutical grade sodium [99mTc] pertechnetate from low specific activity 99Mo using an automated 99Mo/99mTc-TCM-autosolex generator, J. Radioanal. Nucl. Chem. **302** 2 (2014) 781–790.

[28] ZYKOV, M.P., ROMANOVSKII, V.N., WESTER, D.W., et al., Use of extraction generator for preparing a 99mTc radiopharmaceutical, Radiochem. **43** 3 (2001) 297–300.

[29] EGOROV, A.V., ZIKOV, M.P., KORPUSOV, G.V., ROMANOVSKY, V.N., FILYANIN, A.J., Production of 99mTc on the centralized generator in St. Petersburg, J. Nucl. Biol. Med. **38** 3 (1994) 399–402.
[30] AVAGYAN, R., et al., Photo-production of Mo-99/Tc-99m with electron linear accelerator beam, Nucl. Med. Biol. **41** 8 (2014) 705–709.
[31] ANDERSSON, J., et al., Separation of TcO_4^- and MoO_4^{2-} using a PEG coated C18 SPE cartridge, J. Nucl. Med. **54** Suppl. 2 (2013) S1001.
[32] BENARD, F., et al., Cross-linked polyethylene glycol beads to separate Tc-99m-pertechnetate from low-specific-activity molybdenum, J. Nucl. Med. **55** 11 (2014) 1910–1914.
[33] VLCEK, J., et al., Thermal separation of ^{99m}Tc from molybdenum trioxide. II. Separation of 99mTc from molybdenum trioxide at temperatures above 650°C, Radiochem. Radioanal. Lett. **20** 1 (1974) 23–31.
[34] RÖSCH, F., NOVGORODOV, A., QAIM, S., Thermochromatographic separation of 94mTc from enriched molybdenum targets and its large scale production for nuclear medical application, Radiochim. Acta **64** 2 (1994) 113–120.
[35] BIGOTT, H.M., et al., Advances in the production, processing and microPET image quality of technetium-94m, Nucl. Med. Biol. **33** 7 (2006) 923–933.
[36] TUOMINEN, S.M., Preparation and sintering of fine molybdenum powder, Powder Technol. **30** 1 (1981) 73–76.
[37] SELIVANOVA, S., et al., Radioisotopic purity of sodium pertechnetate ^{99m}Tc produced with a medium-energy cyclotron: implications for internal radiation dose, image quality, and release specifications, J. Nucl. Med. **56** 10 (2015) 1600–1608.
[38] EUROPEAN COMMISSION, EudraLex, The Rules Governing Medicinal Products in the European Union, Volume 4, EU Guidelines to Good Manufacturing Practice, Medicinal Products for Human and Veterinary Use, Annex 3: Manufacture of Radiopharmaceuticals (2008),
http://ec.europa.eu/health/files/eudralex/vol-4/2008_09_annex3_en.pdf
[39] EUDRALEX, Eudralex, The Rules Governing Medicinal Products in the European Union, Volume 4, Good Manufacturing Practice, Medicinal Products for Human and Veterinary Use, Part II: Basic Requirements for Active Substances used as Starting Materials (2014),
http://ec.europa.eu/health/files/eudralex/vol-4/2014-08_gmp_part1.pdf

Annex I

PUBLICATIONS RESULTING FROM THE COORDINATED RESEARCH PROJECT

I–1. PUBLICATIONS ON THEORETICAL TOPICS

CELLER, A., HOU, X., BÉNARD, F., RUTH, T., Theoretical modelling of yields for proton induced reactions on natural and enriched molybdenum targets, Phys. Med. Biol. **56** (2011) 5469–5484.

ESPOSITO, J., et al., Evaluation of ^{99}Mo and ^{99m}Tc productions based on a high-performance cyclotron, Sci. Technol. Nucl. Install. **2013** (2013) 1–14.

GAGNON, K., et al., Cyclotron production of ^{99m}Tc: Experimental measurement of the ^{100}Mo(p,x)^{99}Mo, ^{99m}Tc, and ^{99g}Tc excitation functions from 8 to 18 MeV, Nucl. Med. Biol. **38** (2011) 907–916.

HOU, X., et al., Graphical user interface for yield and dose estimations for cyclotron-produced technetium, Phys. Med. Biol. **59** (2014) 3337–3352.

MANENTI, S., et al., The excitation functions of Mo-100(p,x)Mo-99 and Mo-100(p,2n)Tc-99m, Appl. Radiat. Isot. **94** (2014) 344–348.

PUPILLO, G., ESPOSITO, J., GAMBACCINI, M., HADDAD, F., MICHEL, N., Experimental cross section evaluation for innovative ^{99}Mo production via the (α,n) reaction on Zr-96 target, J. Radioanal. Nucl. Chem. **302** 2 (2014) 911–917.

PUPILLO, G., ESPOSITO, J., GAMBACCINI, M., HADDAD, F., MICHEL, N., Accelerator-based production of ^{99}Mo: A comparison between the ^{100}Mo(p,x) and ^{96}Zr(α,n) reactions, J. Radioanal. Nucl. Chem. **305** 1 (2015) 73–78.

TAKÁCS, S., HERMANNE, A., DITRÓI, F., TÁRKÁNYI, F., AIKAWA, M., Reexamination of cross sections of the ^{100}Mo(p,2n)^{99m}Tc reaction, Nucl. Instr. Meth. B **347**(2015) 26–38.

TANGUAY, J., et al., Quantitative analysis of relationships between irradiation parameters and the reproducibility of cyclotron-produced ^{99m}Tc yields, Phys. Med. Biol. **60** (2015) 3883–3903.

UCCELLI, L., et al., Influence of the generator in-growth time on the final radiochemical purity and stability of ^{99m}Tc radiopharmaceuticals, Sci. Technol. Nucl. Install. **2013** (2013) 379283.

I–2. PUBLICATIONS ON TARGETRY

AVETISYAN, A., et al., The powdered molybdenum target preparation technology for 99mTc production on C-18 cyclotron, Int. J. Eng. Sci. Innov. Technol. **4** 3 (2015) 37–44.

AVILA-RODRIGUEZ, M.A., et al., The use of radiochromic films to measure and analyze the beam profile of charged particle accelerators, Appl. Radiat. Isot. **67** (2009) 2025–2028.

GAGNON, K., et al., Cyclotron production of 99mTc: Experimental measurement of the 100Mo(p,x)99Mo, 99mTc, and 99gTc excitation functions from 8 to 18 MeV, Nucl. Med. Biol. **38** (2011) 907–916.

GAGNON, K., et al., Letter to the editor: Experimental cross section measurements for the 100Mo(p,x)101Tc, 96Nb, and 97Nb reactions in the energy range of 10 to 18 MeV, Nucl. Med. Biol. **39** (2012) 923–925.

HANEMAAYER, V., et al., Solid targets for 99mTc production on medical cyclotrons, J. Radioanal. Nucl. Chem. **299** (2014) 1007–1011.

MORLEY, T.J., et al., The deposition of smooth metallic molybdenum from aqueous electrolytes containing molybdate ions, Electrochem. Commun. **15** (2012) 78–80.

SKLIAROVA, H., et al., Niobium-based sputtered thin films for corrosion protection of proton-irradiated liquid water targets for [18F] production, J. Phys. D: Appl. Phys. **47** (2014) 045306.

SKLIAROVA, H., et al., Niobium-niobium oxide multilayered coatings for corrosion protection of proton-irradiated liquid water targets for [18F] production, Thin Solid Films **591** (2015) 316–322.

SKLIAROVA, H., AZZOLINI, O., JOHNSON, R.R., PALMIERI, V., Co-sputtered amorphous Nb–Ta, Nb–Zr and Ta–Zr coatings for corrosion protection of cyclotron targets for [18F] production, J. Alloys Compd. **639** (2015) 488–495.

STOLARZ, A., et al., Molybdenum targets produced by mechanical reshaping, J. Radioanal. Nucl. Chem. **305** (2015) 947–952.

I–3. PUBLICATIONS ON PROCESSING

BENARD, F., et al., Cross-linked polyethylene glycol beads to separate 99mTc-pertechnetate from low specific activity molybdenum, J. Nucl. Med. **55** (2014) 1910–1914.

CHATTOPADHYAY, S., et al., Pharmaceutical grade sodium [99mTc] pertechnetate from low specific activity 99Mo using an automated 99Mo/99mTc-TCM-autosolex generator, J. Radioanal. Nucl. Chem. **302** (2014) 781–790.

CHATTOPADHYAY, S., et al., "An automated computer controlled module for preparation of sodium [99mTc] pertechnetate using (n,γ) 99Mo-molybdate solution: TCM-AUTODOWNA generator", Proc. 46th Annual Conference of Indian Soc. of Nuclear Medicine (SNMICON-2014, December, Kolkata), SINP, Kolkata (2014) 26–27.

GUMIELA, M., et al., A new simple way separation of 99mTc from 100Mo target, Nucl. Med. Biol. **41** 7 (2014) 649.

MORLEY, T.J., et al., An automated module for the separation and purification of cyclotron-produced 99mTcO4-, Nucl. Med. Biol. **39** (2012) 551–559.

PARUS, J., et al., Production of 99mTc in medical cyclotrons (Alternative methods for production of 99mTc), Postępy Techniki Jądrowej **57** 3 (2014) 19–22.

RICHARDS, V.N., et al., Production and separation of (186g)Re from proton bombardment of (186)WC, Nucl. Med. Biol. **42** 6 (2015) 530–535.

WOJDOWSKA, W., et al., Studies on the separation of 99mTc from large excess of molybdenum, Nucl. Med. Rev. Cent.East. Eur. **18** 2 (2015) 65–69.

I–4. PUBLICATIONS ON DOSIMETRY

HOU, X., CELLER, A., GRIMES, J., BÉNARD, F., RUTH T., Theoretical dosimetry estimations for radioisotopes produced by proton induced reactions on natural and enriched molybdenum targets, Phys. Med. Biol. **57** (2012) 1499–1515.

I–5. PUBLICATIONS ON RECYCLING

GAGNON, K., et. al., Cyclotron production of 99mTc: Recycling of enriched 100Mo metal targets, Appl. Radiat. Isot. **70** (2012) 1685–1690.

I–6. PUBLICATIONS ON THE TOTAL PROCESS

BÉNARD, F., et al., Implementation of multi-curie production of 99mTc by conventional medical cyclotrons, J. Nucl. Med. **55** (2014) 1017–1022.

GAGNON, K., Cyclotron Production of Technetium-99m, PhD Thesis, Univ. Alberta (2012).

GUÉRIN, B., et al., Cyclotron production of 99mTc: An approach to the medical isotope crisis, J. Nucl. Med. **51** (2010) 13N–16N.

RICHARDS, V.N., et al., Cyclotron Production of (99m)Tc using (100)Mo2C targets, Nucl. Med. Biol. **40** 7 (2013) 939–945.

SCHAFFER, P., et al., Direct production of 99mTc via 100Mo(p,2n) on small medical cyclotrons, Phys. Procedia **66** (2015) 383–395.

Annex II

CONTENTS OF THE ATTACHED CD-ROM

The final reports of the coordinated research project is available on the attached CD-ROM.

CONTRIBUTORS TO DRAFTING AND REVIEW

Al-Rayyes, A.H.	Atomic Energy Commission of Syria, Syrian Arab Republic
Al-Rumayan, F.	King Faisal Specialist Hospital and Research Centre, Saudi Arabia
Avetisyan, A.	National Science Laboratory Foundation, Armenia
Chattopadhyay, S.	Variable Energy Cyclotron Centre, India
Esposito, J.	Legnaro National Laboratories, Italy
Fujibayashi, Y.	National Institute of Radiological Sciences, Japan
Haji-Saied, M.	International Atomic Energy Agency
Lapi, S.	Washington University School of Medicine, United States of America
McQuarrie, S.A.	University of Alberta, Canada
Mikołajczak, R.	National Centre for Nuclear Research, Poland
Ruth, T. J.	TRIUMF and the British Columbia Cancer Agency, Canada
Salvini, A.	University of Pavia, Italy
Takacs, S.	Institute for Nuclear Research, Hungary

Research Coordination Meetings

Vancouver, Canada: 16–20 April 2012
Legnaro, Italy: 7–11 October 2013
Vienna, Austria: 22–26 June 2015

IAEA
International Atomic Energy Agency

No. 25

ORDERING LOCALLY

In the following countries, IAEA priced publications may be purchased from the sources listed below or from major local booksellers.

Orders for unpriced publications should be made directly to the IAEA. The contact details are given at the end of this list.

CANADA

Renouf Publishing Co. Ltd

22-1010 Polytek Street, Ottawa, ON K1J 9J1, CANADA
Telephone: +1 613 745 2665 • Fax: +1 643 745 7660
Email: order@renoufbooks.com • Web site: www.renoufbooks.com

Bernan / Rowman & Littlefield

15200 NBN Way, Blue Ridge Summit, PA 17214, USA
Tel: +1 800 462 6420 • Fax: +1 800 338 4550
Email: orders@rowman.com Web site: www.rowman.com/bernan

CZECH REPUBLIC

Suweco CZ, s.r.o.

Sestupná 153/11, 162 00 Prague 6, CZECH REPUBLIC
Telephone: +420 242 459 205 • Fax: +420 284 821 646
Email: nakup@suweco.cz • Web site: www.suweco.cz

FRANCE

Form-Edit

5 rue Janssen, PO Box 25, 75921 Paris CEDEX, FRANCE
Telephone: +33 1 42 01 49 49 • Fax: +33 1 42 01 90 90
Email: formedit@formedit.fr • Web site: www.form-edit.com

GERMANY

Goethe Buchhandlung Teubig GmbH

Schweitzer Fachinformationen
Willstätterstrasse 15, 40549 Düsseldorf, GERMANY
Telephone: +49 (0) 211 49 874 015 • Fax: +49 (0) 211 49 874 28
Email: kundenbetreuung.goethe@schweitzer-online.de • Web site: www.goethebuch.de

INDIA

Allied Publishers

1st Floor, Dubash House, 15, J.N. Heredi Marg, Ballard Estate, Mumbai 400001, INDIA
Telephone: +91 22 4212 6930/31/69 • Fax: +91 22 2261 7928
Email: alliedpl@vsnl.com • Web site: www.alliedpublishers.com

Bookwell

3/79 Nirankari, Delhi 110009, INDIA
Telephone: +91 11 2760 1283/4536
Email: bkwell@nde.vsnl.net.in • Web site: www.bookwellindia.com

ITALY

Libreria Scientifica "AEIOU"

Via Vincenzo Maria Coronelli 6, 20146 Milan, ITALY
Telephone: +39 02 48 95 45 52 • Fax: +39 02 48 95 45 48
Email: info@libreriaaeiou.eu • Web site: www.libreriaaeiou.eu

JAPAN

Maruzen-Yushodo Co., Ltd

10-10 Yotsuyasakamachi, Shinjuku-ku, Tokyo 160-0002, JAPAN
Telephone: +81 3 4335 9312 • Fax: +81 3 4335 9364
Email: bookimport@maruzen.co.jp • Web site: www.maruzen.co.jp

RUSSIAN FEDERATION

Scientific and Engineering Centre for Nuclear and Radiation Safety

107140, Moscow, Malaya Krasnoselskaya st. 2/8, bld. 5, RUSSIAN FEDERATION
Telephone: +7 499 264 00 03 • Fax: +7 499 264 28 59
Email: secnrs@secnrs.ru • Web site: www.secnrs.ru

UNITED STATES OF AMERICA

Bernan / Rowman & Littlefield

15200 NBN Way, Blue Ridge Summit, PA 17214, USA
Tel: +1 800 462 6420 • Fax: +1 800 338 4550
Email: orders@rowman.com • Web site: www.rowman.com/bernan

Renouf Publishing Co. Ltd

812 Proctor Avenue, Ogdensburg, NY 13669-2205, USA
Telephone: +1 888 551 7470 • Fax: +1 888 551 7471
Email: orders@renoufbooks.com • Web site: www.renoufbooks.com

Orders for both priced and unpriced publications may be addressed directly to:

Marketing and Sales Unit
International Atomic Energy Agency
Vienna International Centre, PO Box 100, 1400 Vienna, Austria
Telephone: +43 1 2600 22529 or 22530 • Fax: +43 1 2600 29302 or +43 1 26007 22529
Email: sales.publications@iaea.org • Web site: www.iaea.org/books

INTERNATIONAL ATOMIC ENERGY AGENCY
VIENNA
ISBN 978–92–0–102916–4
ISSN 2413–9556